Federal University of Paraíba
Center for Exact and Natural Sciences
Graduate Program in Physics

Ivanilson da Silva Lima

Gravitational Potentials Modified by Extra Dimensions: An Analysis of Alpha Decay in the Context of the Brane-World Model

João Pessoa, PB - Brazil
February, 2026

Ivanilson da Silva Lima

Gravitational Potentials Modified by Extra Dimensions: An Analysis of Alpha Decay in the Context of the Brane-World Model

Dissertation submitted to the Graduate Program in Physics of the Federal University of Paraíba, as part of the requirements to obtain the degree of Master in Physics.

Supervisor: Prof. Dr. Fábio Leal de Melo Dahia

João Pessoa, PB - Brazil
February, 2026

Catalogação na publicação
Seção de Catalogação e Classificação

L732g Lima, Ivanilson da Silva.
Gravitational potentials modified by extra dimensions : an analysis of alpha decay in the context of the Brane-world model / Ivanilson da Silva Lima. - João Pessoa, 2026.
86 f. : il.

Orientação: Fábio Leal de Melo Dahia.
Dissertação (Mestrado) - UFPB/CCEN.

1. Dimensões extras de grande escala. 2. Modelos de Branas. 3. Interação gravitacional modificada. 4. Decaimento alfa. I. Dahia, Fábio Leal de Melo. II. Título.

UFPB/BC CDU 53=111(043)

Elaborado por JONISMAR KENDYS DA SILVA LEAO - CRB-4/2332

Universidade Federal da Paraíba
Centro de Ciências Exatas e da Natureza
Programa de Pós-Graduação *Stricto Sensu* em Física

Ata da Sessão Pública da Defesa de dissertação de **Mestrado** do aluno **Ivanilson da Silva Lima**, candidato ao Título de Mestre em Física na Área de Concentração Gravitação e Cosmologia.

Aos vinte e seis dias do mês de fevereiro do ano de dois mil e vinte e seis, às 15h00, na sala virtual meet.google.com/bmz-ykae-zwd, reuniram-se os membros da Banca Examinadora constituída para avaliar a dissertação de Mestrado, na área de Gravitação e Cosmologia, de **Ivanilson da Silva Lima**. A banca foi composta pelos(as) professores(as) doutores(as): Fábio Leal de Melo Dahia (PPGF/UFPB), orientador e presidente da banca examinadora, Jansen Brasileiro Formiga (PPGF/UFPB) e Marcos Antônio Anacleto (UFCG). Dando início aos trabalhos, o Prof. Fábio Leal de Melo Dahia comunicou aos presentes a finalidade da reunião. A seguir, passou a palavra para o candidato para que o mesmo fizesse, oralmente, a exposição da pesquisa de dissertação intitulada "*Potenciais Gravitacionais modificados por dimensões extras: Uma análise do decaimento alfa no contexto de modelos de mundo-brana*". Concluída a exposição, o candidato foi arguido pela Banca Examinadora, que emitiu o parecer **"aprovado".** Assim sendo, deve a Universidade Federal da Paraíba expedir o respectivo diploma de Mestre em Física na forma da lei. E para constar, Ana Beatriz Cândido Vieira, Assistente em Administração, redigiu a presente ata que vai assinada pelos membros da Banca Examinadora. João Pessoa, Paraíba, **26 de fevereiro de 2026**.

gov.br
Documento assinado digitalmente
FABIO LEAL DE MELO DAHIA
Data: 26/02/2026 17:11:07-0300
Verifique em https://validar.iti.gov.br

Prof. Dr. Fábio Leal de Melo Dahia
Orientador - PPGF/UFPB

gov.br
Documento assinado digitalmente
JANSEN BRASILEIRO FORMIGA
Data: 26/02/2026 17:16:29-0300
Verifique em https://validar.iti.gov.br

Prof. Dr. Jansen Brasileiro Formiga
PPGF/UFPB

gov.br
Documento assinado digitalmente
MARCOS ANTONIO ANACLETO
Data: 26/02/2026 21:43:49-0300
Verifique em https://validar.iti.gov.br

Prof. Dr. Marcos Antônio Anacleto
UFCG

To my dear grandfather (*in memoriam*)

Acknowledgements

I thank God above all for this achievement. Getting here was not an easy task, and I know that if it were not for the grace of Christ in my life, giving me strength to overcome the most difficult moments, I would have achieved nothing.

I express my deepest gratitude to the Federal University of Paraíba, especially to the Center for Exact and Natural Sciences, for providing a stimulating academic environment conducive to learning. The infrastructure, resources, and support made available were essential to my education throughout the master's program, enabling me to acquire the knowledge and experience necessary for the completion of this work. Without this support, the development of this research would not have been possible.

I am deeply grateful to my supervisor, Prof. Dr. Fábio Leal de Melo Dahia, for his invaluable guidance, constant support, and unrestricted availability throughout this journey. His dedicated attention, insightful supervision, and exemplary patience were essential for the development of this work. I also extend my gratitude to Prof. Dr. Thierry Marcelino Passerat de Silans for his excellent supervision during my teaching internship; to Prof. Dr. Valdir Barbosa Bezerra, Prof. Dr. Eugênio Ramos Bezerra de Mello, Prof. Dr. Albert Petrov, and to the other faculty members of the Physics Department who contributed to my academic training.

I am grateful to my mother, Maria de Fátima da Silva, and my father, Ivan Costa Lima, who have always done their best to ensure that I had access to a quality education; to my brother Ivisson; to my dear nephew Davi Lucas; to my brothers and sisters in the church, who have always supported me, prayed for me and my family, and lent me a helping hand whenever I needed it.

I am eternally grateful to my grandfather Inácio and my aunt Antônia (in memoriam), who always encouraged me to study and always believed in my potential.

I am grateful to all the friends and colleagues I met during my academic journey at the Federal University of Paraíba: Gessiane, Fernando, João Artur, Kaio, Joelson Max, Pedro Formiga, Elvis, Igor, Leilane, Lameque, Luan, Eliza, Ana Rafaely, Gabriel Bandeira, João Elias, as well as the other colleagues, for the moments of support and friendship throughout this arduous journey.

Finally, I thank the Coordenação de Aperfeiçoamento de Pessoal de Nível Superior (CAPES) for the financial support.

"Those who sow with tears will reap with songs of joy."

Psalms 126:5

Resumo

Neste trabalho, apresentamos uma introdução às teorias de dimensões extras de grande escala, nas quais são previstas modificações da interação gravitacional em escalas microscópicas. Em seguida, revisamos a teoria do decaimento alfa proposta por Gamow e a estendemos para um cenário que envolve dimensões extras, com o objetivo de investigar a influência de um potencial gravitacional modificado sobre a taxa de decaimento de núcleos radioativos pesados. No regime de curtas distâncias, quando comparadas ao tamanho das dimensões extras, a modificação do potencial gravitacional é descrita por um comportamento do tipo lei de potência. No regime de longas distâncias, por outro lado, empregam-se correções do tipo Yukawa para caracterizar o comportamento assintótico do potencial gravitacional modificado. Com base nesse arcabouço teórico e utilizando dados experimentais de decaimento alfa de 158 isótopos, foi possível estabelecer vínculos experimentais independentes para os parâmetros dos modelos de dimensões extras por meio da técnica de ajuste por mínimos quadrados. Em nossa análise, consideramos cenários com diferentes números de dimensões extras e impusemos restrições aos principais parâmetros do modelo, incluindo o raio nuclear efetivo, o comprimento de Planck em dimensões extras e os parâmetros associados à parametrização de Yukawa.

Palavras-chave: Dimensões Extras de Grande Escala; Modelos de Branas; Interação Gravitacional Modificada; Decaimento Alfa.

Abstract

In this work, we present an introduction to large extra-dimensional theories, in which modifications to the gravitational interaction are predicted at microscopic scales. We then review Gamow's theory of alpha decay and extend it to a scenario involving extra dimensions, with the aim of investigating the influence of a modified gravitational potential on the decay rate of heavy radioactive nuclei. In the short-distance regime, compared with the size of the extra dimensions, the modification of the gravitational potential is described by a power-law behavior. In the long-distance regime, on the other hand, Yukawa-type corrections are employed to characterize the asymptotic behavior of the modified gravitational potential. Based on this theoretical framework, and using experimental alpha-decay data from 158 isotopes, we were able to establish independent experimental constraints on the parameters of extra-dimensional models by means of a least-squares fitting technique. In our analysis, scenarios with different numbers of extra dimensions were considered, and constraints were imposed on the main model parameters, including the effective nuclear radius, the higher-dimensional Planck length, and the parameters associated with the Yukawa parametrization.

Keywords: Large Extra Dimensions; Brane-world Models; Modified Gravitational Interaction; Alpha Decay.

List of Figures

List of Tables

List of Abbreviations and Acronyms

ADD Arkani-Hamed–Dimopoulos–Dvali

CERN European Organization for Nuclear Research

EWT Electroweak Theory

GNL Geiger–Nuttall Law

GR General Relativity

GUT Grand Unified Theory

KK Kaluza–Klein

LED Large Extra Dimensions

LHC Large Hadron Collider

NIST National Institute of Standards and Technology

NNDC National Nuclear Data Center

NSPU Natural System of Planck Units

PSF Poisson Summation Formula

QCD Quantum Chromodynamics

QED Quantum Electrodynamics

QFD Quantum Flavordynamics

RCS Reduced Chi-Squared

TISE Time-Independent Schrödinger Equation

TOE Theory of Everything

UGC Universal Gravitational Constant

WKB Wentzel–Kramers–Brillouin

List of Symbols

α	Interaction amplification factor in Yukawa parameterization
$\Gamma(x)$	Gamma function
γ	Gamow factor of alpha decay
γ'	Modified Gamow factor
δ	Number of compact extra dimensions
ε_0	Vacuum permittivity
λ	Characteristic length scale in Yukawa parameterization
λ_m	Linear mass density (mass per unit length)
μ	Reduced mass
ρ	Matter density (mass per unit three-volume)
$\rho^{(n)}$	Matter density (mass per unit n-volume)
σ	Standard deviation
τ	Lifetime of the radioactive nucleus
Φ_m	Flux of gravitational field through a given surface
$\phi(r)$	Gravitational potential
$\tilde{\chi}^2$	Reduced chi-squared
ψ	Eigenfunction of the particle
A_{d}	Mass number of the daughter nucleus
A_{p}	Mass number of the parent nucleus
A_α	Mass number of the emitted alpha particle
c	Speed of light in vacuum
G	Universal Gravitational Constant
$G^{(D)}$	Gravitational Constant in a spacetime with D dimensions
$\hbar$	Reduced Planck Constant
I_0	Modified Bessel function of the first kind
K_α	Kinetic energy of the alpha particle
l_{P}	Planck length in four dimensions

$l_{\mathrm{P}}^{(D)}$ Planck length in a spacetime with D dimensions

m_{d} Mass of the daughter nucleus

M_{P} Mass of the parent nucleus

m_{P} Planck mass in four dimensions

$m_{\mathrm{P}}^{(D)}$ Planck mass in a spacetime with D dimensions

m_{α} Mass of the alpha particle

p Momentum

Q Energy released during alpha decay

R_1, R_2, R_3 Free parameters of the nucleus radius

r_1 Radius of the parent nucleus

r_2 Turning point

r_2' Modified turning point

$T_{1/2}$ Half-life of the radioactive nucleus

Th Thorium

t_{P} Planck time in four dimensions

$t_{\mathrm{P}}^{(D)}$ Planck time in a spacetime with D dimensions

U Uranium

v Average speed of the particle

V_{C} Coulomb potential energy

V_{G} Gravitational potential energy

Z_{d} Atomic number of the daughter nucleus

Contents

1 Introduction

Below, we present a brief historical overview of the key ideas that led to the development of extra-dimensional theories in modern physics, from their earliest formulations to more recent models. We then offer a concise discussion of the alpha-decay process, highlighting the theoretical aspects essential for its understanding. Next, we explain how this nuclear phenomenon can be employed as a sensitive tool to probe potential signatures of extra dimensions. Finally, we conclude the chapter by outlining the general structure and organization of the remainder of this work.

1.1 A Historical Overview of Higher-Dimensional Physics

The idea that physical space might contain dimensions beyond the three observable spatial ones has a long history, deeply intertwined with the development of modern theoretical physics. The first attempts to incorporate extra dimensions emerged in the early 20th century, motivated by the ambitious goal of unifying the fundamental interactions. In the 1910s, the Finnish physicist Gunnar Nordström proposed a relativistic theory of gravitation that, although based on a scalar field rather than a tensorial metric, introduced for the first time the idea of an additional spatial dimension as a means to unify gravitation and electromagnetism [1–4]. In 1914, he suggested that a five-dimensional universe, with the extra dimension not directly observable, could reproduce in four observable dimensions both gravitational effects and the behavior of electromagnetic fields. This proposal is now recognized as the first extra-dimensional theory in physics.

Although Nordström's theory of gravitation was considered experimentally inferior to Albert Einstein's General Relativity (GR), since it failed to predict phenomena such as the bending of light observed during the 1919 solar eclipse, his work marked a crucial step in the idea that physical laws could emerge from a spatial structure richer than the one directly perceived. Nordström's pioneering contribution paved the way for more robust and mathematically consistent developments, most notably the celebrated Kaluza–Klein (KK) theory.

Until the beginning of the 20th century, the two fundamental interactions known were gravitational and electromagnetic interactions. It was during this period that, in 1919, Theodor Kaluza sent Einstein a manuscript (published two years later, in 1921) presenting the results of a hypothesis he had developed [5–7]. In this work, Kaluza proposed a unification of Maxwell's theory of electromagnetism with Einstein's GR, showing that both could be incorporated elegantly into a single mathematical framework if one assumed the existence of an additional spatial dimension in the universe. To make this extension viable, Kaluza introduced the so-called cylindricity condition, according to which no physical quantity should depend explicitly on the fifth coordinate. This assumption removed unwanted degrees of freedom and allowed Maxwell's field equations to be recovered exactly from the extended five-dimensional metric.

A few years later, in 1926, Oskar Klein made a crucial contribution to the model by suggesting that this fifth dimension is unobservable because it is compactified into a tiny circle of extremely small radius, on the order of the Planck length [8, 9]. Klein's proposal not only provided a geometric explanation for the invisibility of the extra dimension but also introduced a quantum character to the theory, consistent with the recent advances of the time by Heisenberg and Schrödinger. In doing so, it transformed the Kaluza–Klein model into the first concrete example of unification between fundamental interactions through compactified extra dimensions.

Since then, two additional fundamental interactions have joined the set of forces known in physics: the weak and strong nuclear forces. The weak interaction acts between subatomic particles and is responsible for various radioactive decay processes, also playing a significant role in phenomena such as nuclear fission and fusion. Although there exists a formulation known as Quantum Flavordynamics (QFD) to describe it, this terminology is rarely used, as the weak force is more comprehensively treated within the Electroweak Theory (EWT). Its range is extremely short, smaller than the diameter of a proton, which confines it essentially to the subatomic domain [10, 11].

In turn, the strong interaction is described by Quantum Chromodynamics (QCD) and constitutes the mechanism responsible for keeping protons and neutrons bound within atomic nuclei, as well as for confining quarks and gluons inside hadrons. Its typical range, about 10^{-15} meters, is very small, but its intensity is extraordinarily high: it is the most powerful of the four fundamental interactions, being approximately 100 times stronger than electromagnetism, 10^6 times stronger than the weak interaction, and 10^{38} times stronger than gravitation [12–14].

With the establishment of these two new forces in the 20th century, it became natural to seek a theory capable of unifying all fundamental interactions within a single conceptual framework. Over the decades, several proposals emerged, and a remarkable feature shared by many of these theories is the requirement, or at least the possibility, of extra dimensions beyond the four familiar dimensions of spacetime. As an example, one may mention string theory, in which elementary particles are not treated as point-like objects but rather as vibrating one-dimensional entities.

String theory was originally developed in the late 1960s and early 1970s as an attempt, ultimately never fully successful, to describe hadrons, that is, subatomic particles such as protons and neutrons that interact via the strong nuclear force. However, with the development of QCD, it became clear that the strong interaction could be more accurately explained by a gauge field theory based on the dynamics of quarks and gluons [15]. This advance shifted string theory away from its initial purpose; nonetheless, the theory gained new momentum when it was discovered that its mathematical structure provides a natural framework for incorporating quantum gravity. Since then, modern formulations of the theory, including superstring theory and M-theory, have required the existence of compactified extra spatial dimensions, which allow for a consistent description of the fundamental interactions together with supersymmetry and the presence of the graviton as a vibrational mode of the string [16–18].

These theories robustly predict that spacetime contains more dimensions than the four perceived macroscopically, thereby establishing a deep connection between the quest for unification and the notion of additional dimensions. By the end of the 20th century, the idea that extra dimensions might play a fundamental role in the structure of the universe reemerged even more explicitly in the so-called brane theories, in which our observable universe is interpreted as a "hypersurface" embedded in a higher-dimensional space. This conceptual framework culminated, among other developments, in the Arkani-Hamed–Dimopoulos–Dvali (ADD) model [19, 20], which explores large extra dimensions as a possible solution to the hierarchy problem.

In 1998, the celebrated ADD model was proposed, redefining in an innovative way the role of extra dimensions in fundamental physics. This model embraces the idea of Large Extra Dimensions (LED) and suggests that, instead of being compactified at imperceptibly small scales, the additional dimensions could in fact be relatively large, which would drastically modify gravity at short distances. According to the ADD proposal, only gravity could propagate freely through the multidimensional bulk, while the other interactions (such as those described by QED) remain confined to our 3-D brane (or 3-brane). The supplementary space, consisting of the additional dimensions, is assumed to be compact and characterized by a radius of size R. This hypothesis leads to an important consequence: the theory predicts that, due to the existence of the extra dimensions, the gravitational force would be amplified at length scales much smaller than R, potentially producing deviations from the inverse-square law of gravitation [21, 22]. Depending on the specific features of the model considered, this characteristic scale could be as large as the submillimeter range without conflicting with observational data.

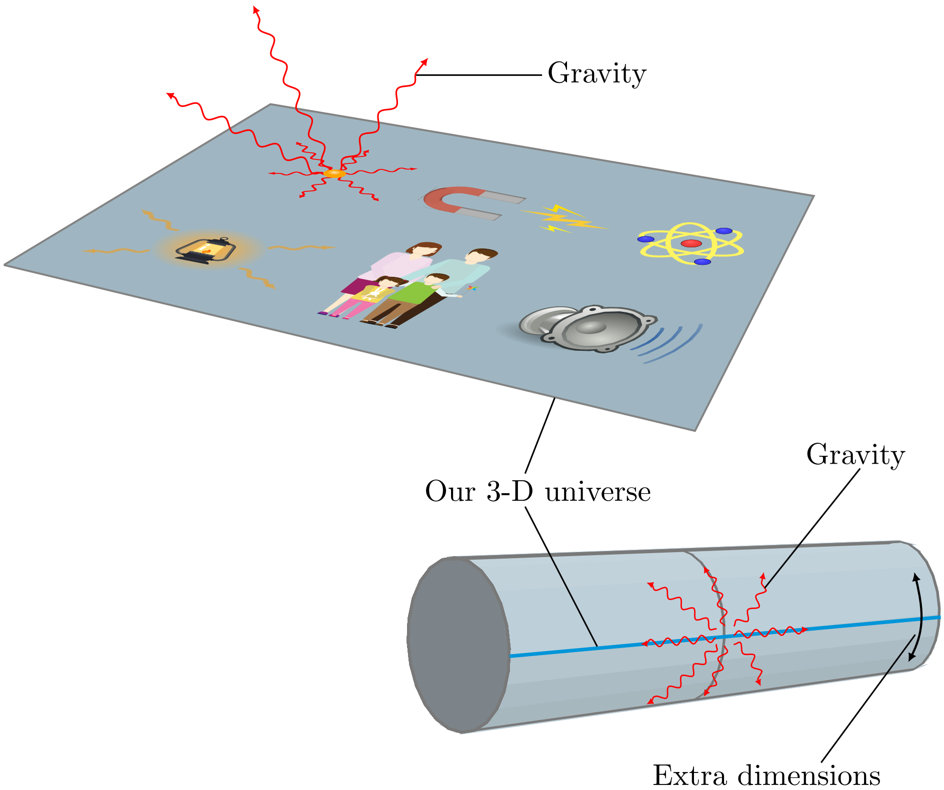

Figure 1 – Our universe may exist on a brane, or membrane, within the extra dimensions. The blue line running along the cylinder (below, on the right) and the horizontal plane represent our three-dimensional universe, to which all known particles and forces, except gravity, are confined. Gravity (red lines) propagates through all dimensions. The extra dimensions can be as large as submillimeter scales without conflicting with any existing observations. Source: Own authorship.

The approach introduced by the ADD model opened the door to revisiting long-standing problems discussed within the scientific community using new theoretical tools, such as the hierarchy problem between the electroweak scale and the Planck scale [19, 20, 23–25]. In this context, the ADD model emerges as a realistic candidate for progress toward a Grand Unified Theory (GUT) or even a Theory of Everything (TOE), by embedding gravitation and the fundamental interactions within the same higher-dimensional framework.

The Fig. 1 illustrates this concept: our three-dimensional brane appears as a sheet, where matter and all non-gravitational forces are confined, whereas the extra dimension is depicted as a cylinder through which gravity freely escapes, propagating across the additional directions of the higher-dimensional spacetime. This geometric, and simultaneously physical, perspective revived debates concerning the nature of space and gravity, and provided the foundation for a wide range of proposals and experiments aiming to search for signatures of extra dimensions at submillimeter, atomic, and nuclear scales.

In Section 2.1, we return to the discussion of the ADD model, exploring some of its features in a bit more detail.

1.2 The Alpha Decay Process

Radioactive atoms that are nuclear-level unstable naturally tend to seek greater stability. To reach a more stable state, such atoms emit particles and/or electromagnetic radiation through processes known as decay reactions. When these processes occur spontaneously, the emitted radiation may be of three types: alpha, beta, or gamma.

Heavy nuclei can undergo alpha decay. A representative example is the reaction $\mathrm{U}^{238} \to \mathrm{Th}^{234} + \alpha$, illustrated in Fig. 2, in which Uranium-238 transforms into the isotope Thorium-234 while emitting an alpha particle (a Helium nucleus). In the alpha-decay model developed by G. Gamow [26], the parent nucleus (in this case, Uranium) is described as a bound state composed of the daughter nucleus (Th) and the alpha particle. The kinetic energy of the emitted particle, E, which consists of two protons and two neutrons, is determined by the difference between the rest masses before and after the reaction, according to the relativistic expression $E = mc^2$ [27]. Inside the nucleus, the alpha particle is subject to an attractive nuclear interaction, which Gamow approximated using a square potential well. Outside the nucleus, however, it experiences a repulsive Coulomb interaction of electrostatic origin.

The energy E of the alpha particle is lower than the height of the potential barrier, which would classically prevent it from appearing outside the nucleus. Nonetheless, due to quantum tunneling, there exists a finite probability for the alpha particle to penetrate the barrier and be emitted. The lifetime of the parent nucleus is directly connected to this transmission probability, which can be estimated by applying the WKB approximation to the Schrödinger equation [28–32].

The central objective of this work is to investigate possible indications of the existence of extra dimensions within the nuclear domain, examining how such dimensions could modify the alpha decay of radioactive nuclei. To this end, we extend Gamow's theory of alpha decay by introducing an additional modification to the potential energy experienced by the alpha particle. This modification arises from the brane-world framework (the ADD model), which predicts an enhancement of the gravitational potential in a spacetime containing extra spatial dimensions.

In the context of the brane-world model, the extra-dimensional space is compact and characterized by a radius of size R. In this scenario, the gravitational interaction becomes stronger at short distances ($r \ll R$), and the modified gravitational potential acquires a power-law behavior proportional to $1/r^{1+\delta}$, where δ is the number of extra dimensions. Conversely, at large distances compared to R, the gravitational potential must asymptotically return to its usual three-dimensional form. Nevertheless, even in this regime, additional gravitational corrections appear. To first approximation, these corrections can be described by a Yukawa-type term, $\alpha \exp(-r/\lambda)$, where α represents the interaction-strength amplification factor and λ defines the characteristic length scale at which the correction becomes significant [22, 33, 34].

Thus, in a scenario with extra dimensions, in addition to the Coulomb interaction, the only one considered in Gamow's original model, the modified gravitational interaction between the emitted alpha particle and the residual nucleus must also be taken into account during the decay process. Based on this, we aim to determine the effects of this additional term on the decay rate of radioactive nuclei and to compare the resulting theoretical predictions with the available experimental data. This analysis will enable us to establish independent constraints on the parameters of extra-dimensional models.

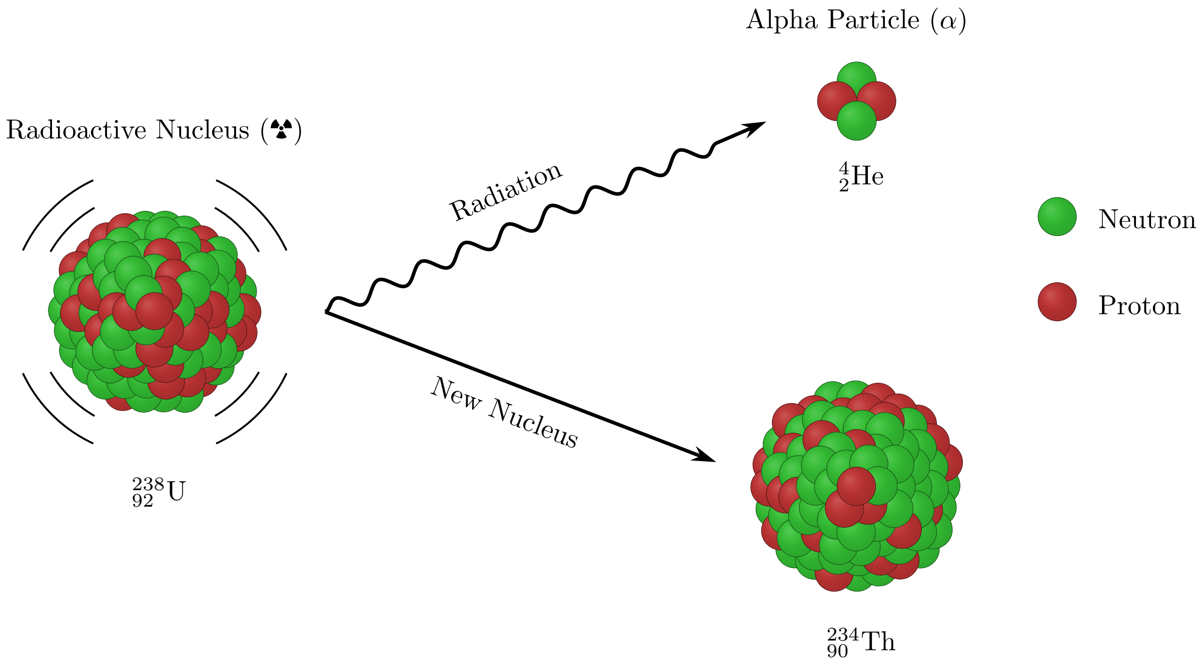

Figure 2 – Illustrative scheme of the alpha decay process. The unstable radioactive nucleus emits an alpha particle, composed of two protons and two neutrons, which escapes the nuclear potential barrier through the quantum tunneling effect. This process results in the formation of a lighter and generally more stable daughter nucleus. Source: Own authorship.

We have divided the content of this work into six chapters. In Chapter 1, *Introduction*, we present a brief historical overview of several prominent theories in physics that involve extra dimensions, as well as an introduction to the alpha-decay process. The objectives of the present work are also outlined within this context. In Chapter 2, *Theoretical Foundations*, we provide a review of the foundations of large-extra-dimension theories, with particular emphasis on the ADD model. In Chapter 3, *The Alpha Decay Theory*, we revisit the theory of alpha decay as originally proposed by G. Gamow. In Chapter 4, *Alpha Decay in Extra-Dimensional Scenarios*, we extend Gamow's theory to frameworks involving extra dimensions and present the possible effects that such dimensions may have on the alpha-decay process. In Chapter 5, *Results and Discussion*, using experimental alpha-decay data from 158 isotopes, we obtain independent experimental constraints on the parameters of the model and discuss the results obtained. Finally, in Chapter 6, *Conclusion*, we provide a brief summary of the material presented throughout the work and discuss the relevance of the results obtained. We also conclude with perspectives for future research in this area.

2 Theoretical Foundations

In this chapter, we present the main theoretical elements that form the foundation of this work. We begin with a brief introduction to the ADD model, highlighting its motivations and fundamental assumptions. Next, we analyze the gravitational potential in different scenarios with extra dimensions, including the study of long-distance corrections that arise in such contexts.

Furthermore, we discuss the relationship between the Planck length and the gravitational constant in spaces of different dimensionalities, as well as how the Newtonian gravitational constant relates to the gravitational constant in models with compact extra dimensions. Finally, we address the hierarchy problem and examine the possible size of the extra dimensions by analyzing representative scenarios and their physical implications.

2.1 The ADD Model

The Arkani-Hamed–Dimopoulos–Dvali (ADD) model is one of the most well-known large extra dimension models in the literature. Historically, the ADD model can be regarded as one of the most influential proposals within the framework of theories that seek to extend our understanding of gravity beyond the traditional paradigm [20, 25]. Unlike the original Kaluza–Klein (KK) formulation, in which the extra dimensions are compactified at scales close to the Planck length and thus inaccessible to direct observation with current technologies, the ADD model allows these additional dimensions to have significantly larger compactification radii, potentially reaching the submillimeter scale without conflicting with the available experimental data [5, 8, 9].

One of the main motivations for the development of this model is related to the so-called hierarchy problem, which concerns the large disparity between the electroweak scale and the Planck scale [19]. In the context of the ADD model, this discrepancy can be alleviated by the hypothesis that gravity propagates freely through the extra dimensions, while matter and the other fundamental fields remain confined to a four-dimensional hypersurface, commonly referred to as a brane. This feature significantly alters the strength of gravitational interaction at small scales, suggesting that gravity could manifest itself much more intensely than predicted by Newton's law in regimes below the compactification radius.

This possibility opens the way for both theoretical and experimental investigations. On the one hand, the amplification of the gravitational potential at microscopic scales could introduce observable effects in systems where gravity is usually negligible, such as in the atomic or nuclear domain. On the other hand, the absence of empirical evidence for such deviations provides experimental bounds on the parameters of the model, namely the number of additional dimensions and the value of the compactification radius. In this sense, the ADD model stands out not only for offering an elegant alternative to the hierarchy problem, but also for providing a theoretical framework that can be directly confronted with experimental results at scales accessible to current technologies, such as, for example, the LHC experiments at CERN [22].

2.2 Gravitational Potential in an Extradimensional Space

The analysis of gravitational potentials in different scenarios is an essential tool for understanding how gravity may manifest itself at scales beyond the usual regime. By first establishing the Newtonian gravitational potential in a four-dimensional spacetime, we can then explore its generalization to an arbitrary number of spatial dimensions. In this section, we intend to discuss the effects of extra dimensions on the gravitational field.

Let us therefore begin our investigation by reviewing the calculation of the usual Newtonian gravitational potential in a (3+1)-dimensional spacetime. According to the differential form of Gauss's law for gravity, the gravitational field $\mathbf{g}$ satisfies the following relation:

$$\nabla \cdot \mathbf{g} = -4\pi G\rho, \tag{2.1}$$

where ρ is the matter density (mass per unit three-volume) and G is the Universal Gravitational Constant (UGC).

Suppose we are interested in determining the gravitational field of a body of mass m with spherical symmetry [33–35]. Consider a body of mass m, a *two-sphere* $S^2(r)$ of radius r centered around the massive body and a *three-ball* $B^3(r)$ whose boundary is the two-sphere[1]. In the three-dimensional space $\mathbb{R}^3$ with coordinates x_1, x_2 and x_3, we can write the two-sphere and the three-ball as follows:

$$S^2(r) = x_1^2 + x_2^2 + x_3^2 = r^2, \tag{2.2}$$

and

$$B^3(r) = x_1^2 + x_2^2 + x_3^2 \leq r^2. \tag{2.3}$$

According to the divergence theorem, we have

$$\int_{B^3} (\nabla \cdot \mathbf{g}) d^3V = \oint_{S^2} \mathbf{g} \cdot d\mathbf{A} = \Phi_m, \tag{2.4}$$

where Φ_m is the flux of $\mathbf{g}$ through S^2. Let's first solve the integral in S^2. Using spherical symmetry, we have

$$\oint_{S^2} \mathbf{g} \cdot d\mathbf{A} = g_r \text{vol}(S^2(r)) = g_r 4\pi r^2, \tag{2.5}$$

where g_r is the radial component of the gravitational field $\mathbf{g}$ and $\text{vol}(S^2(r)) = 4\pi r^2$ is the area of the sphere. On the other hand, calculating the integral of the matter density over the entire volume of the three-ball, we obtain the total mass of the body

$$\int_{B^3} (\nabla \cdot \mathbf{g}) d^3V = -4\pi G m. \tag{2.6}$$

Thus, from Eqs.(2.5) and (2.6), using spherical coordinates, we can write the gravitational field in (3+1)-dimensions as:

$$\mathbf{g}(r) = -\frac{Gm}{r^2}\hat{\mathbf{r}}. \tag{2.7}$$

From the gravitational field $\mathbf{g}$, we can determine the potential using the fact that $\mathbf{g}$ is a conservative field. Thus, we can write $\mathbf{g}$ in terms of the gradient of a scalar field:

$$\mathbf{g} = -\nabla\phi. \tag{2.8}$$

[1] The superscripts in S or B denote the dimensionality of the space in question.

Using spherical coordinates in Eq.(2.8), we can obtain the scalar field:

$$\phi(r) = -\frac{Gm}{r}. \tag{2.9}$$

The Eq.(2.9) is the usual form for the Newtonian gravitational potential of a body of mass m in a four-dimensional spacetime [33–37].

Now, we can use analogous reasoning and generalize this method to calculate the gravitational potential generated by a body of mass m in a space with non-compact $(n+1)$ dimensions[2]. So, suppose we have an $(n-1)$-sphere $S^{n-1}(r)$ of radius r centered on a body of mass m, where $S^{n-1}(r)$ is the contour of an n-ball $B^n(r)$. In this more general scenario, we can define spheres and balls as subspaces of $\mathbb{R}^n$:

$$S^{n-1}(r) = x_1^2 + x_2^2 + \cdots + x_n^2 = r^2, \tag{2.10}$$

and

$$B^n(r) = x_1^2 + x_2^2 + \cdots + x_n^2 \leq r^2. \tag{2.11}$$

Just like for the usual case, we will also have a Gaussian law for gravity in this scenario[3]:

$$\nabla \cdot \mathbf{g} = -4\pi G^{(n+1)} \rho^{(n)}, \tag{2.12}$$

where $\rho^{(n)}$ is the matter density (mass per unit n-volume) and $G^{(n+1)}$ is the $(n+1)$-dimensional gravitational constant [33, 34]. Let's compute the integral of Eq.(2.12) over the n-ball. Then,

$$\int_{B^n} (\nabla \cdot \mathbf{g}) d^n V = -4\pi G^{(n+1)} \int_{B^n} \rho^{(n)} d^n V. \tag{2.13}$$

The integral of the matter density $\rho^{(n)}$ over the entire volume of B^n gives us the total mass of the body. Now, applying the divergence theorem to this scenario,

$$\int_{B^n} (\nabla \cdot \mathbf{g}) d^n V = \oint_{S^{n-1}} \mathbf{g} \cdot d\mathbf{A} = \Phi_m, \tag{2.14}$$

where Φ_m is the flux of $\mathbf{g}$ through S^{n-1}. Evaluating the integral in S^{n-1}, we obtain

$$\oint_{S^{n-1}} \mathbf{g} \cdot d\mathbf{A} = g(r) \mathrm{vol}(S^{n-1}(r)), \tag{2.15}$$

where $\mathrm{vol}(S^{n-1}(r))$ is the volume of the $(n-1)$-sphere. With a little effort, it is possible to show that the volume of the $(n-1)$-sphere is (see Appendix A):

$$\mathrm{vol}(S^{n-1}(r)) = \frac{2\pi^{n/2} r^{n-1}}{\Gamma(n/2)}. \tag{2.16}$$

With this, we obtain the gravitational field generated by a mass m in a space with n spatial dimensions:

$$\mathbf{g}(r) = g(r)\hat{\mathbf{r}} = -\frac{2\Gamma\left(n/2\right) G^{(n+1)} m}{\pi^{\frac{n}{2}-1} r^{n-1}} \hat{\mathbf{r}}. \tag{2.17}$$

[2] By *"non-compact dimensions"* we mean that the extra dimensions are "large" compared to the Planck length.

[3] It is important to emphasize that, even in a scenario with an arbitrary number of spatial dimensions, physical quantities such as gravitational field and gravitational potential maintain the same physical units as in the usual scenario.

Now, let's derive the gravitational potential for this scenario. To do this, we will start with the fundamental theorem for gradients, which tells us that the line integral of the gradient of a scalar function F evaluated along a path C is given by:

$$\int_{\mathbf{a}}^{\mathbf{b}} (\nabla F) \cdot d\mathbf{l} = F(\mathbf{b}) - F(\mathbf{a}). \tag{2.18}$$

Just as for the classical case, Eq.(2.8), let's do $\mathbf{g}(r) = -\nabla\phi$. Considering infinity as the initial position and r as the final position, we can write the following:

$$-\int_{\infty}^{r} (\nabla\phi) \cdot d\mathbf{l} = -[\phi(r) - \phi(\infty)] = -\phi(r). \tag{2.19}$$

Using Eq.(2.17), we obtain the expression for the gravitational potential for long distances generated by a mass immersed in a space of non-compact $(n{+}1)$ dimensions:

$$\phi(r) = -\frac{2\Gamma\left(n/2\right) G^{(n+1)} m}{(n-2)\pi^{\frac{n}{2}-1} r^{n-2}}. \tag{2.20}$$

In Eq.(2.17), we can notice that for small values of r, the magnitude of the gravitational field grows faster than in Eq.(2.7). Thus, Eq.(2.17) tells us that the gravitational interaction becomes stronger for short distances, when compared to Eq.(2.7).[4]

2.3 Gravitational Potential in a Space with One Extra-Compact Dimension

Let's explicitly determine the potential generated by a mass located in a multi-dimensional universe in which the extra dimension is compact. Up to this point, all our analysis of the gravitational potential in scenarios with additional dimensions has not taken into account the characteristic size of the extra dimensions. Now, however, we shall treat these dimensions as finite, that is, compact. This condition, introduced in the ADD model, has important implications for both the theory and its phenomenology. In this new context, we assume that the extra dimension is compact with the topology of a circle of radius l (illustration on the left in Fig. 3). Since gravity is the only interaction able to access these dimensions, the behavior of its field lines will be determined by the resulting cylindrical geometry [35, 38].

Let us then consider an observer located at a point O, who observes a mass m placed at a certain position in the universe. Due to the compact nature of the extra dimension, the gravitational field lines originating from m travel around the circular space, winding repeatedly until they reach the observer at point O. To visualize this situation more clearly, imagine cutting the cylinder and unrolling it (see Fig. 4). We then obtain a plane with the mass m placed at its center, while the observer at O is reached by several field lines originating from the mass. From the observer's point of view, the gravitational influence does not come from a single mass alone, but rather from multiple masses (m_1, m_2,$\cdots$) distributed along a line passing through the center of the original mass (illustration at the center of Fig. 3). We refer to these apparent sources observed by O as *topological images*. The minimum separation between two successive images is $2\pi l$, which corresponds precisely to the size of the compact extra dimension. If the observer is located at a distance

[4] Note that for $(n{+}1)$ non-compact dimensions we will have $(n{-}3)$ supplementary dimensions.

R much larger than l, the images will appear to be uniformly and continuously distributed along the extra dimension (illustration on the right in Fig. 3). In this approximation, Gauss's law can be applied to calculate the field generated by this effective line of masses.

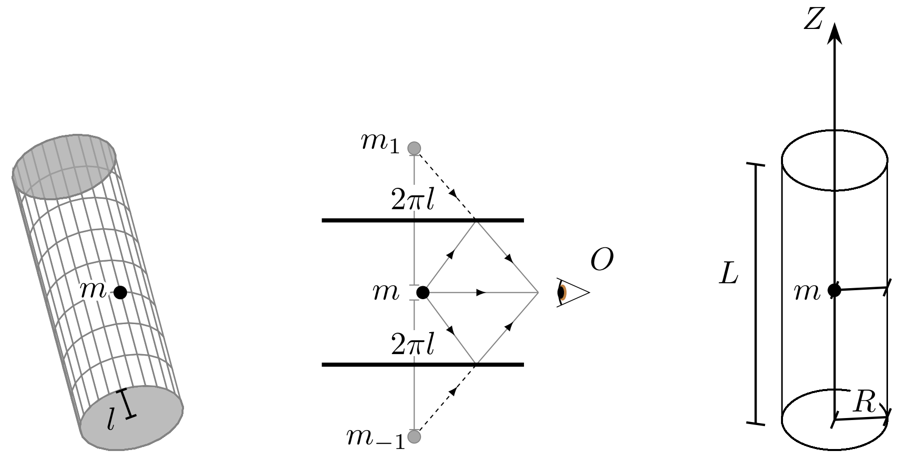

Figure 3 – *On the left:* mass located at a specific point in the universe. *In the center:* the cylinder is represented by an "open" space with topological identifications (the observer feels the influence of several topological images). *On the right:* a situation where the observer is very distant from the mass and observes a virtually continuous distribution of these masses. Source: Own authorship.

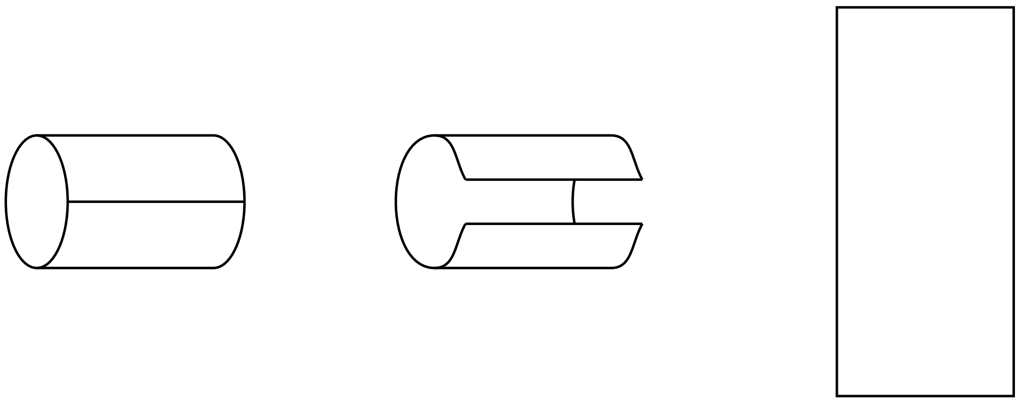

Figure 4 – Cylinder cut laterally, with the cut in the direction of its length. Source: Own authorship.

The situation we will investigate can be represented as shown in the illustration on the right of Fig. 3, where the masses are located on the axis representing the extra dimension. The cylinder of height L corresponds to our Gaussian 'surface'. Since the space we are considering has four spatial dimensions, the base of the cylinder is a sphere, rather than a circle. Let us consider again Gauss's law, where the area integral is performed over the Gaussian surface:

$$\oint \mathbf{g} \cdot d\mathbf{A} = -4\pi G^{(5)} M_{\text{int}}, \tag{2.21}$$

where M_{int} is the amount of topological mass contained in the continuous line within the cylindrical Gaussian surface. Since the topological masses are arranged along a line that passes through each of them, and since $2\pi l$ is the separation distance between one topological image and another, the number of charges contained in a line of length L (length of the cylindrical Gaussian surface) will be equal to $L/2\pi l$. Therefore, we have that M_{int} will be:

$$M_{\text{int}} = \frac{L}{2\pi l} m. \tag{2.22}$$

By the symmetry of the matter distribution, we have that $\mathbf{g}$ is perpendicular to the additional dimension and will depend only on the radial coordinate R of the Gaussian surface, where, in turn, we will have: $\mathbf{g} \cdot d\mathbf{A} = g(R)dA$. With this, Eq.(2.21) becomes

$$\oint g(R)dA = -4\pi G^{(5)} \left(\frac{L}{2\pi l} m \right). \tag{2.23}$$

Since the base of the Gaussian "cylinder" we are dealing with is a sphere, its total area will then be $(4\pi R^2)L$. Therefore,

$$g(R)(4\pi R^2)L = -4\pi G^{(5)} \left(\frac{L}{2\pi l} m \right). \tag{2.24}$$

Isolating the radial component $g(R)$, we can write the gravitational field for this scenario as follows:

$$\mathbf{g}(R) = -\frac{G^{(5)} m}{2\pi l R^2} \hat{\mathbf{e}}_R. \tag{2.25}$$

To calculate the gravitational potential, we will proceed in the same way as we did in Eq.(2.8), where we now have $\mathbf{g}(R) = -\nabla\phi(R)$. Thus, using Eq.(2.18),

$$-\int_{\infty}^{R} (\nabla\phi(R')) \cdot d\mathbf{l} = -\left[\phi(R) - \phi(\infty)\right] = -\phi(R). \tag{2.26}$$

On the other hand, we have

$$\int_{\infty}^{R} \mathbf{g}(R') \cdot d\mathbf{l} = -\int_{\infty}^{R} \frac{G^{(5)} m}{2\pi l R'^2} dR' = \frac{G^{(5)} m}{2\pi l R}. \tag{2.27}$$

With this, the gravitational potential will be

$$\phi(R) = -\frac{G^{(5)} m}{2\pi l R}. \tag{2.28}$$

Let's make the following identification[5]:

$$G^{(4)} = \frac{G^{(5)}}{2\pi l}. \tag{2.29}$$

Therefore, we will have

$$\phi(R) = -\frac{G^{(4)} m}{R}. \tag{2.30}$$

Thus, for large distances compared to the radius of the extra dimension ($R \gg l$), we recover the expression valid in (3+1)-dimensional space [36–38].

[5] We will see this type of relationship in more detail in the next sections.

2.4 Long-Distance Gravitational Potential Corrections in the Brane Model

In this section, we will determine an exact expression for the gravitational potential produced by a mass m in a universe with compact extra dimensions. To do this, we will use the method of topological images (or image masses), analogous to what we saw in the previous section, which will allow us to obtain the total gravitational potential generated by each of the system's image masses in the covering space [33, 34]. In this case, we will assume that the extra dimensions are compact and have a circular topology, with R as their radius.

In the brane model, the gravitational potential produced by a particle of mass m in a space with δ non-compact extra dimensions, $\mathbb{R}^3 \times \mathbb{R}^\delta$, follows a power law:

$$\phi(\mathbf{r}) = -\frac{G^{(4+\delta)}m}{|\mathbf{r}-\mathbf{r}'|^{1+\delta}}, \tag{2.31}$$

where $\mathbf{r}'$ is the vector that locates the mass m and the gravitational constant for this scenario we are denoting by $G^{(4+\delta)}$.

For a supplementary space with δ compact extra dimensions, $\mathbb{R}^3 \times (S^1 \times \cdots \times S^1)$, the location of any point in this space is determined from its coordinates $(x, y, z, w_1, \cdots, w_\delta)$. So, in this case, we will have to consider the extra parameters $(w_1, w_2, \cdots, w_\delta)$ to determine the position of the mass m in the supplementary space. The three-brane would correspond to the space in which $w_i = 0,\ i = 1, \cdots \delta$. Suppose the mass m is at the origin. Then, its position vector will be given by:

$$\mathbf{r}' = (0, 0, 0, 0, \cdots, 0). \tag{2.32}$$

The effect of the compact topology S^1 on the potential can be simulated by means of a set of image masses that are scattered in the supplementary space $\mathbb{R}^\delta$. These images must be separated from each other by a certain distance that is equal to an integer multiple of the length of the extra dimension ($2\pi R$), that is, for each image mass, its position will be given by:

$$\mathbf{r}'_{p_1,\cdots,p_\delta} = (0, 0, 0, 2\pi R p_1, \cdots, 2\pi R p_\delta), \tag{2.33}$$

where each p_i is an integer. The image mass $(p_1, \cdots, p_\delta)$ produces a gravitational potential of the form:

$$\phi_{p_1,\cdots,p_\delta}(\mathbf{r}) = -\frac{G^{(4+\delta)}m}{\left|\mathbf{r}-\mathbf{r}'_{p_1,\cdots,p_\delta}\right|^{1+\delta}}. \tag{2.34}$$

In ambient space, the position vector of any point is given by

$$\mathbf{r} = (x, y, z, w_1, ..., w_\delta). \tag{2.35}$$

With this, we can calculate the norm of the vector $\mathbf{r} - \mathbf{r}'_{p_1,\cdots,p_\delta}$:

$$\left|\mathbf{r}-\mathbf{r}'_{p_1,\cdots,p_\delta}\right|^2 = \left(\mathbf{r}-\mathbf{r}'_{p_1,\cdots,p_\delta}\right)\cdot\left(\mathbf{r}-\mathbf{r}'_{p_1,\cdots,p_\delta}\right). \tag{2.36}$$

Calculating the inner product in the above equation, it is simple to show that

$$\left|\mathbf{r}-\mathbf{r}'_{p_1,\cdots,p_\delta}\right| = \left[s^2 + \sum_{j=1}^{\delta}\left(w_j - (2\pi R)p_j\right)^2\right]^{1/2}, \tag{2.37}$$

where $s^2 = x^2 + y^2 + z^2$. Thus, the potential generated by a single topological mass will be:

$$\phi_{p_1,\cdots,p_\delta}(\mathbf{r}) = -\frac{G^{(4+\delta)}m}{\left[s^2 + \sum_{j=1}^{\delta}\left(w_j - (2\pi R)p_j\right)^2\right]^{\frac{1+\delta}{2}}}. \tag{2.38}$$

Therefore, the resulting gravitational potential is the sum of the potentials produced by each of the image masses:

$$\phi(\mathbf{r}) = -\sum_{(p_1,\cdots,p_\delta)\in\mathbb{Z}^\delta} \frac{G^{(4+\delta)}m}{\left[s^2 + \sum_{j=1}^{\delta}\left(w_j - (2\pi R)p_j\right)^2\right]^{\frac{1+\delta}{2}}}. \tag{2.39}$$

Now, let's explore Eq.(2.39) and obtain a simpler expression for the gravitational potential. First, note that the function given above is periodic in the directions transverse to the brane, that is, with respect to the coordinates w. Thus, we can represent it as a Fourier series.

So, based on this line of reasoning, we will proceed with our analysis starting from the *Poisson Summation Formula* (see Appendix B). As an example, let's first consider a function $F(t)$. Suppose that F is a periodic function and therefore can be represented by means of a Fourier series as follows:

$$F(t) = \sum_{p=-\infty}^{+\infty} f(t + pT) = \sum_{k=-\infty}^{+\infty} g(k/T)\frac{e^{\frac{2\pi ikt}{T}}}{T}, \tag{2.40}$$

where T is the period of F and $g(k/T)$ is the Fourier transform of $f(t)$ [39, 40]. With this, we can make an analogy between Eq.(2.40) and our gravitational potential in the brane model, through the following relations:

$$\phi_{p_1,\cdots,p_\delta}(\mathbf{r}) \equiv f(t + pT) \quad \text{and} \quad \phi(\mathbf{r}) \equiv F(t). \tag{2.41}$$

Thus, from Eq.(2.38),

$$f(t + pT) \equiv -\frac{G^{(4+\delta)}m}{\left[s^2 + \sum_{j=1}^{\delta}\left(w_j - (2\pi R)p_j\right)^2\right]^{\frac{1+\delta}{2}}}. \tag{2.42}$$

In our case, we have $t \equiv w_j$ and $T \equiv 2\pi R$.[6] Therefore, the expression for $f(t) \equiv f(w_1, \cdots, w_\delta)$ will be:

$$f(w_1, ..., w_\delta) \equiv -\frac{G^{(4+\delta)}m}{\left[s^2 + \sum_{j=1}^{\delta} {w_j}^2\right]^{\frac{1+\delta}{2}}} = -\frac{G^{(4+\delta)}m}{\left[s^2 + w^2\right]^{\frac{1+\delta}{2}}}, \tag{2.43}$$

where $w^2 = |\mathbf{w}|^2 = \sum_{j=1}^{\delta} {w_j}^2$. So, being $\phi(\mathbf{r}) \equiv F(w_1, \cdots, w_\delta)$,

$$\begin{aligned}
\phi(\mathbf{r}) &= \sum_{p=-\infty}^{+\infty} f(w_1 + p(2\pi R), \cdots, w_\delta + p(2\pi R)) \\
&= \sum_{k_1=-\infty}^{+\infty} \cdots \sum_{k_\delta=-\infty}^{+\infty} g\left(\frac{k_1}{2\pi R}, \cdots, \frac{k_\delta}{2\pi R}\right) \frac{e^{\frac{2\pi ik_1 w_1}{2\pi R}}}{2\pi R} \cdots \frac{e^{\frac{2\pi ik_\delta w_\delta}{2\pi R}}}{2\pi R} \\
&= \sum_{k_1=-\infty}^{+\infty} \cdots \sum_{k_\delta=-\infty}^{+\infty} g\left(\frac{k_1}{2\pi R}, \cdots, \frac{k_\delta}{2\pi R}\right) \frac{e^{\frac{i(k_1 w_1 + \ldots + k_\delta w_\delta)}{R}}}{(2\pi R)^\delta},
\end{aligned}$$

[6] Without loss of generality, let us consider that T is the same for all extra dimensions.

or simply

$$\phi(\mathbf{r}) = \sum_{\mathbf{k}\in\mathbb{Z}^\delta} g\left(\frac{k_1}{2\pi R}, \cdots, \frac{k_\delta}{2\pi R}\right) \frac{e^{\frac{i\mathbf{k}\cdot\mathbf{w}}{R}}}{(2\pi R)^\delta}, \tag{2.44}$$

where

$$g\left(\frac{k_1}{2\pi R}, \cdots, \frac{k_\delta}{2\pi R}\right) = \int_{\mathbb{R}^\delta} f(w_1, \cdots, w_\delta) e^{-\frac{i\mathbf{k}\cdot\mathbf{w}}{R}} d^\delta w. \tag{2.45}$$

Using the relation in Eq.(2.43), we have that

$$\phi(\mathbf{r}) = -\frac{G^{(4+\delta)}m}{(2\pi R)^\delta} \sum_{\mathbf{k}\in\mathbb{Z}^\delta} e^{\frac{i\mathbf{k}\cdot\mathbf{w}}{R}} \int_{\mathbb{R}^\delta} \frac{e^{-\frac{i\mathbf{k}\cdot\mathbf{w}}{R}}}{\left[s^2+w^2\right]^{\frac{1+\delta}{2}}} d^\delta w. \tag{2.46}$$

This is the simplified expression in Cartesian coordinates for the modified potential of Eq.(2.39).

Now, let's explore Eq.(2.46) a little further to obtain an expression for the modified gravitational potential in spherical coordinates. First, recall that in three-dimensional spherical coordinates (x, y, z) the radial coordinate r of a point is related to the Cartesian coordinates of that point by the following expression: $r^2 = x^2 + y^2 + z^2$.

In Eq.(2.46), the integral is expressed in terms of $w_1, w_2, \cdots, w_\delta$, and we know that $w^2 = w_1^2 + w_2^2 + \cdots + w_\delta^2$. So, w is our radial variable for spherical coordinates in δ dimensions. In turn, the angular variables will be $\theta_1, \theta_2, \cdots, \theta_{\delta-1}$. Using Appendix C, it is straightforward to show that Eq.(2.46) will be:

$$\phi(\mathbf{r}) =$$
$$-\frac{G^{(4+\delta)}m}{(2\pi R)^\delta} \sum_{\mathbf{k}\in\mathbb{Z}^\delta} e^{\frac{i\mathbf{k}\cdot\mathbf{w}}{R}} \int_0^{2\pi}\int_0^{\pi}...\int_0^{\pi}\int_0^{\infty} \frac{e^{-\frac{i\mathbf{k}\cdot\mathbf{w}}{R}}}{\left[s^2+w^2\right]^{\frac{1+\delta}{2}}} w^{\delta-1}\sin^{\delta-2}\theta_1 \sin^{\delta-3}\theta_2 ... \sin\theta_{\delta-2} dw d\theta_1 d\theta_2 ... d\theta_{\delta-1}.$$

Computing the $\delta - 2$ outer integrals[7], as in Appendix C, by setting $\mathbf{k}' = -\mathbf{k}/R$ in the above equation, and assuming that θ_1 is the angle between $\mathbf{k}'$ and $\mathbf{w}$, we will have:

$$\phi(\mathbf{r}) = -\frac{G^{(4+\delta)}m}{(2\pi R)^\delta} \sum_{\mathbf{k}\in\mathbb{Z}^\delta} e^{-i\mathbf{k}'\cdot\mathbf{w}} \mathrm{vol}(S^{\delta-2}) \int_0^\pi \int_0^\infty \frac{e^{ik'w\cos\theta_1}}{\left[s^2+w^2\right]^{\frac{1+\delta}{2}}} w^{\delta-1}\sin^{\delta-2}\theta_1 dw d\theta_1. \tag{2.47}$$

The integrals in the above equation can be solved by doing a separation:

$$\int_0^\pi \int_0^\infty \frac{e^{ik'w\cos\theta_1}}{\left[s^2+w^2\right]^{\frac{1+\delta}{2}}} w^{\delta-1}\sin^{\delta-2}\theta_1 dw d\theta_1 = \int_0^\infty \frac{w^{\delta-1}}{\left[s^2+w^2\right]^{\frac{1+\delta}{2}}} dw \int_0^\pi e^{ik'w\cos\theta_1} \sin^{\delta-2}\theta_1 d\theta_1. \tag{2.48}$$

We can use the following identity[8] for the second integral in Eq.(2.48):

$$J_\nu(z) = \frac{\left(\frac{z}{2}\right)^\nu}{\Gamma\left(\nu+\frac{1}{2}\right)\Gamma\left(\frac{1}{2}\right)} \int_0^\pi e^{\pm iz\cos\theta} \sin^{2\nu}\theta d\theta\ , \quad \mathrm{Re}\left(\nu+\frac{1}{2}\right) > 0,$$

[7] The integrals involving the variables $\theta_2, \theta_3, \cdots, \theta_{\delta-1}$.

[8] Ch. 8, formula 8.411 (7) on page 912 of Ref. [41].

where J_ν is the Bessel function of the first kind, $\delta - 2 \equiv 2\nu \rightarrow \nu \equiv \frac{\delta}{2} - 1$, $z \equiv k'w$ and $\theta \equiv \theta_1$. Thus, we will have

$$J_{\frac{\delta}{2}-1}\left(k'w\right) = \frac{\left(\frac{k'w}{2}\right)^{\frac{\delta}{2}-1}}{\Gamma\left(\frac{\delta-1}{2}\right)\Gamma\left(\frac{1}{2}\right)} \int_0^\pi e^{ik'w\cos\theta_1} \sin^{\delta-2}\theta_1 d\theta_1.$$

In our case, we will use the following identities:

$$\Gamma\left(\frac{\delta-1}{2}\right) = \frac{2\pi^{\frac{\delta-1}{2}}}{\mathrm{vol}(S^{\delta-2})} \quad \text{and} \quad \Gamma\left(\frac{1}{2}\right) = \pi^{1/2}.$$

Thus, our integral can be written as follows:

$$\int_0^\pi e^{ik'w\cos\theta_1} \sin^{\delta-2}\theta_1 d\theta_1 = J_{\frac{\delta}{2}-1}\left(k'w\right) \frac{2^{\delta/2}\pi^{\delta/2}w^{1-\delta/2}}{k'^{\frac{\delta}{2}-1}\mathrm{vol}(S^{\delta-2})}.$$

Substituting this result into Eq.(2.48), we will have

$$\int_0^\infty \frac{w^{\delta-1}}{\left[s^2+w^2\right]^{\frac{1+\delta}{2}}} dw \int_0^\pi e^{ik'w\cos\theta_1} \sin^{\delta-2}\theta_1 d\theta_1 = \frac{2^{\delta/2}\pi^{\delta/2}}{k'^{\frac{\delta}{2}-1}\mathrm{vol}(S^{\delta-2})} \int_0^\infty \frac{w^{\delta/2}}{\left[s^2+w^2\right]^{\frac{1+\delta}{2}}} J_{\frac{\delta}{2}-1}\left(k'w\right) dw. \tag{2.49}$$

Now, to evaluate the integral of Eq.(2.49), we will use the following identity[9]:

$$\int_0^\infty \frac{x^{\nu+1}}{\left(a^2+x^2\right)^{\nu+3/2}} J_\nu(bx) dx = \frac{\pi^{1/2}b^\nu}{2^{\nu+1}ae^{ab}\Gamma\left(\nu+\frac{3}{2}\right)}\ ,\ \mathrm{Re}(a) > 0,\ b > 0,\ \mathrm{Re}(\nu) > -1, \tag{2.50}$$

where we can identify the following terms: $a \equiv s$, $b \equiv k'$, $x \equiv w$ and $\nu \equiv \frac{\delta}{2} - 1$. Then,

$$\int_0^\infty \frac{w^{\frac{\delta}{2}}}{\left[s^2+w^2\right]^{\frac{1-\delta}{2}}} J_{\frac{\delta}{2}-1}(k'w) dw = \frac{\pi^{1/2}k'^{\frac{\delta}{2}-1}}{2^{\delta/2}se^{sk'}\Gamma\left(\frac{1+\delta}{2}\right)}. \tag{2.51}$$

Substituting this result into Eq.(2.49), we will have

$$\int_0^\infty \frac{w^{\delta-1}}{\left[s^2+w^2\right]^{\frac{1+\delta}{2}}} dw \int_0^\pi e^{ik'w\cos\theta_1} \sin^{\delta-2}\theta_1 d\theta_1 = \frac{\pi}{se^{sk'}}. \tag{2.52}$$

Thus, the modified gravitational potential $\phi(\mathbf{r})$ of Eq.(2.47) can be rewritten as:

$$\phi(\mathbf{r}) = -\frac{G^{(4+\delta)}m}{s} \frac{\pi\mathrm{vol}(S^{\delta-2})}{(2\pi R)^\delta} \sum_{\mathbf{k}\in\mathbb{Z}^\delta} e^{-sk'} e^{-i\mathbf{k}'\cdot\mathbf{w}}. \tag{2.53}$$

For simplicity, we consider $w = |\mathbf{w}| = 0$ and thus we have[10]

$$\phi(\mathbf{r}) = -\frac{G^{(4+\delta)}m}{r} \frac{\pi\mathrm{vol}(S^{\delta-2})}{(2\pi R)^\delta} \sum_{\mathbf{k}\in\mathbb{Z}^\delta} e^{-rk'}. \tag{2.54}$$

[9] Ch. 6, formula 6.565 (3) on page 678 of Ref. [41].

[10] In this case, setting $|\mathbf{w}| = 0$ means we have $r = s$.

where $r^2 = x^2 + y^2 + z^2$ and $k'^2 = (k_1/R)^2 + \cdots + (k_\delta/R)^2$. Now, to obtain the usual expression of the Newtonian gravitational potential with correction terms, we conclude that we must relate $G^{(4+\delta)}$ to the Universal Gravitational Constant G as follows:

$$G \equiv \frac{G^{(4+\delta)}\pi \mathrm{vol}(S^{\delta-2})}{(2\pi R)^\delta}. \tag{2.55}$$

Thus, we are left with the following expression:

$$\phi(\mathbf{r}) = -\frac{Gm}{r} \sum_{\mathbf{k}\in\mathbb{Z}^\delta} e^{-rk'}. \tag{2.56}$$

This is the gravitational potential on the brane assuming that the brane is embedded in a higher-dimensional space with δ compact extra dimensions. As a first approximation, we can calculate the correction to the potential by taking only the largest terms, that is, the terms with $k' = 0$ and $k' = 1$. By doing this, with some mathematical manipulations, it is simple to show that the result obtained will be:

$$\phi(r) = -\frac{Gm}{r}\left(1 + \alpha e^{-r/R}\right). \tag{2.57}$$

The factor α in Eq.(2.57) concerns degeneracy[11], where in this case $\alpha = 2\delta$. The above expression is known in the literature as a *Yukawa-type expression*[12,13] [22, 32, 42–44]. Note that for $r \gg R$, the usual Newtonian potential is recovered. The Yukawa parameter would give us the correction for long distances. In turn, for short distances the potential would be given by Eq.(2.31).

Now, returning to Eq.(2.56), we can explore the summation to obtain a simpler expression for the exact potential. To do this, we rewrite the summation as follows[14]:

$$\sum_{\mathbf{k}\in\mathbb{Z}^\delta} e^{-rk'} = \sum_{\mathbf{k}\in\mathbb{Z}^\delta} e^{-\frac{rk}{R}} \longrightarrow \sum_{k\in\mathbb{Z}} e^{-\frac{rk}{R}} = \sum_{k=-\infty}^{+\infty} \left(e^{-\frac{r}{R}}\right)^k. \tag{2.58}$$

It is possible to show that the summation in the second equality above can be expressed by $\coth(r/2R)$. Therefore, the exact expression for the gravitational potential at long distances generated by all the image masses of a system considering a single compact extra dimension will be given by:

$$\phi(r) = -\frac{Gm}{r}\coth\left(\frac{r}{2R}\right). \tag{2.59}$$

2.5 Gravitation and Planck's Length

Gravitation is formally described by Einstein's general theory of relativity, in which the geometry of spacetime is determined by the distribution of energy and momentum.

---

11 Here, degeneracy means the number of compact extra dimensions that have the same compactification radius R.

12 Named after Japanese physicist Hideki Yukawa, who was the first Japanese to receive a Nobel Prize in Physics (1949) for formulating the meson hypothesis, based on theoretical work on nuclear forces. His work pioneered the study of strong interactions.

13 Over the years, the Yukawa form has appeared so frequently in studies of natural phenomena that it has come to be called *Yukawa Parameterization.*

14 For simplicity, we have considered the particular case of just a single compact extra dimension.

However, in situations where gravitational fields are weak and the velocities involved are small compared to the speed of light, the Newtonian formulation of gravity provides an adequate description. In such regimes, the simplicity of the Newtonian framework allows one to explore certain fundamental concepts in a more accessible way, without resorting to the full apparatus of general relativity.

In this context, beginning in this section and extending through Sections 2.6 and 2.7, we will employ Newtonian gravity to discuss the definition of the Planck length in different scenarios and to examine how the gravitational constants are modified when additional spatial dimensions are compactified. Although conducted within a simplified framework, this analysis reveals essential properties of gravity in multidimensional settings and provides valuable insights that also extend to the full relativistic treatment.

Newton's law of gravitation in four dimensions states that the force of attraction between two masses m_1 and m_2 separated by a distance r is given by

$$|\mathbf{F}^{(4)}| = \frac{Gm_1m_2}{r}, \tag{2.60}$$

where G is the Universal Gravitational Constant. Moreover, by analyzing the units not only of G, but also of the physical constants c and $\hbar$, we observe that they can be expressed in terms of three fundamental quantities: length, mass, and time:

$$[G] = \frac{L^3}{MT^2}, \quad [c] = \frac{L}{T} \quad \text{and} \quad [\hbar] = \frac{ML^2}{T}. \tag{2.61}$$

The numerical value for the constant G is determined experimentally [34]:

$$G = 6.674 \times 10^{-11}\frac{\mathrm{m}^3}{\mathrm{kg}\cdot\mathrm{s}^2}. \tag{2.62}$$

Thus, the three fundamental constants can be written as follows:

$$G = 6.674 \times 10^{-11}\frac{\mathrm{m}^3}{\mathrm{kg}\cdot\mathrm{s}^2}, \quad c = 2.998 \times 10^{8}\frac{\mathrm{m}}{\mathrm{s}}, \quad \hbar = 1.055 \times 10^{-34}\frac{\mathrm{kg}\cdot\mathrm{m}^2}{\mathrm{s}}. \tag{2.63}$$

In the Natural System of Planck Units (NSPU), the physical quantities G, c and $\hbar$ have unitary values, being written as:

$$G = 1\frac{l_{\mathrm{P}}^3}{m_{\mathrm{P}}t_{\mathrm{P}}^2}, \quad c = 1\frac{l_{\mathrm{P}}}{t_{\mathrm{P}}}, \quad \hbar = 1\frac{m_{\mathrm{P}}l_{\mathrm{P}}^2}{t_{\mathrm{P}}}, \tag{2.64}$$

where l_{P}, m_{P}, and t_{P} are the Planck length, Planck mass, and Planck time, respectively. With some mathematical manipulation, it is possible to show that the values of l_{P}, m_{P}, and t_{P} are:

$$l_{\mathrm{P}} = \sqrt{\frac{G\hbar}{c^3}} = 1.616 \times 10^{-33}\mathrm{cm}, \tag{2.65a}$$

$$m_{\mathrm{P}} = \sqrt{\frac{\hbar c}{G}} = 2.176 \times 10^{-5}\mathrm{g}, \tag{2.65b}$$

$$t_{\mathrm{P}} = \sqrt{\frac{G\hbar}{c^5}} = 5.391 \times 10^{-44}\mathrm{s}. \tag{2.65c}$$

These are the values of quantities in the NSPU in four-dimensional spacetime. Since these quantities involve the constants G, which represents gravitation, c (Special Relativity), and $\hbar$ (quantum), it is commonly assumed that these values represent the scale at which the effects of quantum gravity can be important.

2.6 Planck's Quantities in Various Dimensions

The Planck length in Eq.(2.65a) is a four-dimensional quantity. However, we can calculate the Planck length, and the other Planck quantities, in any dimension using the constants $G^{(D)}$, c, and $\hbar$. Here, D represents the number of dimensions of spacetime. To determine the Planck length in multiple dimensions, we must first determine the units of $G^{(D)}$. Consider the gravitational potential ϕ of a mass distribution in (3+1)-dimensions [33–35]:

$$\nabla^2\phi = 4\pi G\rho, \tag{2.66}$$

where ρ is the volumetric mass density, that is, the mass per unit three-volume. Analogously to this case, for a space with D dimensions, we will have:

$$\nabla^2\phi^{(D)} = 4\pi G^{(D)}\rho^{(D-1)}, \tag{2.67}$$

where $\rho^{(D-1)}$ is the mass per unit $(D-1)$-volume. Since the units of $\nabla^2\phi$ and $\nabla^2\phi^{(D)}$ must be the same, by comparing the units of Eqs.(2.66) and (2.67), we conclude that $G^{(D)}$ must have the following units:

$$[G^{(D)}] = L^{D-4}[G]. \tag{2.68}$$

Since the constants G, c and $\hbar$ have unitary values in the NSPU, and this relation is valid for both $(3+1)$ dimensions and D dimensions, with some algebraic manipulations, we can rewrite the Planck quantities in D dimensions in terms of l_P, m_P and t_P:

$$\left(l_\text{P}^{(D)}\right)^{D-2} = l_\text{P}^2\frac{G^{(D)}}{G}, \tag{2.69a}$$

$$\left(m_\text{P}^{(D)}\right)^{D-2} = \left(\frac{m_\text{P}^{D-3}}{c^{D-4}}\right)^2\frac{G^{D-3}}{G^{(D)}}, \tag{2.69b}$$

$$\left(t_\text{P}^{(D)}\right)^{D-2} = t_\text{P}^2\frac{G^{(D)}}{Gc^{D-4}}. \tag{2.69c}$$

where $l_\text{P}^{(D)}$, $m_\text{P}^{(D)}$ and $t_\text{P}^{(D)}$ are the Planck length, Planck mass and Planck time in D dimensions, respectively.

2.7 Gravitational Constants and Compactification

If string theory is correct, our world indeed possesses a multidimensional structure. In this context, the fundamental theory of gravity is formulated in a multidimensional space, characterized by a specific value of the corresponding Planck length. Since, however, we observe only four dimensions, the additional ones must be compactified into a space of small volume. The effective four-dimensional Planck length arises from this configuration and depends both on the volume of the extra dimensions and on the value of the multidimensional Planck length.

These observations indicate that the effective four-dimensional Planck length, whose known value is on the order of 10^{-33} cm, may not coincide with the fundamental Planck length defined in higher-dimensional theories. In this scenario, the fundamental Planck length could be significantly larger than the value traditionally associated with the four-dimensional world. In this section, we investigate how compactification influences the gravitational constants.

Our goal is to understand how the gravitational constant in four dimensions, $G^{(4)}$ (which we shall denote simply by G), relates to the gravitational constant in five dimensions, $G^{(5)}$. For an effectively four-dimensional spacetime to exist, it is necessary to assume the compactification of one spatial dimension. The size of this extra dimension plays a fundamental role in the relation between the gravitational constants. To analyze this effect clearly, we consider a five-dimensional spacetime in which one of the dimensions forms a circle of radius R. In this framework, starting from the value of $G^{(5)}$, we aim to derive the corresponding expression for G.

Let (x^1, x^2, x^3) denote the three spatial dimensions of infinite extent, and x^4 a compactified dimension of circumference $2\pi R$ (Fig. 5). A uniform ring of total mass M is placed along the circle at $x^1 = x^2 = x^3 = 0$, establishing a constant mass distribution along the x^4 dimension [34]. We are interested in the gravitational potential $\phi^{(5)}$ generated by this distribution. In this case, the gravitational potential does not depend on the coordinate x^4. The total mass M can then be expressed as:

$$\text{total mass} = M = 2\pi R\lambda_m, \tag{2.70}$$

where λ_m denotes the linear mass density (mass per unit length).

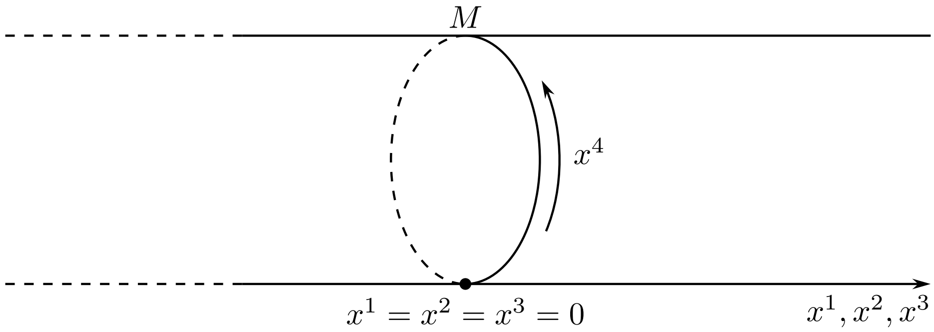

Figure 5 – A universe with four spatial dimensions, where the extra dimension x^4 is compactified into a circle of radius R. A uniform ring with total mass M extends along this compactified direction. Source: Own authorship.

If we wanted to determine the mass density along x^4, Eq.(2.70) would be enough, since that is exactly what it tells us. However, since we want to determine the mass density considering (x^1, x^2, x^3, x^4), which we will denote by $\rho^{(4)}$, we have to look at the points that have mass and that relate to both (x^1, x^2, x^3) and x^4. As we can see in Fig. 5, of all the points, the only one that satisfies the criteria mentioned above is $x^1 = x^2 = x^3 = 0$.

Thus, given the configuration of the system in question, it is convenient that we try to express $\rho^{(4)}$ in terms of the Dirac delta function[15] [31, 39, 40, 45]. In this case, since the only point with mass that concerns (x^1, x^2, x^3, x^4) is the point $x^1 = x^2 = x^3 = 0$, and since λ_m is constant along x^4, we will have:

$$\rho^{(4)} = \lambda_m \delta(x^1)\delta(x^2)\delta(x^3). \tag{2.71}$$

[15] Recall that the delta function $\delta(x)$ can be viewed as a singular function whose value is zero except for $x = 0$ and such that the integral $\int_{-\infty}^{+\infty} dx\delta(x) = 1$. This integral implies that if x has units of length, then $\delta(x)$ has units of inverse length.

If we integrate $\rho^{(4)}$ over the whole space, we obtain Eq.(2.70):

$$\begin{aligned} \int \rho^{(4)} d^4V &= \int_{-\infty}^{+\infty}\int_{-\infty}^{+\infty}\int_{-\infty}^{+\infty}\int_{0}^{2\pi R} \lambda_m \delta(x^1)\delta(x^2)\delta(x^3) dx^4 dx^1 dx^2 dx^3 \\ &= 2\pi R \lambda_m \\ &= M. \end{aligned} \tag{2.72}$$

For the effectively four-dimensional observer the mass is point-like, and it is located at $x^1 = x^2 = x^3 = 0$. To find the mass density in (3+1) dimensions, $\rho^{(3)}$ (which we will denote simply by ρ), simply integrate $\rho^{(4)}$ over all x^4:

$$\rho = \int_0^{2\pi R} \rho^{(4)} dx^4 = M\delta(x^1)\delta(x^2)\delta(x^3). \tag{2.73}$$

From Eqs.(2.70), (2.71) and (2.73), we can note the following relationship:

$$\rho^{(4)} = \frac{1}{2\pi R}\rho. \tag{2.74}$$

Thus, we can apply the above relation to the calculation of gravitational potential in (4+1) dimensions. In this scenario, Poisson's equation for gravity will be:

$$\nabla^2 \phi^{(5)} = 4\pi G^{(5)} \rho^{(4)} = 4\pi G^{(5)} \frac{\rho}{2\pi R}. \tag{2.75}$$

As we noted earlier, $\phi^{(5)}$ is independent of x^4, so the above Laplacian is four-dimensional. Since the four-dimensional effective gravitational potential is $\phi^{(5)}$, the above equation takes the form of the gravitational equation in (3+1) dimensions:

$$\nabla^2 \phi = 4\pi G \rho. \tag{2.76}$$

Thus, from Eqs.(2.75) and (2.76), we conclude that

$$\frac{G^{(5)}}{G} = 2\pi R = l_C, \tag{2.77}$$

where l_C is the length of the extra compact dimension. The Eq.(2.77) shows us a relationship between the strength of the gravitational constants and the size of the extra dimension. This relationship can be generalized to the case where there is more than one extra dimension:

$$\frac{G^{(D)}}{G} = (l_C)^{D-4}, \tag{2.78}$$

where l_C is the common length of each of the extra dimensions. When the extra dimensions are compactified into circles of different radii, the expression on the right-hand side above must be replaced by the product of these lengths. This product corresponds to the volume V_C of the compact extra dimensions, so that

$$\frac{G^{(D)}}{G} = V_C. \tag{2.79}$$

2.8 Large Extra Dimensions and the Hierarchy Problem

One of the most persistent open questions in modern physics is the so-called hierarchy problem, which concerns the enormous disparity between the strengths of the fundamental interactions. Among these, gravity stands out as the weakest, exerting a negligible influence when compared with the other fundamental forces. Within the framework of brane-world models, this apparent weakness could be understood as a consequence of the existence of additional spatial dimensions, through which the gravitational field can propagate [19, 20, 25, 46]. In this context, the relationship between the higher-dimensional and the effective four-dimensional gravitational constants, and consequently between their associated Planck lengths, becomes of central importance.

From the results obtained in the previous sections, we have established the relation between the Planck length and the gravitational constant in different dimensions (Section 2.6), as well as how these gravitational constants are related under compactification (Section 2.7). We are therefore ready to determine how the fundamental Planck length in a higher-dimensional theory with compactification is related to the Planck length in the effectively four-dimensional theory.

Then, from Eqs.(2.69a) and (2.78), we can rewrite the length of the extra dimension, l_C, in terms of the Planck length in (3+1) dimensions, l_{P}, and in D dimensions, $l_{\mathrm{P}}^{(D)}$, as follows:

$$l_C = l_{\mathrm{P}}^{(D)} \left(\frac{l_{\mathrm{P}}^{(D)}}{l_{\mathrm{P}}} \right)^{\frac{2}{D-4}} . \tag{2.80}$$

The hierarchy problem can be addressed by assuming that the Planck length in a D-dimensional space is of the same order of magnitude as the electroweak scale, that is, $l_{\mathrm{P}}^{(D)} \sim 10^{-18}$ cm. By imposing this condition in Eq.(2.80), and considering that $l_{\mathrm{P}} \sim 10^{-33}$ cm, one obtains a relation between the size of the extra dimension, l_C, and the number of additional spatial dimensions:

$$l_C \sim 10^{-18} \left(10^{15}\right)^{\frac{2}{D-4}} \text{ cm.} \tag{2.81}$$

Considering the case of only one extra dimension ($D = 5$), we obtain $l_C \sim 10^7$ km, a distance greater than twenty times the average separation between the Earth and the Moon. Such a result makes the existence of only one additional dimension in this model untenable, since a dimension of that scale would certainly have already been detected experimentally. For the case of two extra dimensions ($D = 6$), the length of each additional dimension would be

$$l_C \sim 10^{-3} \text{ cm.} \tag{2.82}$$

This value is close to the smallest distance at which Newtonian gravitational laws have been accurately tested (the submillimeter scale) [22, 38], making a model with two extra dimensions compatible with experimental observations. Thus, any deviation from the inverse-square law at this scale could serve as strong evidence for the existence of additional dimensions.

It is noteworthy that as the number of extra dimensions increases, the characteristic length of each of them decreases. Even in the case of $D = 10$ (six extra dimensions), as proposed by superstring theories, the resulting size would be $l_C \sim 10^{-13}$ cm, still much larger than the Planck length l_{P}.

3 The Alpha Decay Theory

In the model proposed by G. Gamow, the alpha decay of radioactive nuclei is interpreted as the result of the quantum tunneling of the alpha particle through a potential barrier. This phenomenon, which has no analogue in classical physics, has become one of the most remarkable examples of the probabilistic nature of quantum mechanics. The analysis of tunneling is usually carried out using the WKB approximation, whose formulation and application will be discussed below.

3.1 The WKB Approximation

The Wentzel–Kramers–Brillouin (WKB) approximation is a sophisticated mathematical method used to obtain approximate solutions of differential equations in which the highest-order derivative is multiplied by a small parameter ε [28–30, 47]. Thus, for a differential equation of the form:

$$\varepsilon \frac{d^n y}{dx^n} + a(x)\frac{d^{n-1}y}{dx^{n-1}} + \cdots + k(x)\frac{dy}{dx} + m(x)y = 0, \tag{3.1}$$

we assume that the solution has the following form:

$$y(x) \sim \exp\left[\frac{1}{\delta}\sum_{n=0}^{\infty}\delta^n S_n(x)\right], \tag{3.2}$$

in the limit where $\delta \to 0$.

3.2 Application of the WKB Method to the Schrödinger's Equation

The WKB approximation can be used to solve the Schrödinger's equation and obtain its approximate solutions. Consider the Time-Independent Schrödinger Equation (TISE) in one dimension [32, 44, 48–51]:

$$-\frac{\hbar^2}{2m}\frac{d^2}{dx^2}\psi(x) + V(x)\psi(x) = E\psi(x). \tag{3.3}$$

For convenience, let's rewrite the eigenfunction ψ as an exponential of another function ϕ:

$$\psi(x) = e^{\phi(x)}. \tag{3.4}$$

Using the notation ϕ' for the first derivative of ϕ and ϕ'' for the second derivative, it is simple to show that Eq.(3.3) can be rewritten as:

$$\phi''(x) + \left(\phi'(x)\right)^2 = \frac{2m}{\hbar^2}\left[V(x) - E\right]. \tag{3.5}$$

Suppose ϕ is a complex function. Without loss of generality, we can separate ϕ' in terms of its real and imaginary parts, introducing the real functions A and B:

$$\phi'(x) = A(x) + iB(x), \tag{3.6}$$

where

$$\phi(x) = \int_{x_0}^{x} A(x')dx' + i\int_{x_0}^{x} B(x')dx'. \tag{3.7}$$

Since $\psi = e^{\phi}$, the amplitude of ψ will be

$$\exp\left[\int_{x_0}^{x} A(x')dx'\right].$$

On the other hand, the phase of ψ will be

$$\int_{x_0}^{x} B(x')dx'.$$

With this, Eq.(3.5) becomes

$$A'(x) + iB'(x) + [A(x) + iB(x)]^2 = \frac{2m}{\hbar^2}\left[V(x) - E\right]. \tag{3.8}$$

Separating the Eq.(3.8) into two parts (real and imaginary), we have

$$A'(x) + A^2(x) - B^2(x) = \frac{2m}{\hbar^2}\left[V(x) - E\right], \tag{3.9}$$

and

$$B'(x) + 2A(x)B(x) = 0. \tag{3.10}$$

Now, we can expand A and B into power series of $\hbar$ as follows:

$$A(x) = \frac{1}{\hbar}\sum_{n=0}^{\infty}\hbar^n A_n(x) \quad \text{and} \quad B(x) = \frac{1}{\hbar}\sum_{n=0}^{\infty}\hbar^n B_n(x).$$

To achieve a good classical limit, we must consider only the first terms in the expressions above, that is, we will consider the following approximations:

$$A(x) \approx \frac{1}{\hbar}A_0(x) + A_1(x) \quad \text{and} \quad B(x) \approx \frac{1}{\hbar}B_0(x) + B_1(x). \tag{3.11}$$

Therefore, from Eq.(3.9), we will have:

$$\frac{1}{\hbar^2}\left[A_0^2 - B_0^2\right] + \frac{1}{\hbar}\left[A_0' + 2A_0A_1 - 2B_0B_1\right] + A_1' + A_1^2 - B_1^2 = \frac{2m}{\hbar^2}\left[V - E\right]. \tag{3.12}$$

On the other hand, from Eq.(3.10), it results

$$\frac{2}{\hbar^2}A_0B_0 + \frac{1}{\hbar}\left[B_0' + 2A_0B_1 + 2A_1B_0\right] + B_1' + 2A_1B_1 = 0. \tag{3.13}$$

For very small $\hbar$, terms with some negative power of $\hbar$ will dominate. Thus, from Eqs.(3.12) and (3.13), we can equate terms with the same power in $\hbar$. For terms of order $\hbar^{-2}$:

$$A_0^2 - B_0^2 = 2m\left[V - E\right], \tag{3.14a}$$

$$A_0B_0 = 0. \tag{3.14b}$$

Likewise, for terms of order $\hbar^{-1}$:

$$A_0' + 2A_0A_1 - 2B_0B_1 = 0, \tag{3.15a}$$

$$B_0' + 2A_0B_1 + 2A_1B_0 = 0. \tag{3.15b}$$

Using Eqs.(3.14) and (3.15), we will consider two possible situations, which will lead us to solutions with completely different physical interpretations [31, 32, 44].

3.2.1 The "Classical" Region

Suppose the amplitude of ψ varies slowly compared to the phase. In this case, we can make $A_0 = 0$ in Eqs.(3.14) and, with that, we will have

$$B_0(x) = \pm\sqrt{2m\,[E - V(x)]}. \tag{3.16}$$

On the other hand, from Eq.(3.15a), considering $B_0 \neq 0$, we have that

$$B_1(x) = 0. \tag{3.17}$$

Replacing Eq.(3.16) in Eq.(3.15b) it is possible to show that

$$A_1(x) = \frac{d}{dx}\left\{\ln\,[2m\,(E - V(x))]^{-1/4}\right\}. \tag{3.18}$$

In this way, we will have

$$\begin{aligned} A(x) &\approx \frac{d}{dx}\left\{\ln\,[2m\,(E - V(x))]^{-1/4}\right\}, \\ B(x) &\approx \pm\frac{1}{\hbar}\sqrt{2m\,[E - V(x)]}. \end{aligned} \tag{3.19}$$

Now using Eqs.(3.7) and (3.4), we obtain the following solution for Schrödinger's equation:

$$\psi(x) \approx \frac{C_1}{\sqrt[4]{2m\,[E - V(x)]}} e^{\pm\frac{i}{\hbar}\int_{x_0}^{x}\sqrt{2m[E - V(x')]}dx'}, \tag{3.20}$$

where C_1 is constant. Note that, implicitly in Eq.(3.20), it is suggested that we must have $E > V$, which is precisely the type of situation studied in Classical Mechanics (see Fig. 6) [31, 36, 37].

3.2.2 The "Non-Classical" Region

Returning to Eqs.(3.14), suppose that the phase of ψ varies slowly compared to the amplitude. In this case, we can make $B_0 = 0$ and, from this, it follows that

$$A_0(x) = \pm\sqrt{2m\,[V(x) - E]}. \tag{3.21}$$

From Eqs.(3.15a) and (3.21), it is possible to obtain

$$A_1(x) = \frac{d}{dx}\left\{\ln\,[2m\,(V(x) - E)]^{-1/4}\right\}. \tag{3.22}$$

On the other hand, from Eq.(3.15b), assuming $A_0 \neq 0$,

$$B_1(x) = 0. \tag{3.23}$$

Summarizing all these results, we have

$$\begin{aligned} A(x) &\approx \pm\frac{1}{\hbar}\sqrt{2m\,[V(x) - E]} + \frac{d}{dx}\left\{\ln\,[2m\,(V(x) - E)]^{-1/4}\right\}, \\ B(x) &\approx 0. \end{aligned} \tag{3.24}$$

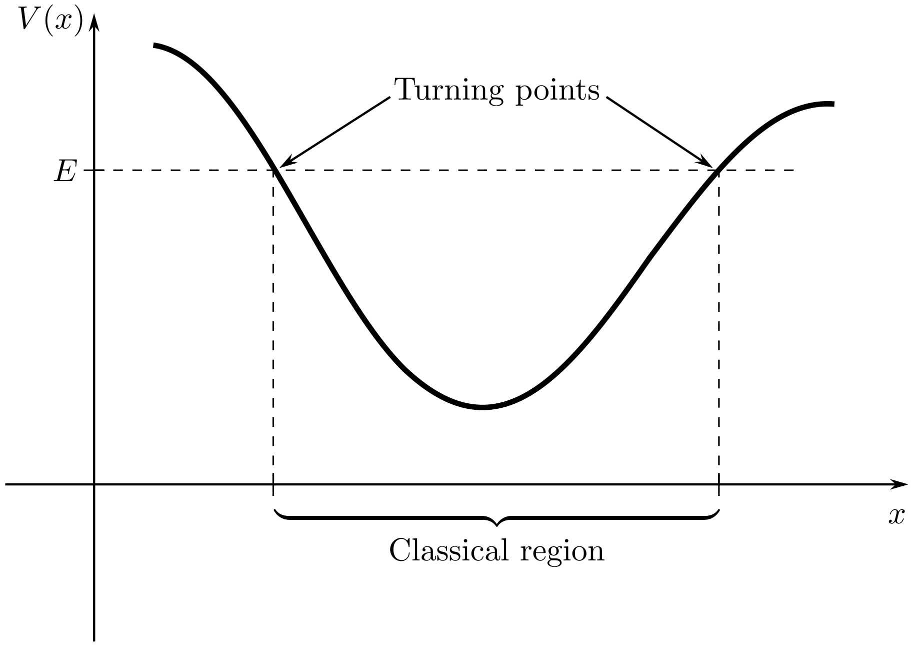

Figure 6 – Classically, the particle is limited to the region where $E \geq V(x)$. Source: Own authorship.

From Eqs.(3.7) and (3.4)), we find the following solution to Schrödinger's equation:

$$\psi(x) \approx \frac{C_2}{\sqrt[4]{2m\left[V(x)-E\right]}} e^{\pm\frac{1}{\hbar}\int_{x_0}^{x}\sqrt{2m[V(x')-E]}dx'}, \tag{3.25}$$

where C_2 is constant. Note that, unlike Eq.(3.20), the exponential is now real. The Eq.(3.25), implicitly, suggests that we must have $E < V$, a situation that, classically, is impossible, as the particle cannot have access to regions where its total energy is less than its own potential energy. This phenomenon is known in the literature as *Quantum Tunneling* [31, 32].

3.3 Quantum Tunneling

Consider the problem of a particle moving in the positive x-direction and scattering from a rectangular potential barrier with a ripple on top, as shown in Fig. 7. For regions of zero potential, the general solution of the Time-Independent Schrödinger Equation, Eq.(3.3), is written as a linear combination of complex exponentials. Thus, for the region $x < 0$, we will have the solution:

$$\psi(x) = Ae^{ikx} + Be^{-ikx}\ , \text{ with } k \equiv \frac{\sqrt{2mE}}{\hbar}. \tag{3.26}$$

In Eq.(3.26) the coefficient A is interpreted as the *amplitude of the incident wave* and B is the *amplitude of the reflected wave*. On the other hand, for the region $x > a$, the eigenfunction ψ will be composed of just a single term, as we assume that in this region there are no obstacles that could cause any reflection of the particle and, therefore, the term with the reflection amplitude is discarded.

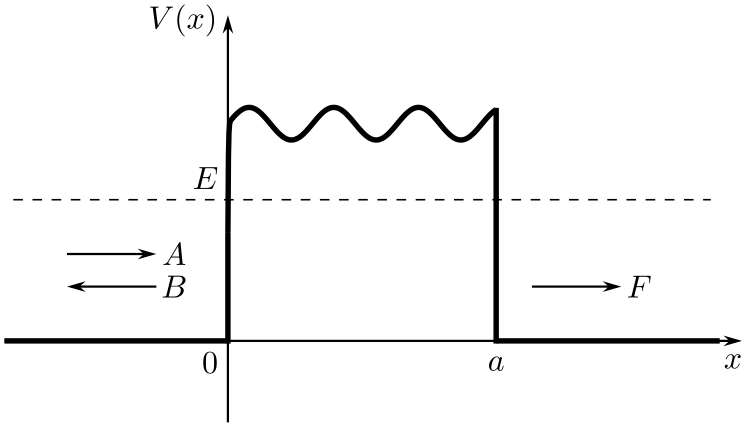

Figure 7 – Spreading of a rectangular barrier with a ripple on top. Source: Own authorship.

Therefore, for the region $x > a$, we will have

$$\psi(x) = Fe^{ikx}, \tag{3.27}$$

where F is the *amplitude of the transmitted wave.*

Although we have $E < V$, quantum mechanics says that there is a non-zero probability of the particle crossing the potential barrier and appearing on the other side (transmission probability). To determine the particle transmission probability, we first need to obtain the *probability current density*, which is calculated as:

$$J(x) = \frac{i\hbar}{2m}\left[\psi\frac{d}{dx}\psi^* - \psi^*\frac{d}{dx}\psi\right]. \tag{3.28}$$

In terms of J, the particle transmission probability is given by:

$$T = \frac{|J_t(x)|}{|J_i(x)|}, \tag{3.29}$$

where J_i is the probability current density for the incident wave and J_t the probability current density for the transmitted wave. Thus, by Eqs.(3.26) and (3.27), we have

$$J_i(x) = \frac{\hbar k}{m}|A|^2 \quad \text{and} \quad J_t(x) = \frac{\hbar k}{m}|F|^2. \tag{3.30}$$

That way,

$$T = \frac{|F|^2}{|A|^2}. \tag{3.31}$$

For the region $0 < x < a$, the WKB approximation tells us that the eigenfunction should be:

$$\begin{aligned}\psi(x) \approx \frac{C}{\sqrt[4]{2m\,[V(x)-E]}}e^{\frac{1}{\hbar}\int_0^x \sqrt{2m[V(x')-E]}dx'} + \\ \frac{D}{\sqrt[4]{2m\,[V(x)-E]}}e^{-\frac{1}{\hbar}\int_0^x \sqrt{2m[V(x')-E]}dx'}.\end{aligned} \tag{3.32}$$

Now, if the potential barrier is very high or very wide, the probability of transmission will be small. In this case, the coefficient of the exponentially increasing term (C) must be small (and would be zero if the barrier were infinitely wide). Therefore, it is reasonable to consider only the term that decreases exponentially as an approximation. With that, we can summarize the behavior of ψ as follows:

$$\psi(x) : \begin{cases} Ae^{ikx} + Be^{-ikx}, \ x < 0, \\ \dfrac{D}{\sqrt[4]{2m\left[V(x) - E\right]}} e^{-\frac{1}{\hbar}\int_0^x \sqrt{2m[V(x')-E]}dx'}, \ 0 < x < a, \\ Fe^{ikx}, \ x > a. \end{cases} \tag{3.33}$$

Figure 8 illustrates the behavior of the eigenfunction of Eq.(3.33) for the potential analyzed.

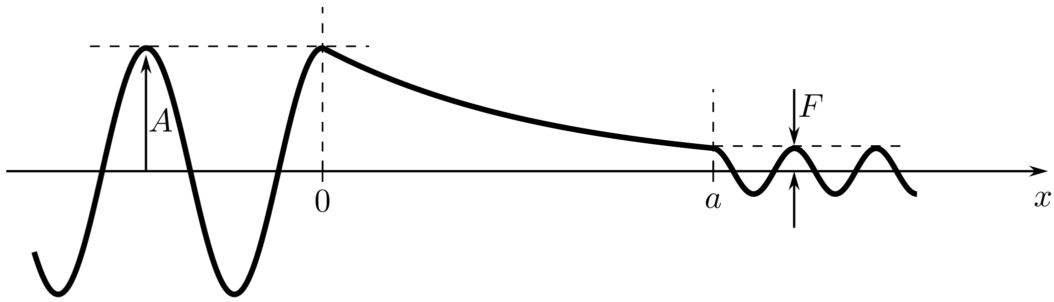

Figure 8 – Qualitative eigenfunction structure for spreading a high barrier and broad. Source: Own authorship.

3.3.1 Boundary conditions

Due to the continuity of ψ in $x = 0$, we have

$$A + B \approx \frac{D}{\sqrt[4]{2m\left[V(0) - E\right]}}. \tag{3.34}$$

Since ψ must also be continuous at $x = a$, then

$$\frac{D}{\sqrt[4]{2m\left[V(a) - E\right]}} \approx Fe^{ika}e^{\gamma}. \tag{3.35}$$

As long as $V(0)$ and $V(a)$ are approximately equal, from Eqs.(3.34) and (3.35),

$$A \approx Fe^{ika}e^{\gamma} \Rightarrow \frac{F}{A}e^{ika} \approx e^{-\gamma}. \tag{3.36}$$

Calculating the squared modulus on both sides of Eq.(3.36) and substituting in Eq.(3.31), it is simple to show that the *Probability of Particle Transmission* through potential barrier will be:

$$T \approx e^{-2\gamma} \ , \ \text{with} \ \gamma = \frac{1}{\hbar}\int_0^a \sqrt{2m\left[V(x) - E\right]}dx, \tag{3.37}$$

where the tunneling exponent γ is known in the literature as the *Gamow Factor*, or Gamow–Sommerfeld factor [52].

3.4 Gamow's Theory of Alpha Decay

In the early 20th century, it was already known that radioactive substances exhibit characteristic exponential decay rates, or half-lives, and that the emitted radiation possesses well-defined energies. In 1928, George Gamow, working in Göttingen with mathematical assistance from Nikolai Kochin, developed the first theoretical explanation of alpha decay (the spontaneous emission of an alpha particle, composed of two protons and two neutrons) in terms of quantum tunneling [26]. Independently, Ronald W. Gurney and Edward U. Condon arrived at a similar theoretical framework, although their results were less quantitatively precise than Gamow's [53, 54].

From a classical standpoint, an alpha particle should remain confined within the nucleus due to the immense energy required to overcome the strong nuclear potential barrier. The disintegration of the nucleus, therefore, would not occur spontaneously. Quantum mechanics, however, allows for a finite probability that the particle can penetrate, or "tunnel through", the potential barrier and escape. By solving a model potential for the nucleus, Gamow derived from first principles a relation between the half-life of alpha decay and the energy of the emitted particle, a result that had previously been established empirically as the Geiger–Nuttall Law (GNL) [55].

Some years later, the term Gamow factor (or Gamow-Sommerfeld factor) was introduced to describe the tunneling probability for incoming charged particles penetrating the Coulomb barrier and participating in nuclear reactions.

Gamow's theoretical framework treats the alpha decay process as a quantum mechanical phenomenon governed by the principles of tunneling. In this model, the atomic nucleus is regarded as a potential well in which the alpha particle is initially bound by the strong nuclear force. Although classically the particle would remain trapped within this potential, quantum mechanics allows for a finite probability of penetration through the barrier, enabling the particle to escape and be emitted from the nucleus [31, 32, 44].

According to Gamow[1], the nuclei of radioactive elements can be understood as a combination of potentials that give rise to two distinct regions:

i. **Internal region (attractive nuclear interaction):** inside the nucleus, the alpha particle is subjected to a short-range attractive force responsible for keeping it confined. This region can be represented, to a first approximation, by a finite square potential well whose outer boundary corresponds approximately to the radius of the parent nucleus, r_1.

ii. **External region (repulsive Coulomb interaction):** upon reaching the nuclear boundary, the alpha particle, with charge $2q$, begins to interact with the daughter nucleus, of charge[2] $Z_\mathrm{d}q$, through the repulsive electrostatic interaction. In this region, the potential is dominated by the Coulomb term, which decreases inversely with distance. For $r_1 < r < r_2$, the total energy of the particle, E, is lower than the potential barrier, V, and the escape occurs via quantum tunneling through the potential barrier. For $r > r_2$, where $E > V$, the particle is no longer bound and moves away from the daughter nucleus under the influence of the residual Coulomb

[1] The analysis developed in this work is restricted to the case in which alpha decay occurs between the ground states of the parent and daughter nuclei.

[2] The subscripts "p" and "d" will be used to denote quantities referring to the parent and daughter nuclei, respectively.

potential, behaving approximately as a free particle with kinetic energy corresponding to the difference between E and $V(r)$.

Figure 9 illustrates the effective potential described above, showing the confinement and barrier regions. The points r_1 and r_2 mark, respectively, the nuclear boundary and the outer turning point, where the alpha particle emerges after the tunneling process.

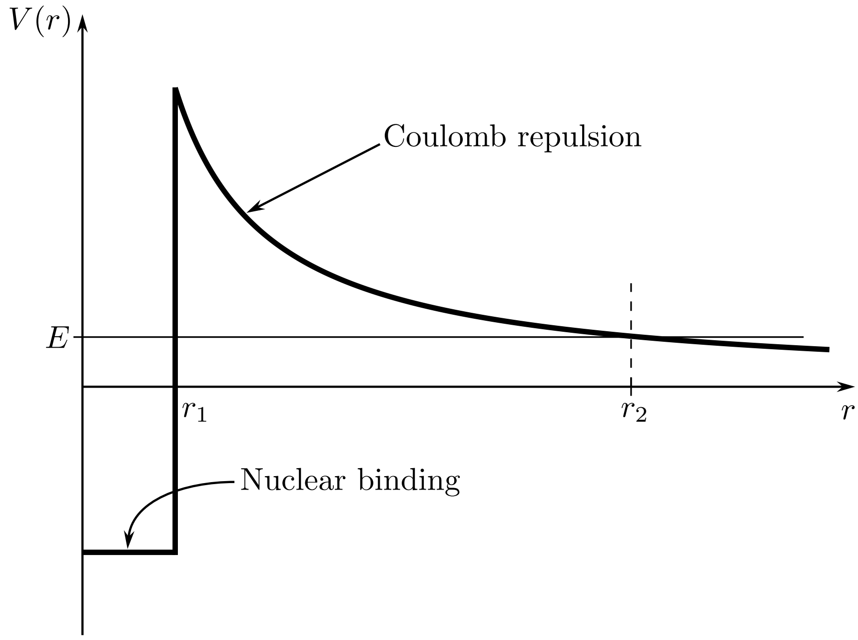

Figure 9 – Gamow's model for the potential energy of an alpha particle in a radioactive nucleus. Source: Own authorship.

Let E be the energy of the emitted alpha particle. The turning point r_2 can be determined from the Coulomb potential energy:

$$\frac{1}{4\pi\varepsilon_0}\frac{2Z_\mathrm{d}q^2}{r_2} = E. \tag{3.38}$$

To determine the probability of alpha particle transmission, we will use the result of Eq.(3.37), where now the gamma factor will be as follows:

$$\gamma = \frac{1}{\hbar}\int_{r_1}^{r_2}\sqrt{2\mu\left[V_\mathrm{C}(r) - E\right]}dr, \tag{3.39}$$

where r_1 is the radius of the parent nucleus, r_2 the classical turning point (see Fig. 9), $\mu = m_\alpha m_\mathrm{d}/(m_\alpha + m_\mathrm{d})$ the reduced mass, and V_C the Coulomb potential energy. Thus, using Eq.(3.38), we can write

$$\gamma = \frac{\sqrt{2\mu E}}{\hbar}\int_{r_1}^{r_2}\sqrt{\frac{r_2 - r}{r}}dr. \tag{3.40}$$

Let's make the following change of variable:

$$r = r_2\sin^2 u \;\Rightarrow\; dr = 2r_2\sin u\cos u du. \tag{3.41}$$

With this, we will have

$$\int \sqrt{\frac{r_2 - r}{r}} dr = r_2 \left[u + \sin u \cos u \right].$$

The Eq.(3.41) allows us to return to the variable r:

$$\sin u = \sqrt{\frac{r}{r_2}} \;\Rightarrow\; u = \sin^{-1} \sqrt{\frac{r}{r_2}}. \tag{3.42}$$

Using the identity $\cos u = \sqrt{1 - \sin^2 u}$ and Eq.(3.42), we will have

$$\int \sqrt{\frac{r_2 - r}{r}} dr = r_2 \sin^{-1} \sqrt{\frac{r}{r_2}} + \sqrt{r(r_2 - r)}.$$

Using this result in Eq.(3.40), we obtain

$$\begin{aligned} \gamma &= \frac{\sqrt{2\mu E} r_2}{\hbar} \left\{ \frac{\pi}{2} - \sin^{-1} \sqrt{\frac{r_1}{r_2}} - \frac{1}{r_2} \sqrt{r_1 r_2 \left(1 - \frac{r_1}{r_2}\right)} \right\} \\ &= \left(\frac{q^2}{4\pi\varepsilon_0} \right) \sqrt{\frac{2\mu}{E}} \frac{2Z_{\mathrm{d}}}{\hbar} \left\{ \frac{\pi}{2} - \sin^{-1} x - x\sqrt{1 - x^2} \right\}, \end{aligned} \tag{3.43}$$

where $x = \sqrt{r_1/r_2}$. In Eq.(3.43), we can consider the following expansion for small x:

$$\frac{\pi}{2} - \sin^{-1} x - x\sqrt{1 - x^2} = \frac{\pi}{2} - 2x + \frac{x^3}{3} + \frac{x^5}{20} + \frac{x^7}{56} + \cdots. \tag{3.44}$$

In the literature, it is common to consider the terms of the expansion up to x^3 [56], the higher order terms are discarded because $x \ll 1$ (which implies $r_1 \ll r_2$). Thus, from Eqs.(3.43) and (3.44), we will have:

$$\gamma = \left(\frac{q^2}{4\pi\varepsilon_0} \right) \frac{\pi\sqrt{2\mu}}{\hbar} \frac{Z_{\mathrm{d}}}{\sqrt{E}} - \left(\frac{q^2}{4\pi\varepsilon_0} \right)^{1/2} \frac{4\sqrt{\mu}}{\hbar} \sqrt{Z_{\mathrm{d}} r_1} + \left(\frac{q^2}{4\pi\varepsilon_0} \right)^{-1/2} \frac{\sqrt{\mu}}{3\hbar} \sqrt{\frac{r_1^3}{Z_{\mathrm{d}}}} E. \tag{3.45}$$

To simplify the notation, we can define the following coefficients:

$$K_1(\mu) = \left(\frac{q^2}{4\pi\varepsilon_0} \right) \frac{\pi\sqrt{2\mu}}{\hbar}, \quad K_2(\mu) = \left(\frac{q^2}{4\pi\varepsilon_0} \right)^{1/2} \frac{4\sqrt{\mu}}{\hbar} \quad \text{and} \quad K_3(\mu) = \left(\frac{q^2}{4\pi\varepsilon_0} \right)^{-1/2} \frac{\sqrt{\mu}}{3\hbar}. \tag{3.46}$$

With this, Eq.(3.45) becomes[3]

$$\gamma = K_1(\mu) \frac{Z_{\mathrm{d}}}{\sqrt{E}} - K_2(\mu) \sqrt{Z_{\mathrm{d}} r_1} + K_3(\mu) \sqrt{\frac{r_1^3}{Z_{\mathrm{d}}}} E. \tag{3.47}$$

We could also consider only the first two terms of the expansion in Eq.(3.44), which would yield the first two terms of Eq.(3.47), corresponding to the terms with K_1 and K_2. Although this simplified expression contains less information than the full result presented

[3] Note that for Eq.(3.45) to be dimensionless the coefficients of Eq.(3.46) must have the following units of magnitude: K_1 must have units $[\text{energy}]^{1/2}$, K_2 must have units $[\text{length}]^{-1/2}$ and K_3 must have units $[\text{length}]^{-3/2} * [\text{energy}]^{-1}$.

in Eq.(3.47), it remains highly relevant, as its form directly recalls the empirical GNL, Eq.(D.1).

Assuming that the alpha particle oscillates inside the nucleus with an average velocity v, the mean time between "collisions" with the potential "wall" is approximately $2r_1/v$. Thus, the collision frequency is $v/2r_1$. As previously discussed, the probability of the particle escaping in a single collision is $e^{-2\gamma}$ (according to Eq.(3.37)), so the probability of emission per unit time is $(v/2r_1)e^{-2\gamma}$. Consequently, the *lifetime* of the parent nucleus can be expressed as [31, 43]:

$$\tau = \frac{2r_1}{v} e^{2\gamma}. \tag{3.48}$$

Although the exact value of v is unknown, assuming $v \ll c$ (where c is the speed of light in vacuum), we can employ the classical expression for the kinetic energy of the alpha particle, $E = (1/2)\mu v^2$, to estimate v. This approximation slightly underestimates the true value of v, but it remains a reasonable approach within the non-relativistic regime relevant to alpha decay.

In nuclear physics, it is more common to express results in terms of the half-life, $T_{1/2}$, rather than the lifetime τ, with both quantities related by $T_{1/2} = \tau \ln 2$. Thus, we obtain the following theoretical expression for the half-life of the alpha-decay process:

$$T_{1/2} = r_1 \sqrt{\frac{2\mu}{E}} e^{2\gamma} \ln 2. \tag{3.49}$$

The expression obtained in Eq.(3.49) encapsulates the central result of Gamow's theory, quantitatively establishing the connection between the tunneling factor and the half-life of radioactive nuclei that emit alpha particles. Although highly successful, this model relies exclusively on the nuclear interaction and the Coulomb potential, neglecting possible corrections arising from other interactions. However, in broader physical scenarios, such as those that admit compactified extra dimensions, additional contributions may modify the shape of the potential barrier and, consequently, the very dynamics of alpha decay. Thus, in the following chapter, we extend Gamow's formalism to investigate how modified gravitational potentials affect both the classical turning point and the Gamow factor, allowing us to assess the consequences of these extensions for the observed half-lives.

3.5 Energy Dissipated in Alpha Decay

The energy released in alpha decay, commonly denoted in the literature by Q, appears as the total kinetic energy of the system after emission, that is, the sum of the kinetic energies of the alpha particle and the daughter nucleus. Let M_p be the mass of the parent nucleus, m_d the mass of the daughter nucleus, and m_α the mass of the alpha particle.

Before the alpha particle is emitted, the initial system is composed solely of the parent nucleus (see Fig. 2). Assuming that the parent nucleus is initially at rest, its total energy is given only by its relativistic rest energy, according to Einstein's well-known expression [57, 58]:

$$E_{\text{total}} = M_\mathrm{p} c^2, \tag{3.50}$$

where c is the speed of light in vacuum.

After emission, the system consists of two particles: the alpha particle and the daughter nucleus. The total energy of the system remains conserved, but it is now redistributed among the rest energies of the two final particles and the kinetic energy released in the process. Thus, we can write:

$$E_{\text{total}} = Q + m_{\text{d}}c^2 + m_{\alpha}c^2. \tag{3.51}$$

Hence, by energy conservation, the energy released in alpha decay is simply the difference between the mass of the parent nucleus and the sum of the masses of the decay products:

$$Q = \left(M_{\text{p}} - m_{\text{d}} - m_{\alpha}\right)c^2. \tag{3.52}$$

As follows directly from Eq.(3.52), alpha decay can occur only if $Q > 0$, since only in such cases is there sufficient energy to be converted into the kinetic energy of the final particles [27]. For this reason, only certain heavy nuclei are energetically capable of undergoing alpha decay.

Since the final system consists of just two particles, conservation of momentum requires the alpha particle and the daughter nucleus to recoil with equal and opposite momenta, which we denote by p. Thus, using energy conservation, we have:

$$Q = \frac{p^2}{2m_{\alpha}} + \frac{p^2}{2m_{\text{d}}} = \frac{p^2}{2m_{\alpha}}\left(1 + \frac{m_{\alpha}}{m_{\text{d}}}\right) = \frac{p^2}{2\mu}, \tag{3.53}$$

where $\mu = m_{\alpha}m_{\text{d}}/(m_{\alpha} + m_{\text{d}})$ is the reduced mass of the system.

For heavy radioactive nuclei ($m_{\text{d}} \gg m_{\alpha}$), the situation simplifies significantly. Because the daughter nucleus is much more massive than the alpha particle, its kinetic energy after emission is extremely small compared to that of the alpha particle. This follows directly from the relation $K = p^2/2m$: for the same momentum p, the more massive particle acquires much less kinetic energy. Thus, when $m_{\text{d}} \gg m_{\alpha}$, the term $p^2/2m_{\text{d}}$ becomes negligible when compared to $p^2/2m_{\alpha}$. Therefore, to an excellent approximation, nearly all the energy released in alpha decay Q is carried by the alpha particle, and its kinetic energy may be taken as

$$K_{\alpha} \approx Q. \tag{3.54}$$

This approximation is widely used in nuclear physics literature, as it accurately reflects the large mass asymmetry between the alpha particle and the daughter nucleus in alpha decays of heavy nuclei.

4 Alpha Decay in Extra-Dimensional Scenarios

In this chapter, we extend Gamow's theory of alpha decay to a framework that incorporates extra dimensions, as proposed in the brane-world model of Arkani-Hamed–Dimopoulos–Dvali (ADD model). Within this perspective, gravity can propagate through the additional dimensions, modifying the effective potential experienced by the alpha particle during the tunneling process. Our main goal is to investigate how this modification affects the classical turning point and the Gamow factor, introducing corrections arising from the anomalous gravitational interaction associated with the presence of hidden dimensions.

4.1 Extended Gamow Theory of Alpha Decay

In Section 3.4, we saw that the decay model proposed by George Gamow describes the parent nucleus as a bound state between the daughter nucleus and the alpha particle [26, 31, 43]. In this model, the interaction potential consists of two main contributions: an attractive nuclear interaction, which can be approximated by a finite square well, and a repulsive electrostatic (Coulomb) interaction between the daughter nucleus and the alpha particle, as illustrated in Fig. 9.

The total energy of the alpha particle is lower than the height of the potential barrier; however, due to the quantum tunneling effect, there exists a finite probability for the particle to be emitted. The lifetime of the parent nucleus is directly related to this transmission probability, which is obtained through the WKB approximation, leading to Eq.(3.48). Essentially, the tunneling probability depends on both the height and width of the barrier, which in turn vary according to the energy of the emitted particle.

In the nuclear regime, the contribution of Newtonian gravity is completely negligible. However, in the presence of extra dimensions (as described in the ADD model), the gravitational interaction becomes enhanced at short distances. In fact, if R represents the compactification radius, then for distances $r \ll R$, the modified gravitational potential energy between two particles of masses M and m follows a *Power-Law* behavior (see Section 2.4):

$$V_{\mathrm{G}}(r) = -\frac{G^{(4+\delta)}Mm}{r^{1+\delta}}, \tag{4.1}$$

where $G^{(4+\delta)}$ is the gravitational constant in this scenario and δ is the number of extra dimensions[1].

On the other hand, in the long-distance regime, where distances are much larger than the compactification radius, the gravitational potential must asymptotically recover its usual three-dimensional behavior. Nevertheless, even in this domain, corrections arise. To first order (see Section 2.4), the correction terms to the modified gravitational potential

[1] Without loss of generality, we assume that all extra dimensions have a circular topology with the same compactification radius R.

energy take a *Yukawa-type* form:

$$V_G(r) = -\frac{GMm}{r}\left(1 + \alpha e^{-r/\lambda}\right), \tag{4.2}$$

where the parameter α represents the amplification factor of the interaction and λ denotes the characteristic length scale over which the correction becomes significant.

Therefore, to investigate the effects of extra dimensions on the decay rate of radioactive nuclei, it is necessary to account for the influence of the modified gravitational potential energy on the alpha-particle tunneling process. Since the gravitational potential contributes negatively to the total potential energy, it can be expected to modify both the height and width of the barrier (see Fig. 10), effectively narrowing it and thus leading to shorter nuclear lifetimes.

In a brane-world scenario, it becomes necessary to redefine the Gamow factor to adapt it to this new theoretical framework. The modified factor must incorporate the corrections arising from the presence of extra dimensions. Analogous to the conventional case, it can then be expressed as:

$$\gamma' = \frac{\sqrt{2\mu}}{\hbar}\int_{r_1}^{r_2'} \sqrt{V'(r) - E}dr, \tag{4.3}$$

where r_2' is the new turning point and $V' = V_C + V_G$ is the total potential energy, with V_G being the modified gravitational potential energy.

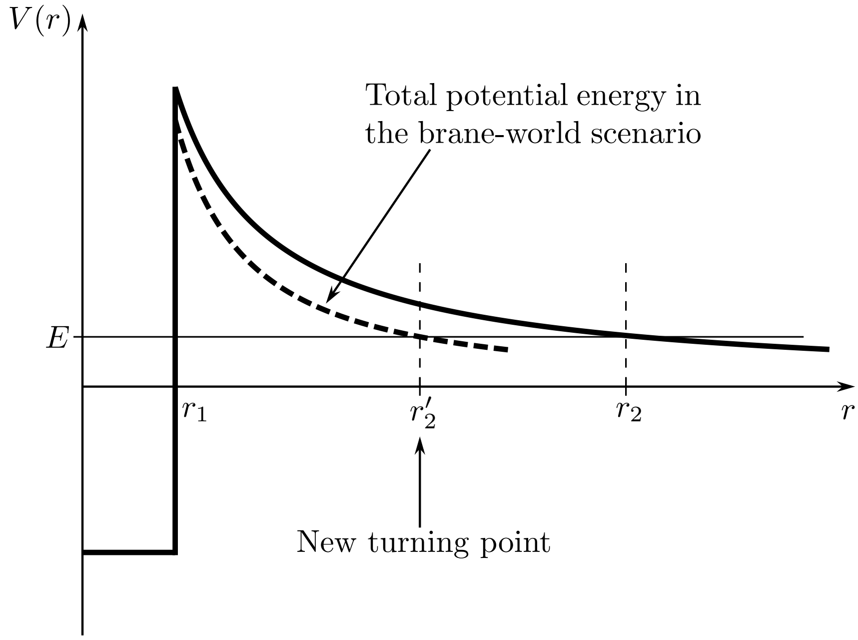

Figure 10 – Modified Gamow model for the potential energy of an alpha particle in a scenario with extra dimensions. Source: Own authorship.

4.2 Calculation of the New Turning Point

Before proceeding with the analysis of γ', we shall first determine the new turning point. This requires evaluating its behavior in both regimes: at short distances, where the effects of the extra dimensions are dominant, and at long distances, where the compactification radius becomes relevant and the gravitational potential approaches its asymptotic three-dimensional form.

4.2.1 New Turning Point Considering the Power Law

In a short-distance regime, the modified gravitational potential energy will be given by a power law: $V_{\mathrm{G}}(r) = -G^{(4+\delta)} M_{\mathrm{d}} \mu / r^{1+\delta}$. Therefore, for simplicity, we can begin by defining the following notations:

$$\mathscr{K} \equiv \frac{Z_{\mathrm{d}} q^2}{2\pi\varepsilon_0} \quad \text{and} \quad \mathscr{G} \equiv G^{(4+\delta)} M_{\mathrm{d}} \mu. \tag{4.4}$$

Let's assume $r_2' = r_2 + \delta r$, where δr is small. Then, at the turning point, we will have

$$V_{\mathrm{C}}(r_2') + V_{\mathrm{G}}(r_2') = E. \tag{4.5}$$

Since V_{G} contributes only a small modification, without loss of generality, we can do

$$V_{\mathrm{C}}(r_2') + V_{\mathrm{G}}(r_2) = E. \tag{4.6}$$

Using the notation from Eq.(4.4) and rewriting Eq.(4.6) in another way,

$$\frac{1}{r_2'} = \frac{1}{r_2 + \delta r} = \frac{1}{r_2\left(1 + \delta r / r_2\right)} = \frac{E}{\mathscr{K}} + \frac{\mathscr{G}}{\mathscr{K} r_2^{1+\delta}}.$$

Assuming $\delta r \ll r_2$, we can perform the following expansion:

$$\frac{1}{r_2\left(1 + \delta r / r_2\right)} \cong \frac{1}{r_2}\left(1 - \frac{\delta r}{r_2}\right).$$

With this, we will have

$$r_2 - \delta r = \frac{E r_2^2}{\mathscr{K}} + \frac{\mathscr{G}}{\mathscr{K} r_2^{\delta-1}}.$$

Using the identity $\mathscr{K}/r_2 = E$, with some mathematical manipulations, it is simple to show that

$$\delta r = -\left(\frac{2\pi\varepsilon_0}{Z_{\mathrm{d}} q^2}\right)^{\delta} G^{(4+\delta)} M_{\mathrm{d}} \mu E^{\delta-1}. \tag{4.7}$$

We can also express this result in terms of the Planck length in a scenario with extra dimensions, $l_{\mathrm{P}}^{(D)}$. From Eqs.(2.69a) and (2.65a), setting $D = 4+\delta$, we can find the following relationship:

$$G^{(4+\delta)} = \frac{\left(l_{\mathrm{P}}^{(4+\delta)}\right)^{2+\delta} c^3}{\hbar}. \tag{4.8}$$

Therefore, we can rewrite Eq.(4.7) as:

$$\delta r = -\left(\frac{2\pi\varepsilon_0}{Z_{\mathrm{d}} q^2}\right)^{\delta} \frac{\left(l_{\mathrm{P}}^{(4+\delta)}\right)^{2+\delta} c^3 M_{\mathrm{d}} \mu E^{\delta-1}}{\hbar}. \tag{4.9}$$

Note that, as expected due to the fact that $V_{\mathrm{G}} < 0$, we have that $r_2' < r_2$, as the negative sign in Eq.(4.9) suggests.

4.2.2 New Turning Point Considering Yukawa's Parameterization

In a long-distance regime compared to the compactification radius of the supplementary dimensions, the gravitational potential of the system exhibits Yukawa-type corrections, where the modified gravitational potential energy can be written as: $V_{\mathrm{G}}(r) = -GM_{\mathrm{d}}\mu/r\left(1+\alpha e^{-r/\lambda}\right)$. To simplify the notation, let's consider:

$$\mathcal{K} \equiv \frac{Z_{\mathrm{d}}q^2}{2\pi\varepsilon_0} \quad \text{and} \quad \mathcal{G} \equiv GM_{\mathrm{d}}\mu. \tag{4.10}$$

Again, let's assume $r_2' = r_2 + \delta r$, assuming that δr is small. Proceeding with reasoning analogous to that of Eq.(4.6), we will have

$$V_{\mathrm{C}}(r_2') + V_{\mathrm{G}}(r_2) = E.$$

Using the notation of Eq.(4.10), we can write

$$\frac{1}{r_2'} = \frac{1}{r_2+\delta r} = \frac{1}{r_2\left(1+\delta r/r_2\right)} = \frac{E}{\mathcal{K}} + \frac{\mathcal{G}}{\mathcal{K}r_2}\left(1+\alpha e^{-r_2/\lambda}\right).$$

Assuming $\delta r \ll r_2$ and proceeding similarly to what we did in the previous section, we will obtain the following result:

$$\delta r = -\frac{GM_{\mathrm{d}}\mu}{E}\left[1+\alpha\exp\left(-\frac{Z_{\mathrm{d}}q^2}{2\pi\varepsilon_0 E\lambda}\right)\right]. \tag{4.11}$$

4.3 Modified Gamow Factor

Returning to Eq.(4.3), we have that the alpha decay will be given in terms of the new Gamow factor:

$$\gamma' = \frac{\sqrt{2\mu}}{\hbar}\int_{r_1}^{r_2'}\sqrt{V_{\mathrm{C}}(r)+V_{\mathrm{G}}(r)-E}\,dr. \tag{4.12}$$

Assuming $V_{\mathrm{G}} \ll V_{\mathrm{C}}$ for the entire interval $r_1 < r < r_2'$, we can calculate the variation of the Gamow factor:

$$\delta\gamma = \gamma' - \gamma, \tag{4.13}$$

where it is implied that $\delta\gamma$ is a small term. By writing γ and γ' explicitly,

$$\begin{aligned}\delta\gamma/\left(\sqrt{2\mu}/\hbar\right) &= \int_{r_1}^{r_2'}\sqrt{V_{\mathrm{C}}(r)+V_{\mathrm{G}}(r)-E}\,dr - \int_{r_1}^{r_2}\sqrt{V_{\mathrm{C}}(r)-E}\,dr\\ &= \int_{r_1}^{r_2'}\sqrt{V_{\mathrm{C}}(r)+V_{\mathrm{G}}(r)-E}\,dr - \int_{r_1}^{r_2'}\sqrt{V_{\mathrm{C}}(r)-E}\,dr - \int_{r_2'}^{r_2}\sqrt{V_{\mathrm{C}}(r)-E}\,dr,\end{aligned}$$

By rewriting the first two integrals in a single form, we will have

$$\delta\gamma/\left(\sqrt{2\mu}/\hbar\right) = \int_{r_1}^{r_2'}\left[\sqrt{V_{\mathrm{C}}(r)+V_{\mathrm{G}}(r)-E} - \sqrt{V_{\mathrm{C}}(r)-E}\right]dr - \int_{r_2'}^{r_2}\sqrt{V_{\mathrm{C}}(r)-E}\,dr. \tag{4.14}$$

Now, we will follow a procedure similar to the calculation of variations, where we define the following quantity analogous to a Lagrangian:

$$L(V) = \sqrt{V-E}. \tag{4.15}$$

Thus, a change in V causes a change in L. For a small change in V, $V' = V + \delta V$, we can write:

$$L(V') = L(V) + \delta L.$$

Rewriting it another way,

$$\delta L = \sqrt{V + \delta V - E} - \sqrt{V - E}. \tag{4.16}$$

Comparing Eq.(4.16) with the integrand in the first integral of Eq.(4.14), we can identify the following terms:

$$V \equiv V_{\mathrm{C}} \quad \text{and} \quad \delta V \equiv V_{\mathrm{G}}. \tag{4.17}$$

Returning to Eq.(4.16), let's expand δL in a Taylor series around V. Then,

$$\begin{aligned}
\delta L = \delta L(V') &= \delta L(V) + \left[\frac{\partial}{\partial V'}\left(\delta L(V')\right)\right]\Bigg|_{V'=V} \delta V + \frac{1}{2!}\left[\frac{\partial^2}{\partial V'^2}\left(\delta L(V')\right)\right]\Bigg|_{V'=V} (\delta V)^2 + \cdots \\
&= 0 + \left[\frac{\partial}{\partial V'}\left(L(V')\right)\right]\Bigg|_{V'=V} \delta V + \frac{1}{2}\left[\frac{\partial^2}{\partial V'^2}\left(L(V')\right)\right]\Bigg|_{V'=V} (\delta V)^2 + \cdots \\
&= \frac{\partial L}{\partial V}\delta V + \frac{1}{2}\frac{\partial^2 L}{\partial V^2}(\delta V)^2 + \cdots .
\end{aligned} \tag{4.18}$$

Using Eq.(4.17), we can write:

$$\begin{aligned}
\frac{\partial L}{\partial V} &= \frac{\partial}{\partial V'} L(V')\Bigg|_{V'=V_{\mathrm{C}}} = \frac{1}{2}\frac{1}{\sqrt{V_{\mathrm{C}} - E}}, \\
\frac{\partial^2 L}{\partial V^2} &= \frac{\partial^2}{\partial V'^2} L(V')\Bigg|_{V'=V_{\mathrm{C}}} = -\frac{1}{4}\frac{1}{[V_{\mathrm{C}} - E]^{3/2}}.
\end{aligned}$$

As we did in Eqs.(4.4) and (4.10), we will use the notation $\mathscr{G}$ for the terms involving the gravitational constant. We will analyze the terms of the expansion in Eq.(4.18) separately, considering their order of $\mathscr{G}$ within the integration interval $[r_1, r_2']$.

i) *First Term*: $\delta L_{(1)} = \frac{\partial L}{\partial V}\delta V$.

$\delta V = V_{\mathrm{G}} \sim \mathcal{O}(\mathscr{G})$ for the entire interval.
$\frac{\partial L}{\partial V} = \frac{1}{2}\frac{1}{\sqrt{V_{\mathrm{C}}(r) - E}} \sim \mathcal{O}(\mathscr{G}^{-1/2})$, around r_2', since $V_{\mathrm{C}}(r) - E \sim \mathcal{O}(\mathscr{G})$ for r close to r_2', by Eq.(4.5).

In this way,

$$\delta L_{(1)} = \frac{\partial L}{\partial V}\delta V \sim \begin{cases} \mathcal{O}(\mathscr{G}^{1/2}), \text{ around } r_2', \\ \mathcal{O}(\mathscr{G}), \text{ in the rest of the interval.} \end{cases}$$

The interval where the variation of the Lagrangian is of order $\mathscr{G}^{1/2}$ is a short domain, with a size on the order of $\mathscr{G}$. If we denote this interval by $\mathscr{I}$, we will have the following result:

$$\int \delta L_{(1)} dr = \int \frac{\partial L}{\partial V}\delta V dr \sim \begin{cases} \mathcal{O}(\mathscr{G}^{3/2}), \text{ integrating in } \mathscr{I}, \\ \mathcal{O}(\mathscr{G}), \text{ integrating in } [r_1, r_2'] - \mathscr{I}. \end{cases}$$

Let's now return to Eq.(4.14) to analyze the integral performed on the interval $[r_2', r_2]$. Since $\sqrt{V_\mathrm{C} - E} \sim \mathcal{O}(\mathscr{G}^{1/2})$ around r_2' and $[r_2', r_2] \sim \mathcal{O}(\mathscr{G})$, we will have

$$\int_{r_2'}^{r_2} \sqrt{V_\mathrm{C}(r) - E}dr \sim \mathcal{O}(\mathscr{G}^{3/2}).$$

Therefore, we arrive at the following conclusion:

$$\delta\gamma_{(1)} \sim \mathcal{O}(\mathscr{G}) + \mathcal{O}(\mathscr{G}^{3/2}).$$

ii) *Second Term*: $\delta L_{(2)} = \frac{\partial^2 L}{\partial V^2}\left(\delta V\right)^2$.

$\left(\delta V\right)^2 = V_\mathrm{G}^2 \sim \mathcal{O}(\mathscr{G}^2)$ for the entire interval.
$\frac{\partial^2 L}{\partial V^2} = -\frac{1}{4}\frac{1}{[V_\mathrm{C}(r)-E]^{3/2}} \sim \mathcal{O}(\mathscr{G}^{-3/2})$, around r_2'.

Therefore,

$$\delta L_{(2)} = \frac{\partial^2 L}{\partial V^2}\left(\delta V\right)^2 \sim \begin{cases} \mathcal{O}(\mathscr{G}^{1/2}), \text{ around } r_2', \\ \mathcal{O}(\mathscr{G}^2), \text{ in the rest of the interval.} \end{cases}$$

Since we have $\mathscr{I} \sim \mathcal{O}(\mathscr{G})$, we conclude that

$$\int \delta L_{(2)} dr = \int \frac{\partial^2 L}{\partial V^2}\left(\delta V\right)^2 dr \sim \begin{cases} \mathcal{O}(\mathscr{G}^{3/2}), \text{ integrating in } \mathscr{I}, \\ \mathcal{O}(\mathscr{G}^2), \text{ integrating in } [r_1, r_2'] - \mathscr{I}. \end{cases}$$

In general, for any order n, it is possible to show that

$$\int \delta L_{(n)} dr = \int \frac{\partial^n L}{\partial V^n}\left(\delta V\right)^n dr \sim \begin{cases} \mathcal{O}(\mathscr{G}^{3/2}), \text{ integrating in } \mathscr{I}, \\ \mathcal{O}(\mathscr{G}^n), \text{ integrating in } [r_1, r_2'] - \mathscr{I}. \end{cases}$$

Therefore, disregarding the higher-order terms in $\mathscr{G}$, we can conclude that $\delta\gamma \sim \mathcal{O}(\mathscr{G}) + \mathcal{O}(\mathscr{G}^{3/2})$. Thus, the first approximation can be calculated as follows:

$$\delta\gamma \approx \frac{\sqrt{2\mu}}{\hbar}\int_{r_1}^{r_2'} \frac{\partial L}{\partial V}\delta V dr.$$

Considering only the $\mathscr{G}$ order terms, we can still do:

$$\delta\gamma \approx \frac{1}{\hbar}\sqrt{\frac{\mu}{2}}\int_{r_1}^{r_2} \frac{V_\mathrm{G}(r)}{\sqrt{V_\mathrm{C}(r) - E}}dr, \tag{4.19}$$

where now the upper limit of the integral is r_2 instead of r_2'.

4.3.1 Variation of the Gamow Factor by the Power Law

From Eq.(4.19), we will calculate the variation of the Gamow factor in a short-distance regime compared to the compactification radius of the supplementary dimensions. To simplify our analysis, we will again use the notation of Eq.(4.4) when convenient.

i) Case with one extra dimension ($\delta = 1$):

$$\begin{aligned}\delta\gamma &\approx -\frac{1}{\hbar}\sqrt{\frac{\mu}{2E}}\int_{r_1}^{r_2}\frac{\mathscr{G}/r^2}{\sqrt{\mathscr{K}/Er-1}}dr \\ &= -\frac{\mathscr{G}}{\hbar}\frac{\sqrt{2\mu E}}{\mathscr{K}}\sqrt{\frac{r_2}{r_1}}\sqrt{1-\frac{r_1}{r_2}}.\end{aligned} \tag{4.20}$$

Let's define $x \equiv r_1/r_2$. In the regime $r_1 \ll r_2$, we can consider the following expansion:

$$\sqrt{1-x} = 1 - \frac{x}{2} - \frac{x^2}{8} + \mathcal{O}(x^3). \tag{4.21}$$

Since we are considering that r_1 is much smaller than r_2, which is precisely what happens for heavy radioactive atoms, the lower-order terms in Eq.(4.21) will dominate. Therefore, Eq.(4.20) becomes:

$$\delta\gamma \approx -\frac{\mathscr{G}}{\hbar}\frac{\sqrt{2\mu E}}{\mathscr{K}}\sqrt{\frac{r_2}{r_1}}\left[1-\frac{r_1}{2r_2}\right]. \tag{4.22}$$

ii) Case with two extra dimensions ($\delta = 2$):

$$\begin{aligned}\delta\gamma &\approx -\frac{1}{\hbar}\sqrt{\frac{\mu}{2E}}\int_{r_1}^{r_2}\frac{\mathscr{G}/r^3}{\sqrt{\mathscr{K}/Er-1}}dr \\ &= -\frac{\mathscr{G}}{3\hbar}\frac{\sqrt{2\mu E}}{\mathscr{K}r_1}\sqrt{\frac{r_2}{r_1}}\sqrt{1-\frac{r_1}{r_2}}\left(1+\frac{2r_1}{r_2}\right).\end{aligned}$$

Using the expansion of Eq.(4.21), just as we did to obtain Eq.(4.22), we will have

$$\delta\gamma \approx -\frac{\mathscr{G}}{3\hbar}\frac{\sqrt{2\mu E}}{\mathscr{K}r_1}\sqrt{\frac{r_2}{r_1}}\left[1+\frac{3r_1}{2r_2}\right]. \tag{4.23}$$

iii) Case with three extra dimensions ($\delta = 3$):

$$\begin{aligned}\delta\gamma &\approx -\frac{1}{\hbar}\sqrt{\frac{\mu}{2E}}\int_{r_1}^{r_2}\frac{\mathscr{G}/r^4}{\sqrt{\mathscr{K}/Er-1}}dr \\ &= -\frac{\mathscr{G}}{15\hbar}\frac{\sqrt{2\mu E}}{\mathscr{K}r_1^2}\sqrt{\frac{r_2}{r_1}}\sqrt{1-\frac{r_1}{r_2}}\left(3+\frac{4r_1}{r_2}+\frac{8r_1^2}{r_2^2}\right).\end{aligned}$$

Using Eq.(4.21), we will have

$$\delta\gamma \approx -\frac{\mathscr{G}}{15\hbar}\frac{\sqrt{2\mu E}}{\mathscr{K}r_1^2}\sqrt{\frac{r_2}{r_1}}\left[3+\frac{5r_1}{2r_2}\right]. \tag{4.24}$$

iv) Case with four extra dimensions ($\delta = 4$):

$$\begin{aligned}\delta\gamma &\approx -\frac{1}{\hbar}\sqrt{\frac{\mu}{2E}}\int_{r_1}^{r_2}\frac{\mathscr{G}/r^5}{\sqrt{\mathscr{K}/Er-1}}dr \\ &= -\frac{\mathscr{G}}{35\hbar}\frac{\sqrt{2\mu E}}{\mathscr{K}r_1^3}\sqrt{\frac{r_2}{r_1}}\sqrt{1-\frac{r_1}{r_2}}\left(5+\frac{6r_1}{r_2}+\frac{8r_1^2}{r_2^2}+\frac{16r_1^3}{r_2^3}\right).\end{aligned}$$

Using Eq.(4.21) again, we will have

$$\delta\gamma \approx -\frac{\mathscr{G}}{35\hbar}\frac{\sqrt{2\mu E}}{\mathscr{K}r_1^3}\sqrt{\frac{r_2}{r_1}}\left[5+\frac{7r_1}{2r_2}\right]. \tag{4.25}$$

By carefully analyzing these results, we can observe the emergence of the following pattern:

$$\delta\gamma \approx -\frac{1}{(2\delta-3)(2\delta-1)}\frac{\mathscr{G}}{\hbar}\frac{\sqrt{2\mu E}}{\mathscr{K}r_1^{\delta-1}}\sqrt{\frac{r_2}{r_1}}\left[(2\delta-3)+(2\delta-1)\frac{r_1}{2r_2}\right].$$

By explicitly writing the physical quantities involved, and using the identity from Eq.(4.8), we can rewrite the general expression for $\delta\gamma$ as follows:

$$\delta\gamma \approx -\frac{2}{(2\delta-3)(2\delta-1)}\sqrt{\frac{\pi\varepsilon_0\mu}{Z_\mathrm{d}}}\frac{\left(l_\mathrm{P}^{(4+\delta)}\right)^{2+\delta}c^3M_\mathrm{d}\mu}{\hbar^2 q r_1^{\delta-\frac{1}{2}}}\left[(2\delta-3)+(2\delta-1)\frac{\pi\varepsilon_0 r_1 E}{Z_\mathrm{d}q^2}\right], \tag{4.26}$$

where $\delta = 1, 2, 3\cdots$ is the number of extra dimensions. As a first approximation, we could take only the first term in brackets in Eq.(4.26), which would disregard the influence of the energy of the emitted alpha particle on the effect caused by the extra dimensions for radioactive isotopes.

4.3.2 Variation of the Gamow Factor by Yukawa Parameterization

Analogously to what we did in the previous section, we will start from Eq.(4.19) using the modified gravitational potential energy with Yukawa correction to calculate the variation of the Gamow factor. Furthermore, we will use Eq.(4.10) to simplify the notation.

So, we will begin by writing the potential energies of Eq.(4.19) explicitly:

$$\delta\gamma \approx -\frac{1}{\hbar}\sqrt{\frac{\mu}{2E}}\int_{r_1}^{r_2}\frac{\frac{\mathscr{G}}{r}\left(1+\alpha e^{-r/\lambda}\right)}{\sqrt{\mathscr{K}/rE-1}}dr. \tag{4.27}$$

Let's separate the integral of Eq.(4.27) into two parts:

$$\int_{r_1}^{r_2}\frac{\frac{1}{r}\left(1+\alpha e^{-r/\lambda}\right)}{\sqrt{r_2/r-1}}dr = \int_{r_1}^{r_2}\frac{1/r}{\sqrt{r_2/r-1}}dr + \alpha\int_{r_1}^{r_2}\frac{e^{-r/\lambda}/r}{\sqrt{r_2/r-1}}dr. \tag{4.28}$$

Considering the first integral on the right-hand side of Eq.(4.28), we can rewrite it as follows:

$$\int_{r_1}^{r_2}\frac{1/r}{\sqrt{r_2/r-1}}dr = \int_{r_1}^{r_2}\frac{dr}{\sqrt{(r_2/2)^2-(r-r_2/2)^2}}. \tag{4.29}$$

Let's now make the following change of variable:

$$x = r - r_2/2 \implies dx = dr. \tag{4.30}$$

Therefore, Eq.(4.29) will look like this:

$$\int_{r_1}^{r_2}\frac{1/r}{\sqrt{r_2/r-1}}dr = \int_{r_1-r_2/2}^{r_2/2}\frac{dx}{\sqrt{(r_2/2)^2-x^2}}. \tag{4.31}$$

Let's make another change of variable:

$$\frac{r_2}{2}\sin\theta = x \implies \frac{r_2}{2}\cos\theta d\theta = dx, \tag{4.32}$$

where the new integration boundaries will now be:

$$\theta_1 = \sin^{-1}\left(\frac{2r_1}{r_2} - 1\right) \quad \text{and} \quad \theta_2 = \pi/2. \tag{4.33}$$

For the case $r_1 \ll r_2$, we will have $\sin^{-1}(2r_1/r_2 - 1) \approx -\pi/2$. Therefore, in the regime $r_1 \ll r_2$, we can write the integration limits as follows:

$$\theta_1 = -\pi/2 + \delta\theta \quad \text{and} \quad \theta_2 = \pi/2, \tag{4.34}$$

where $\delta\theta > 0$ is small. The gray region in Fig. 11 illustrates the interval between the integration limits θ_1 and θ_2. Thus, using Eqs.(4.32) and (4.34), we will have the following result:

$$\int_{r_1}^{r_2} \frac{1/r}{\sqrt{r_2/r - 1}} dr = \int_{\theta_1}^{\theta_2} \frac{\frac{r_2}{2}\cos\theta}{\sqrt{(r_2/2)^2\left(1 - \sin^2\theta\right)}} d\theta = \pi - \delta\theta. \tag{4.35}$$

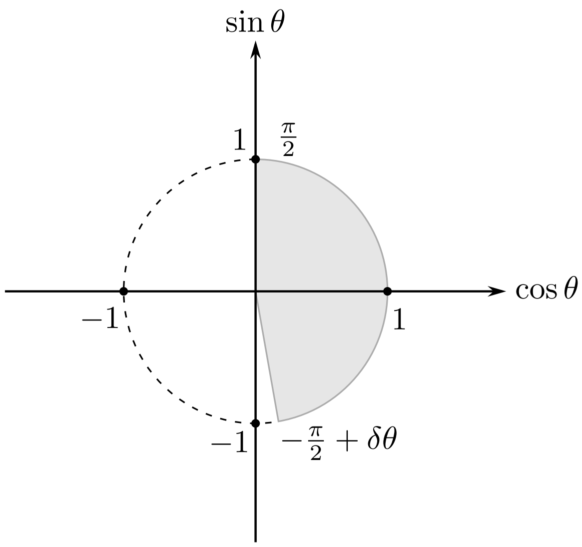

Figure 11 – Integration interval between the upper and lower limits. Source: Own authorship.

Now, let's analyze the second integral on the right-hand side of Eq.(4.28):

$$\int_{r_1}^{r_2} \frac{e^{-r/\lambda}/r}{\sqrt{r_2/r - 1}} dr = \int_{r_1}^{r_2} \frac{e^{-r/\lambda}}{\sqrt{(r_2/2)^2 - (r - r_2/2)^2}} dr. \tag{4.36}$$

Using the change of variable from Eq.(4.30) in our integral, we will have:

$$\int_{r_1}^{r_2} \frac{e^{-r/\lambda}/r}{\sqrt{r_2/r - 1}} dr = e^{-r_2/2\lambda} \int_{r_1 - r_2/2}^{r_2/2} \frac{e^{-x/\lambda}}{\sqrt{(r_2/2)^2 - x^2}} dx.$$

We will also use the change of variable from Eq.(4.32) in this integral:

$$\int_{r_1}^{r_2} \frac{e^{-r/\lambda}/r}{\sqrt{r_2/r-1}}dr = e^{-r_2/2\lambda}\int_{\theta_1}^{\theta_2} e^{-\frac{r_2}{2\lambda}\sin\theta}d\theta, \tag{4.37}$$

where θ_1 and θ_2 are given in Eq.(4.34). With some mathematical manipulation, it's easy to show that we can rewrite the right-hand side of Eq.(4.37) as follows:

$$\begin{aligned}\int_{r_1}^{r_2} \frac{e^{-r/\lambda}/r}{\sqrt{r_2/r-1}}dr &= e^{-r_2/2\lambda}\int_{-\pi/2}^{\pi/2} e^{-\frac{r_2}{2\lambda}\sin\theta}d\theta - \delta\theta \\ &= \pi e^{-r_2/2\lambda} I_0\left(r_2/2\lambda\right) - \delta\theta,\end{aligned} \tag{4.38}$$

where I_0 is the modified Bessel function of the first kind (see Fig. 12) [40, 59, 60].

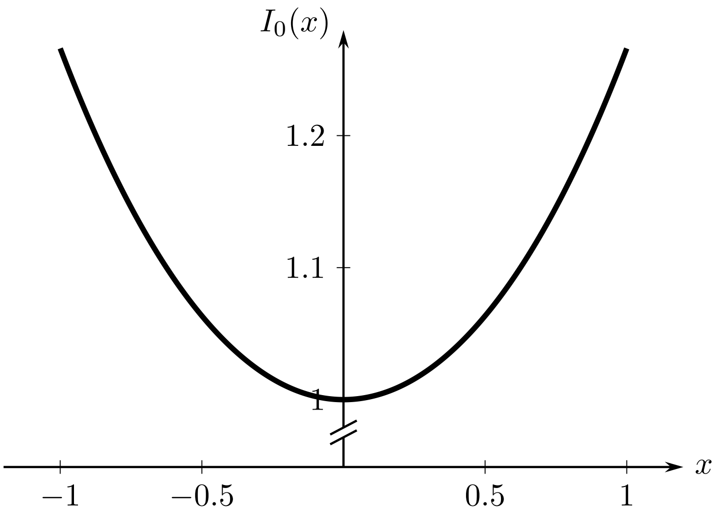

Figure 12 – Modified Bessel function I_0. Source: Own authorship.

Now, let's do a brief analysis to obtain an expression for $\delta\theta$. First, let's look at the following series expansion:

$$\sin^{-1}\left(x-1\right) = -\frac{\pi}{2} + \sqrt{2x} + \frac{x^{3/2}}{6\sqrt{2}} + \frac{3x^{5/2}}{80\sqrt{2}} + \frac{5x^{7/2}}{448\sqrt{2}} + \cdots \quad (x \ll 1). \tag{4.39}$$

Therefore, from Eqs.(4.33), (4.34) and (4.39), we have that the term $\delta\theta$ can be written as follows:

$$\delta\theta = 2\sqrt{\frac{r_1}{r_2}} + \frac{1}{6\sqrt{2}}\left(\frac{2r_1}{r_2}\right)^{3/2} + \frac{3}{80\sqrt{2}}\left(\frac{2r_1}{r_2}\right)^{5/2} + \cdots. \tag{4.40}$$

Therefore, from the results obtained in Eqs.(4.35), (4.38) and (4.40), we have that the variation of the Gamow factor for long distances compared to the compactification radius of the extra dimensions will be:

$$\delta\gamma \approx -\frac{GM_{\mathrm{d}}\mu}{\hbar}\sqrt{\frac{\mu}{2E}}\left\{\pi - \delta\theta + \alpha\left[\pi e^{-r_2/2\lambda} I_0\left(\frac{r_2}{2\lambda}\right) - \delta\theta\right]\right\}. \tag{4.41}$$

The approximate expressions obtained in Eqs.(4.26) and (4.41) for the variation of the Gamow factor play a fundamental role in the analysis developed in this chapter. In particular, these expressions allow for an analytical and transparent identification of how the presence of extra dimensions modifies the Gamow factor in the regime where $r_1 \ll r_2$, a condition that corresponds to the situation most frequently encountered in experimental alpha-decay data. In this limit, the approximations employed are physically well justified and provide a direct interpretation of the influence of extra-dimensional gravitational corrections on the quantum tunneling process.

Despite their conceptual relevance and analytical usefulness, we chose to reserve the detailed presentation of the numerical results and the associated statistical discussion based on these approximate expressions for Appendix F. This decision stems from the fact that such results have a complementary character with respect to the main analysis, serving primarily as a consistency check and as an auxiliary tool for interpreting the results obtained from the complete treatment of the problem.

In the following chapter, whose main objective is to present and discuss the results in a more comprehensive and general manner, without being restricted to the specific regime $r_1 \ll r_2$, we adopt a more complete and robust approach. To this end, we employ Eq.(4.3) in its exact integral form, performing numerical calculations both for the new turning point, r_2', and for the integral that defines the modified Gamow factor itself. This procedure was applied individually to each isotope analyzed, allowing for a more direct and accurate comparison between the theoretical predictions of the extra-dimensional model and the available experimental data.

5 Results and Discussion

In this chapter, we move beyond the purely theoretical developments and apply our extended framework to real experimental data, allowing us to test the behavior and predictive power of the model in practice. With this in mind, we begin by examining one of the key ingredients entering the calculation of the decay rate: the nuclear radius r_1. Although we have not emphasized it properly until now, one of the most relevant physical quantities in Gamow's theory of alpha decay is the nuclear radius. In the literature, several expressions can be found to describe it. Among the most commonly used are the following [31, 56, 61]:

$$r_1 = R_1 A_\mathrm{p}^{1/3}, \tag{5.1a}$$

$$r_1 = R_\alpha + R_2 A_\mathrm{d}^{1/3}, \tag{5.1b}$$

$$r_1 = R_3 \left(A_\alpha^{1/3} + A_\mathrm{d}^{1/3}\right), \tag{5.1c}$$

where[1] A_p is the mass number of the parent nucleus, A_d is the mass number of the daughter nucleus, A_α is the mass number of the emitted alpha particle, R_α is the radius of the emitted alpha particle (in fm), and R_1, R_2, and R_3 are free parameters that can be adjusted based on experimental data. Their values are generally found within the range of 1.0 fm to 2.0 fm [56, 62]. In this chapter, all results presented use r_1 as expressed in Eq.(5.1a).

As mentioned at the end of Chapter 4, the main purpose of this chapter is to advance toward a broader and more consistent analysis, without imposing the specific restriction of the regime $r_1 \ll r_2$. For this reason, all the results and fitting regions presented in the figures of this chapter were obtained using Eq.(4.3) in its complete integral form. This required performing numerical calculations, for each isotope considered, both for the new turning point r_2' and for the integral associated with the modified Gamow factor, thereby allowing a more realistic treatment of the effects of extra-dimensional corrections over the entire relevant range of the potential [63, 64].

For the analysis, we employed the Reduced Chi-Squared (RCS) statistical method[2], usually denoted by $\tilde{\chi}^2$ (see Appendix E), and used an experimental dataset corresponding to the alpha decay of 158 isotopes with even atomic and mass numbers. These data were obtained from the National Nuclear Data Center (NNDC) and the National Institute of Standards and Technology (NIST) databases [65, 66].

5.1 Results for the Power Law

We denote by $\tilde{\chi}_0^2$ the minimum value obtained for the RCS during the fitting procedure. In the short-distance regime, where the modified gravitational potential energy follows the power-law behavior given in Eq.(4.1), the free parameters of the model for each scenario with δ extra dimensions are R_1 and $l_\mathrm{P}^{(4+\delta)}$. The results of the fits, including the optimal values of these parameters that minimize $\tilde{\chi}_0^2$, are presented in Table 1. Each line in the table corresponds to a specific value of δ, allowing for a direct comparison across different extra-dimensional frameworks.

[1] See the second footnote on p. 43.
[2] Also known as the *least squares* method.

Table 1 – Parameter fitting in the short-distance regime using the RCS method. The values shown for the free parameters R_1 and $l_{\mathrm{P}}^{(4+\delta)}$ are those that minimize the RCS.

δ	$\tilde{\chi}_0^2$	R_1 (fm)	$l_{\mathrm{P}}^{(4+\delta)}$ (m)
1	0.8543	1.27	4.4×10^{-17}
2	0.8692	1.49	4.6×10^{-17}
3	0.8692	1.49	1.6×10^{-16}
4	0.8691	1.49	3.4×10^{-16}
5	0.8689	1.49	6.0×10^{-16}
6	0.8687	1.49	9.0×10^{-16}
7	0.8671	1.48	1.4×10^{-15}

A detailed inspection of the second column of Table 1 reveals that the values of $\tilde{\chi}_0^2$ are quite similar across most scenarios, indicating a comparable level of agreement between the model and the experimental data for different numbers of extra dimensions. The only notable exception is the case $\delta = 1$, where the minimum RCS value is slightly smaller. This suggests that, within the context of the power-law potential, the model with a single extra dimension provides a marginally better fit. The third column reinforces this distinction: the fitted value of R_1 for $\delta = 1$ is somewhat smaller than those obtained in the cases with more extra dimensions, although all values remain within a physically reasonable range.

The fourth column of Table 1 contains another striking result. For $\delta = 7$, the fitted value of $l_{\mathrm{P}}^{(4+\delta)}$ reaches the femtometer scale, implying that the higher-dimensional Planck length could be as large as typical nuclear distance scales. This is particularly interesting because it indicates that, even for scenarios with many extra dimensions, the model allows for compactification radii far above the conventional Planck length while still remaining compatible with the observed alpha-decay data. This finding aligns with a central feature of brane-world theories: they naturally accommodate large extra dimensions without conflicting with established experimental constraints [67–70].

To visualize these behaviors more clearly, Fig. 13 displays four color maps corresponding to different values of δ, each illustrating how $\tilde{\chi}^2$ varies throughout the parameter space. The color bar beside each plot provides the scale for interpreting the RCS values, with blue regions indicating better fits. Because the $\delta = 1$ case exhibits a blue region that extends slightly further to the left, toward smaller values of R_1, than in the other scenarios, we set the horizontal axis to show the interval 0.55 fm $\leq R_1 \leq 1.65$ fm in all plots. This unified choice facilitates a direct visual comparison across the four extra-dimensional cases.

A global comparison of the plots in Fig. 13 reveals several consistent patterns. The lower segments of the blue best-fit regions have nearly identical widths for all values of δ, and they are all centered around $R_1 \approx 1.5$ fm, suggesting a strong stability of this parameter across different extra-dimensional models. Moreover, the left boundary of the best-fit strip becomes increasingly curved and irregular as δ grows, indicating a heightened sensitivity of the model to small changes in R_1 when more extra dimensions are present. Another important feature is the widening of the allowed range of $l_{\mathrm{P}}^{(4+\delta)}$ as δ increases. For instance, in the $\delta = 4$ scenario, the best-fit region encompasses values of $l_{\mathrm{P}}^{(4+\delta)}$ around 0.5 fm, reinforcing the possibility that the additional dimensions predicted by LED theories could be as large as femtometer-scale distances.

Taken together, these results strengthen one of the fundamental predictions of the ADD model: extra dimensions need not be confined to ultramicroscopic Planck-scale lengths. Instead, they may extend to nuclear scales while remaining fully consistent with available observational and experimental data derived from alpha-decay systematics.

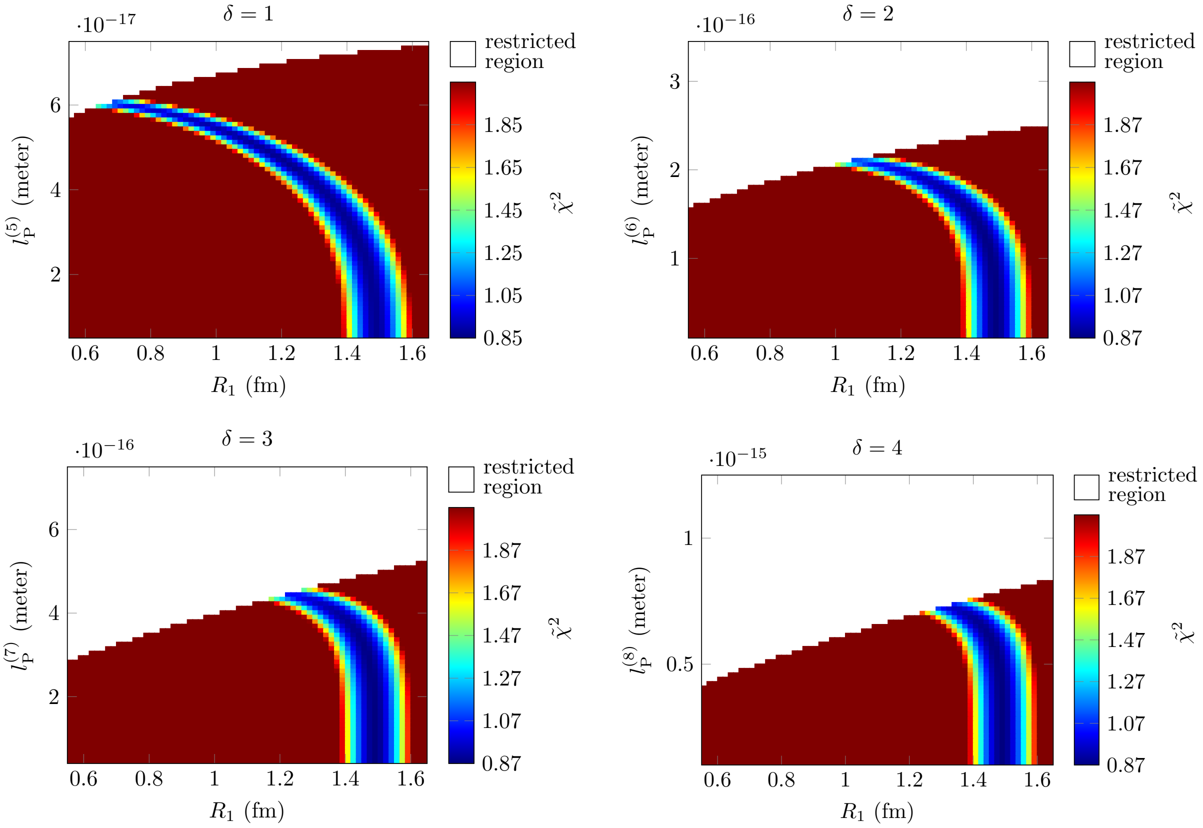

Figure 13 – Color map showing the behavior of $\tilde{\chi}^2$ for four different scenarios. The white constrained regions at the top of each plot indicate that, for those combinations of values of R_1 and $l_{\mathrm{P}}^{(4+\delta)}$, no tunneling occurs because the condition $V_{\mathrm{C}}(r) + V_{\mathrm{G}}(r) < E$ holds throughout the entire interval $[r_1, r_2']$.

5.2 Results for Yukawa Parameterization

In the long-distance regime, the modified gravitational potential energy recovers its usual behavior with a Yukawa-type correction, as given in Eq.(4.2). In this case, the free parameters of our model are R_1, α, and λ. The parameter α is dimensionless, whereas λ has dimensions of length, in accordance with Eq.(4.2). Performing the fit using these free parameters, we obtained the results displayed in Table 2. Furthermore, in Fig. 14 we present the corresponding fit regions[3].

[3] Note that the ranges shown on the α axis and on the λ axis are exactly the same in both the upper and lower plots.

Table 2 – Parameter fitting in the long-distance regime using the RCS method. The values shown for the free parameters R_1, λ and α are those that minimize the RCS.

$\tilde{\chi}_0^2$	R_1 (fm)	λ (m)	α
0.8383	1.37	1.95×10^{-13}	9.82×10^{33}

Examining the value of $\tilde{\chi}_0^2$ in Table 2, we observe that the fit obtained for the model with Yukawa-type corrections yields a slightly better result than those obtained for the power-law case shown in Table 1. This suggests that, for the dataset used, the Yukawa parametrization provides a more efficient description of possible gravitational modifications caused by extra dimensions. Furthermore, when comparing the fitted value of the free parameter associated with the nuclear radius, R_1, with the results presented in Table 1, we note that the value obtained for the Yukawa model lies essentially between the value found for the case $\delta = 1$ (slightly smaller) and the values obtained for the other power-law scenarios with extra dimensions (slightly larger). This indicates that, from a phenomenological standpoint, the Yukawa model tends to produce an intermediate and stable effective nuclear radius, regardless of the structural differences between the two types of gravitational corrections considered.

The value determined for the parameter λ specifies the length scale at which the Yukawa correction becomes relevant within the model. According to Table 2, this scale is of order 10^{-13} m, meaning that the modified gravitational effects would be significant at distances roughly two orders of magnitude larger than the typical nuclear size. This is particularly interesting because it places the scale of gravitational modification at the boundary between nuclear and deep subatomic distances, suggesting the possibility, however speculative, that nuclear phenomena could, in principle, be sensitive to nonstandard gravitational corrections. Moreover, such a scale remains fully compatible with current experimental limits from direct tests of the inverse-square law, which currently probe distances down to the tens of micrometers [71–75]. Thus, values as small as 10^{-13} m, while extremely tiny compared to macroscopic scales, remain far beyond the reach of present-day experimental techniques for testing gravity at such distances.

Comparing the fitted value of the interaction amplification factor, α, with the results found in other analyses in the literature (Refs. [22, 76, 77]), we observe that our result lies close to the upper bounds established in those studies. This suggests that, within the brane-world model and for the dataset analyzed, the strength of the gravitational correction required to achieve a good fit to the half-life data is near the highest value allowed by independent constraints. This result can be interpreted in two ways: (i) the alpha-decay phenomenon might indeed be sensitive to relatively strong gravitational corrections within this parametrization, or (ii) the modified gravitational model, when applied to the nuclear domain, tends to require values of α close to the phenomenologically allowed upper limit in order to remain consistent with the experimental data. In either case, the result highlights the importance of further studies comparing different physical observables and different energy ranges, in order to determine whether this trend is a robust feature or merely a specific consequence of the dataset considered.

Analyzing Fig. 14, in the upper plot, we show the values that the variable R_1 must take in order for the RCS, $\tilde{\chi}^2$, to reach its minimum value at each point (λ, α)

shown; that is, this plot displays the value of R_1 that best fits each pair (λ, α). This figure therefore provides a direct visualization of how the optimal nuclear-radius parameter adjusts itself in response to different combinations of the Yukawa-scale parameter λ and the interaction-strength parameter α.

In the lower plot, we show the behavior of the RCS itself, using the values of R_1 obtained from the upper plot to generate this fit region. Notice how the values of $\tilde{\chi}^2$ change relatively abruptly, transitioning from the blue region (lower values) to the red region (higher values). These sharp transitions delineate the boundary between the parameter combinations that are compatible with the experimental data and those that yield significantly poorer agreement. Another striking feature of this plot is the narrow best-fit region (the darker blue band) located around $\alpha = 9.82 \times 10^{33}$ on the right-hand side. The fact that this optimal region is extremely narrow in α, while remaining extended over several orders of magnitude in λ, indicates that the quality of the fit is much more sensitive to variations in α than to changes in the Yukawa length scale. In other words, for the dataset analyzed, the interaction-amplitude parameter α must take a very specific value in order to reproduce the observed half-lives, whereas λ may still vary considerably without compromising the quality of the fit. This behavior strongly suggests that the best agreement with our data occurs when $\alpha = 9.82 \times 10^{33}$, while λ retains considerable freedom across multiple orders of magnitude.

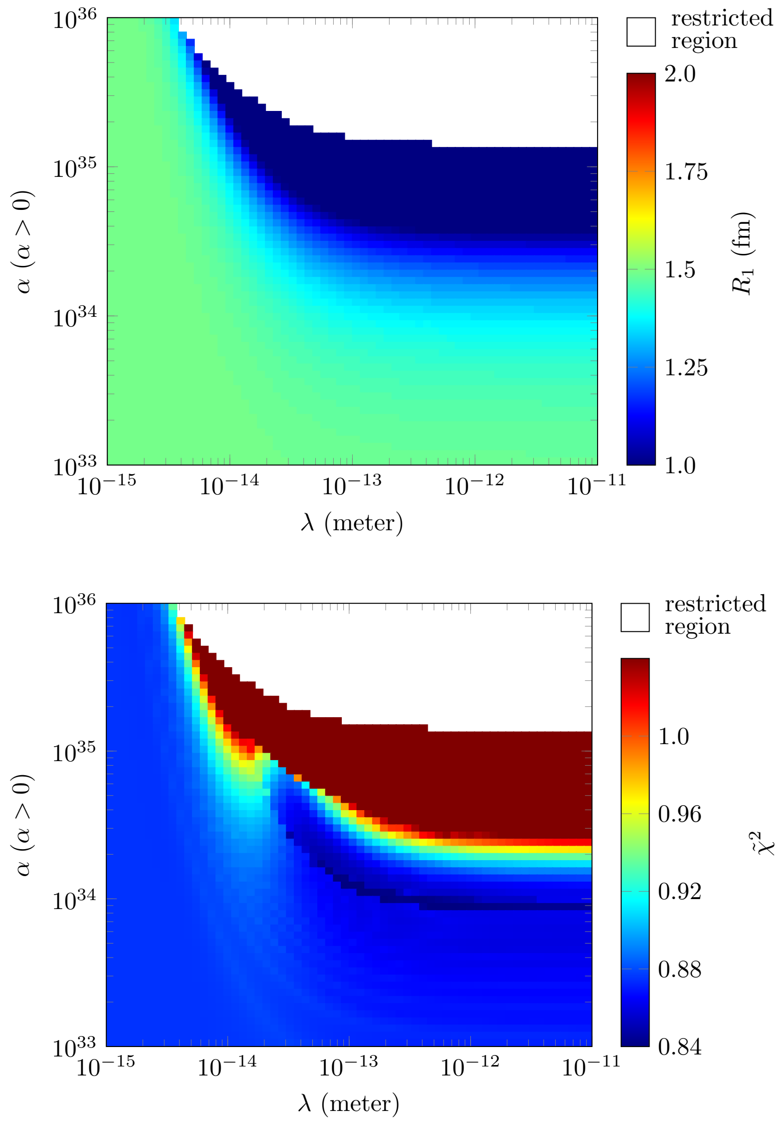

Figure 14 – *Above:* Fit region showing only the free parameters. In this plot, note that the color gradient indicates the values of R_1. *Below:* Fit region showing the behavior of $\tilde{\chi}^2$ for the values of α, λ, and R_1 (with the corresponding parameter values used in this plot displayed in the plot above). The white constrained regions indicate that no tunneling occurs because the condition $V_\mathrm{C}(r) + V_\mathrm{G}(r) < E$ holds throughout the entire interval $[r_1, r_2']$.

6 Conclusion

In this work, we carried out a comprehensive review of the main foundations of LED theories, with particular emphasis on brane-world scenarios, in which only gravity is allowed to propagate through the higher-dimensional space. We also revisited in detail George Gamow's theory of alpha decay, an undeniably important formulation in the history of physics. In addition to being the first successful theoretical explanation of the alpha-decay process in radioactive nuclei, Gamow's model represents a landmark in modern physics, marking the first explicit application of quantum mechanics to the nuclear domain [78].

The central objective of this work was to extend Gamow's original theory to a framework incorporating extra dimensions, in order to investigate how the existence of hidden dimensions might modify the decay rate of heavy nuclei. To achieve this, we examined two distinct types of corrections to the gravitational potential: (i) a power-law behavior valid in the short-distance regime, and (ii) a Yukawa-like parametrization describing the asymptotic behavior of the modified gravitational interaction at larger length scales. Incorporating these theoretical modifications into the extended Gamow factor, and using a dataset of 158 isotopes, we compared the model's predictions with real experimental measurements. This allowed us to identify best-fit regions and impose experimental constraints, obtained independently, on the relevant parameters of each theoretical scenario, such as the effective nuclear radius, the higher-dimensional Planck length, and the Yukawa parameters α and λ.

For the power-law correction, considering scenarios with up to seven extra dimensions ($\delta = 1, \ldots, 7$), our results indicate that the scenario yielding the smallest value of the RCS, $\tilde{\chi}_0^2$, is $\delta = 1$, for which $\tilde{\chi}_0^2 = 0.8543$ (Table 1). To explore the structure of the parameter space in more detail, we constructed color maps of the RCS as functions of the free nuclear-radius parameter R_1 and the higher-dimensional Planck length $l_{\mathrm{P}}^{(4+\delta)}$ for the first four extra-dimensional scenarios (Figure 13). From the corresponding best-fit regions, several noteworthy features emerge. First, the $\delta = 1$ scenario allows a noticeably broader interval of admissible values of R_1 compared with the other cases. Second, for all considered values of δ, the lower portions of the best-fit regions exhibit nearly identical widths and are consistently centered around $R_1 \approx 1.5$ fm, indicating a remarkable stability of this parameter across different extra-dimensional scenarios. Third, with the increase in the number of extra dimensions, the left boundary of the best-fit region gradually acquires a more pronounced curvature, indicating that the model becomes increasingly sensitive to small changes in the parameter R_1 as additional dimensions are introduced. Finally, we observe a systematic widening of the allowed range of $l_{\mathrm{P}}^{(4+\delta)}$ with increasing δ. In particular, for the $\delta = 4$ scenario, the best-fit region includes values of $l_{\mathrm{P}}^{(4+\delta)}$ of the order of 0.5 fm, reinforcing the possibility that the extra dimensions predicted by LED theories could reach femtometer-scale sizes without conflicting with the experimental data considered.

For the Yukawa parametrization, on the other hand, we found a minimum RCS value slightly smaller than that obtained for the best power-law scenario: $\tilde{\chi}_0^2 = 0.8383$ (Table 2). This result indicates that, from a statistical point of view, describing gravitational corrections through a Yukawa-type term provides a slightly more efficient fit to the experimental alpha-decay data. The analysis of the best-fit regions in the parameter space defined by R_1, α, and λ (Figure 14) revealed that the effective nuclear radius remains strongly concentrated around $R_1 \approx 1.5$ fm, once again highlighting the robustness of this parameter regardless of the functional form adopted for the gravitational correction. In addition, another noteworthy feature of this model is the emergence of a narrow best-fit region centered around $\alpha = 9.82 \times 10^{33}$. The fact that this optimal region is extremely narrow in α, while extending over several orders of magnitude in λ (starting at scales of order 10^{-13} m and reaching larger values), indicates that the quality of the fit is far more sensitive to variations in α than to changes in the Yukawa length scale.

Taken together, these results are particularly significant, as they demonstrate that alpha decay, despite being a nuclear process traditionally governed by the strong and electromagnetic interactions, can serve as a sensitive testing tool for modified gravitational theories arising from extra-dimensional models.

In conclusion, it is important to emphasize that this work obtained independent bounds for both the Planck length in higher-dimensional scenarios and for the parameters of the Yukawa parametrization. The independence of these constraints, derived solely from alpha-decay data, without relying on laboratory-scale gravitational experiments or cosmological tests, highlights the relevance and originality of the results presented here.

Finally, with regard to future perspectives, several promising directions may be pursued. From a theoretical standpoint, a more refined analysis could incorporate more realistic nuclear models, going beyond the idealized potential combination used in Gamow's formulation. For example, nuclear potentials widely employed in nuclear physics, such as the Woods–Saxon potential [79], or even approaches based on the liquid-drop description of the atomic nucleus [80–82], could provide more accurate modeling and yield tighter experimental bounds. Additional structural properties of the nucleus, such as spin, quadrupole moment, deformations, and finite-size effects, could also be systematically included [83, 84]. From a technical and computational perspective, refining the discretization grid used in the fitting maps, thereby producing higher-resolution plots, could reveal subtle features in the behavior of $\tilde{\chi}^2$ that remain hidden in lower-resolution plots.

Bibliography

[1] NORDSTRÖM, G. Über die möglichkeit, das elektromagnetische feld und das gravitationsfeld zu vereinigen. *Physikalische Zeitschrift*, v. 15, p. 504–506, 1914. Cited on page 15.

[2] NORDSTRÖM, G. *On the possibility of unifying the electromagnetic and the gravitational fields*. 2007. Disponível em: <https://arxiv.org/abs/physics/0702221>. Cited on page 15.

[3] ISAKSSON, E. *Gunnar Nordström, suomalainen Einstein: painovoiman teoriaa 1910-luvulla*. <https://www.mv.helsinki.fi/home/eisaksso/nordstrom/gunnar.html>. Retrieved 04 December 2025. Cited on page 15.

[4] RAVNDAL, F. *Scalar Gravitation and Extra Dimensions*. 2004. Disponível em: <https://arxiv.org/abs/gr-qc/0405030>. Cited on page 15.

[5] KALUZA, T. Zum unitätsproblem der physik. *Sitzungsberichte der Königlich Preußischen Akademie der Wissenschaften (Berlin*, p. 966–972, 1921. Cited 3 times on pages 15, 21, and 81.

[6] PAIS, A. *Subtle is the Lord: The science and the life of Albert Einstein*. [S.l.]: Oxford University Press, 2005. Cited on page 15.

[7] CHENG, T. *Einstein's Physics: Atoms, Quanta, and Relativity - Derived, Explained, and Appraised*. [S.l.]: OUP Oxford, 2013. ISBN 9780191648762. Cited 2 times on pages 15 and 81.

[8] KLEIN, O. Quantentheorie und fünfdimensionale relativitätstheorie. *Zeitschrift für Physik*, Springer, v. 37, n. 12, p. 895–906, 1926. Cited 3 times on pages 15, 21, and 81.

[9] KLEIN, O. The atomicity of electricity as a quantum theory law. *Nature*, Nature Publishing Group, v. 118, n. 2971, p. 516–516, 1926. Cited 3 times on pages 15, 21, and 81.

[10] GRIFFITHS, D. *Introduction to Elementary Particles*. [S.l.]: Wiley, 2008. (Physics textbook). ISBN 9783527406012. Cited on page 16.

[11] SCHWINGER, J. A theory of the fundamental interactions. *Annals of Physics*, v. 2, n. 5, p. 407–434, 1957. ISSN 0003-4916. Disponível em: <https://www.sciencedirect.com/science/article/pii/0003491657900155>. Cited on page 16.

[12] STRASSLER, M. *The Strengths of the Known Forces*. <https://profmattstrassler.com/articles-and-posts/particle-physics-basics/the-known-forces-of-nature/the-strength-of-the-known-forces/>. Retrieved 04 December 2025. Cited on page 16.

[13] COLLINS, P. D. B.; MARTIN, A. D.; SQUIRES, E. J. *Particle Physics and Cosmology*. 1st. ed. [S.l.]: Wiley VCH, 1989. ISBN 0471600881. Cited on page 16.

[14] OHANIAN, H. *Modern Physics*. [S.l.]: Prentice-Hall, 1987. ISBN 9780135961230. Cited on page 16.

[15] POLITZER, H. D. Reliable perturbative results for strong interactions? *Phys. Rev. Lett.*, American Physical Society, v. 30, p. 1346–1349, Jun 1973. Disponível em: <https://link.aps.org/doi/10.1103/PhysRevLett.30.1346>. Cited on page 16.

[16] BECKER, K.; BECKER, M.; SCHWARZ, J. *String Theory and M-Theory: A Modern Introduction*. [S.l.]: Cambridge University Press, 2006. ISBN 9780521860697. Cited on page 16.

[17] RICKLES, D. *A Brief History of String Theory: From Dual Models to M-Theory*. 1st. ed. [S.l.]: Springer Berlin, Heidelberg, 2014. (The Frontiers Collection). ISBN 9783642451270. Cited on page 16.

[18] CERN. *Supersymmetry*. <https://home.web.cern.ch/science/physics/supersymmetry>. Retrieved 04 December 2025. Cited on page 16.

[19] ARKANI-HAMED, N.; DIMOPOULOS, S.; DVALI, G. The hierarchy problem and new dimensions at a millimeter. *Physics Letters B*, Elsevier, v. 429, n. 3-4, p. 263–272, 1998. Cited 4 times on pages 16, 17, 21, and 36.

[20] ANTONIADIS, I. et al. New dimensions at a millimeter to a fermi and superstrings at a tev. *Physics Letters B*, Elsevier, v. 436, n. 3-4, p. 257–263, 1998. Cited 4 times on pages 16, 17, 21, and 36.

[21] KAPNER, D. J. et al. Tests of the gravitational inverse-square law below the dark-energy length scale. *Physical review letters*, APS, v. 98, n. 2, p. 021101, 2007. Cited on page 17.

[22] MURATA, J.; TANAKA, S. A review of short-range gravity experiments in the lhc era. *Classical and Quantum Gravity*, IOP Publishing, v. 32, n. 3, p. 033001, Jan 2015. ISSN 1361-6382. Disponível em: <http://dx.doi.org/10.1088/0264-9381/32/3/033001>. Cited 6 times on pages 17, 19, 21, 31, 36, and 62.

[23] SHIFMAN, M. Large extra dimensions: Becoming acquainted with an alternative paradigm. *International Journal of Modern Physics A*, World Scientific Pub Co Pte Lt, v. 25, n. 02n03, p. 199–225, jan. 2010. ISSN 1793-656X. Disponível em: <http://dx.doi.org/10.1142/S0217751X10048548>. Cited on page 17.

[24] ARKANI-HAMED, N.; DIMOPOULOS, S.; DVALI, G. Phenomenology, astrophysics, and cosmology of theories with submillimeter dimensions and tev scale quantum gravity. *Physical Review D*, American Physical Society (APS), v. 59, n. 8, mar 1999. ISSN 1089-4918. Disponível em: <http://dx.doi.org/10.1103/PhysRevD.59.086004>. Cited on page 17.

[25] ARKANI-HAMED N.; DIMOPOULOS, S. D. G. The universe's unseen dimensions. *Scientific American*, New York, v. 12, n. 2, p. 66–73, 2002. Cited 3 times on pages 17, 21, and 36.

[26] GAMOW, G. Zur quantentheorie des atomkernes. *Zeitschrift für Physik*, Springer, v. 51, n. 3, p. 204–212, 1928. Cited 4 times on pages 18, 43, 48, and 79.

[27] ROHLF, J. W. *Modern physics from α to Z^0*. 1st. ed. [S.l.]: John Wiley & Sons, Inc, 1994. ISBN 0471572705. Cited 2 times on pages 18 and 47.

[28] WENTZEL, G. Eine verallgemeinerung der quantenbedingungen für die zwecke der wellenmechanik. *Zeitschrift für Physik*, Springer, v. 38, n. 6, p. 518–529, 1926. Cited 2 times on pages 18 and 37.

[29] KRAMERS, H. A. Wellenmechanik und halbzahlige quantisierung. *Zeitschrift für Physik*, Springer, v. 39, n. 10, p. 828–840, 1926. Cited 2 times on pages 18 and 37.

[30] BRILLOUIN, L. La mécanique ondulatoire de schrödinger; une méthode générale de résolution par approximations successives. *CR Acad. Sci*, v. 183, n. 11, p. 24–26, 1926. Cited 2 times on pages 18 and 37.

[31] GRIFFITHS, D. J. *Introduction to Quantum Mechanics*. [S.l.]: New Jersey: Prentice Hall, 1995. Cited 9 times on pages 18, 34, 38, 39, 40, 43, 46, 48, and 59.

[32] COHEN-TANNOUDJI, C.; DIU, B.; LALOË, F. *Quantum Mechanics*. [S.l.]: Wiley, 1977. (A Wiley - Interscience publication, v. 1). ISBN 9782705658335. Cited 6 times on pages 18, 31, 37, 38, 40, and 43.

[33] ZWIEBACH, B. *A First Course in String Theory*. [S.l.]: Cambridge University Press, 2004. (A First Course in String Theory). ISBN 9780521831437. Cited 6 times on pages 19, 22, 23, 27, 33, and 75.

[34] ZWIEBACH, B. *A First Course in String Theory*. 2nd. ed. [S.l.]: New York: Cambridge University Press, 2009. Cited 8 times on pages 19, 22, 23, 27, 32, 33, 34, and 75.

[35] SILVA, A. d. A. *Um Estudo Sobre Dimensões Extras*. Dissertação (Mestrado) — Universidade Federal de Campina Grande (UFCG), 2009. Cited 4 times on pages 22, 23, 24, and 33.

[36] SYMON, K. *Mechanics: 3d Ed.* [S.l.]: Addison-Wesley Publishing Company, 1971. (Addison-wesley series in physics). Cited 3 times on pages 23, 26, and 39.

[37] WATARI, K. *Mecânica Clássica 2*. [S.l.]: Editora Livraria da Física, 2004. ISBN 9788588325159. Cited 3 times on pages 23, 26, and 39.

[38] ROCHA, J. M. *Experimentos com Nêutrons e Gravidade Modificada*. Tese (Doutorado) — Universidade Federal da Paraíba (UFPB), 2025. Cited 3 times on pages 24, 26, and 36.

[39] BUTKOV, E. *Mathematical Physics*. [S.l.]: Addison-Wesley Publishing Company, 1968. (A-W series in advanced physics). ISBN 9780201007275. Cited 2 times on pages 28 and 34.

[40] ARFKEN, G. et al. *Mathematical Methods for Physicists: A Comprehensive Guide*. [S.l.]: Elsevier Science, 2013. ISBN 9780123846549. Cited 3 times on pages 28, 34, and 57.

[41] GRADSHTEYN, I. S.; RYZHIK, I. M. *Table of Integrals, Series, and Products*. 7th. ed. [S.l.]: Academic Press, 2007. ISBN 9780123736376. Cited 2 times on pages 29 and 30.

[42] YUKAWA, H. On the interaction of elementary particles. i. *Proceedings of the Physico-Mathematical Society of Japan. 3rd Series*, The Physical Society of Japan, The Mathematical Society of Japan, v. 17, p. 48–57, 1935. Cited on page 31.

[43] GRIFFITHS, D. *Introduction to Quantum Mechanics*. [S.l.]: Cambridge University Press, 2017. ISBN 9781107179868. Cited 3 times on pages 31, 46, and 48.

[44] MERZBACHER, E. *Quantum Mechanics*. [S.l.]: Wiley, 1998. ISBN 9780471887027. Cited 4 times on pages 31, 37, 38, and 43.

[45] GRIFFITHS, D. *Introduction to Electrodynamics*. [S.l.]: Pearson Education, 2014. ISBN 9780321972101. Cited on page 34.

[46] RANDALL, L.; SUNDRUM, R. Large mass hierarchy from a small extra dimension. *Physical review letters*, APS, v. 83, n. 17, p. 3370, 1999. Cited on page 36.

[47] HALL, B. *Quantum Theory for Mathematicians*. [S.l.]: Springer New York, 2013. (Graduate Texts in Mathematics). ISBN 9781461471165. Cited on page 37.

[48] SCHIFF, L. I. *Quantum Mechanics*. 3rd. ed. [S.l.]: McGraw-Hill Book Company, Inc., 1968. (International Series In Pure And Applied Physics). Cited on page 37.

[49] SAKURAI, J.; NAPOLITANO, J. *Modern Quantum Mechanics*. [S.l.]: Cambridge University Press, 2017. ISBN 9781108422413. Cited on page 37.

[50] GASIOROWICZ, S. *Quantum Physics, 3Rd Ed*. [S.l.]: Wiley India Pvt. Limited, 2007. ISBN 9788126511174. Cited on page 37.

[51] SHANKAR, R. *Principles of Quantum Mechanics*. [S.l.]: Springer US, 2012. (Physics and Astronomy). ISBN 9781475705768. Cited on page 37.

[52] YOON, J.-H.; WONG, C.-Y. Relativistic modification of the gamow factor. *Physical Review C*, American Physical Society (APS), v. 61, n. 4, mar. 2000. ISSN 1089-490X. Disponível em: <http://dx.doi.org/10.1103/PhysRevC.61.044905>. Cited on page 42.

[53] GURNEY, R. W.; CONDON, E. U. Quantum mechanics and radioactive disintegration. *Physical Review*, APS, v. 33, n. 2, p. 127, 1929. Cited on page 43.

[54] FRIEDLANDER, G.; KENNEDY, J.; MILLER, J. *Nuclear and Radiochemistry*. 2nd. ed. [S.l.]: John Wiley & Sons, Inc., 1964. ISBN 0471280208. Cited on page 43.

[55] GEIGER, H.; NUTTALL, J. Lvii. the ranges of the α particles from various radioactive substances and a relation between range and period of transformation. *The London, Edinburgh, and Dublin Philosophical Magazine and Journal of Science*, Taylor & Francis, v. 22, n. 130, p. 613–621, 1911. Cited 2 times on pages 43 and 79.

[56] BROWN, B. A. Simple relation for alpha decay half-lives. *Physical Review C*, APS, v. 46, n. 2, p. 811, 1992. Cited 2 times on pages 45 and 59.

[57] LANDAU, L. D.; LIFSHITZ, E. M. *The Classical Theory of Fields*. 3rd. ed. Headington Hill Hall, Oxford: Pergamon Press Ltd, 1971. v. 2. (Course of Theoretical Physics, v. 2). Cited on page 46.

[58] BERGMANN, P. G.; EINSTEIN, A. *Introduction to the Theory of Relativity*. 180 Varik Street – New York, N.Y. 10014: Dover Publications, Inc, 1976. ISBN 0486632822. Cited on page 46.

[59] ABRAMOWITZ, M.; STEGUN, I. *Handbook of Mathematical Functions: With Formulas, Graphs, and Mathematical Tables*. [S.l.]: Dover Publications, 1965. (Applied mathematics series). ISBN 9780486612720. Cited on page 57.

[60] WATSON, G. *A Treatise on the Theory of Bessel Functions*. [S.l.]: Cambridge University Press, 1995. (Cambridge Mathematical Library). ISBN 9780521483919. Cited on page 57.

[61] QI, C. et al. On the validity of the geiger–nuttall alpha-decay law and its microscopic basis. *Physics Letters B*, Elsevier, v. 734, p. 203–206, 2014. Cited 2 times on pages 59 and 79.

[62] MUGHABGHAB, S. F. *Neutron Cross Sections: Neutron Resonance Parameters and Thermal Cross Sections Part B: Z= 61-100*. [S.l.]: Academic press, 2012. v. 1. Cited on page 59.

[63] HJORTH-JENSEN, M. Computational physics. University of Oslo. 2005. Cited on page 59.

[64] DAMAS, L. *Linguagem C*. 10. ed. Rio de Janeiro: LTC, 2007. ISBN 8521615191. Cited on page 59.

[65] NNDC. *NuDat | Search and plot nuclear structure and decay data interactively*. <https://www.nndc.bnl.gov/nudat3/>. Retrieved 06 December 2025. Cited on page 59.

[66] NIST. *Atomic Weights and Isotopic Compositions for All Elements*. <https://physics.nist.gov/cgi-bin/Compositions/stand_alone.pl>. Retrieved 06 December 2025. Cited on page 59.

[67] KEHAGIAS, A.; SFETSOS, K. Deviations from the 1/r2 newton law due to extra dimensions. *Physics Letters B*, Elsevier BV, v. 472, n. 1–2, p. 39–44, jan. 2000. ISSN 0370-2693. Disponível em: <http://dx.doi.org/10.1016/S0370-2693(99)01421-5>. Cited on page 60.

[68] GIUDICE, G. F.; RATTAZZI, R.; WELLS, J. D. Quantum gravity and extra dimensions at high-energy colliders. *Nuclear Physics B*, Elsevier BV, v. 544, n. 1–2, p. 3–38, abr. 1999. ISSN 0550-3213. Disponível em: <http://dx.doi.org/10.1016/S0550-3213(99)00044-9>. Cited on page 60.

[69] SUNDRUM, R. Effective field theory for a three-brane universe. *Phys. Rev. D*, American Physical Society, v. 59, p. 085009, Mar 1999. Disponível em: <https://link.aps.org/doi/10.1103/PhysRevD.59.085009>. Cited on page 60.

[70] DIMOPOULOS, S.; LANDSBERG, G. Black holes at the large hadron collider. *Phys. Rev. Lett.*, American Physical Society, v. 87, p. 161602, Sep 2001. Disponível em: <https://link.aps.org/doi/10.1103/PhysRevLett.87.161602>. Cited on page 60.

[71] KAPNER, D. J. et al. Tests of the gravitational inverse-square law below the dark-energy length scale. *Phys. Rev. Lett.*, American Physical Society, v. 98, p. 021101, Jan 2007. Disponível em: <https://link.aps.org/doi/10.1103/PhysRevLett.98.021101>. Cited on page 62.

[72] TAN, W.-H. et al. Improvement for testing the gravitational inverse-square law at the submillimeter range. *Phys. Rev. Lett.*, American Physical Society, v. 124, p. 051301, Feb 2020. Disponível em: <https://link.aps.org/doi/10.1103/PhysRevLett.124.051301>. Cited on page 62.

[73] RIDER, A. D. et al. Search for screened interactions associated with dark energy below the 100 μm length scale. *Phys. Rev. Lett.*, American Physical Society, v. 117, p. 101101, Aug 2016. Disponível em: <https://link.aps.org/doi/10.1103/PhysRevLett.117.101101>. Cited on page 62.

[74] GERACI, A. A. et al. Improved constraints on non-newtonian forces at 10 microns. *Phys. Rev. D*, American Physical Society, v. 78, p. 022002, Jul 2008. Disponível em: <https://link.aps.org/doi/10.1103/PhysRevD.78.022002>. Cited on page 62.

[75] SUSHKOV, A. O. et al. New experimental limits on non-newtonian forces in the micrometer range. *Phys. Rev. Lett.*, American Physical Society, v. 107, p. 171101, Oct 2011. Disponível em: <https://link.aps.org/doi/10.1103/PhysRevLett.107.171101>. Cited on page 62.

[76] XU, J. et al. Nuclear constraints on non-newtonian gravity at femtometer scale. *Journal of Physics G: Nuclear and Particle Physics*, IOP Publishing, v. 40, n. 3, p. 035107, fev. 2013. ISSN 1361-6471. Disponível em: <http://dx.doi.org/10.1088/0954-3899/40/3/035107>. Cited on page 62.

[77] KAMYSHKOV, Y.; TITHOF, J.; VYSOTSKY, M. Bounds on new light particles from high-energy and very small momentum transfer np elastic scattering data. *Physical Review D—Particles, Fields, Gravitation, and Cosmology*, APS, v. 78, n. 11, p. 114029, 2008. Cited on page 62.

[78] GRIFFITHS, D. *Mecânica Quântica*. 2. ed. [S.l.]: Pearson Universidades, 2011. ISBN 9788576059271. Cited on page 65.

[79] WOODS, R. D.; SAXON, D. S. Diffuse surface optical model for nucleon-nuclei scattering. *Phys. Rev.*, American Physical Society, v. 95, p. 577–578, Jul 1954. Disponível em: <https://link.aps.org/doi/10.1103/PhysRev.95.577>. Cited on page 66.

[80] GAMOW, G. Mass defect curve and nuclear constitution. *Proceedings of the Royal Society of London. Series A, Containing Papers of a Mathematical and Physical Character*, v. 126, n. 803, p. 632–644, 03 1930. ISSN 0950-1207. Disponível em: <https://doi.org/10.1098/rspa.1930.0032>. Cited on page 66.

[81] WEIZSÄCKER, C. F. von. Zur theorie der kernmassen. *Zeitschrift für Physik*, v. 96, p. 431–458, 1935. Disponível em: <https://api.semanticscholar.org/CorpusID:118231854>. Cited on page 66.

[82] SARTORI, E. *Histoire des femmes scientifiques de l'antiquité au XXe siècle: les filles d'Hypatie*. Plon, 2006. ISBN 9782259202886. Disponível em: <https://books.google.com.br/books?id=3B3KHAAACAAJ>. Cited on page 66.

[83] JACKSON, J. D. *Classical Electrodynamics*. 3rd. ed. 111 River Street, Hoboken, NJ 07030: John Wiley & Sons, Inc, 1998. Includes index. ISBN 0-471-30932-X. Cited on page 66.

[84] FISCHBACH, E.; TALMADGE, C. L. *The Search for Non-Newtonian Gravity*. 1396 Physics Building, West Lafayette, IN 47907-1396 - USA: Springer Science+Business Media New York, 1999. Includes bibliographical references and index. ISBN 978-1-4612-7144-4. Cited on page 66.

[85] SALINAS, S. *Introduction to Statistical Physics*. [S.l.]: Springer New York, 2013. (Graduate Texts in Contemporary Physics). ISBN 9781475735086. Cited on page 75.

[86] PINSKY, M. *Introduction to Fourier Analysis and Wavelets*. [S.l.]: American Mathematical Society, 2023. (Graduate Studies in Mathematics). ISBN 9781470475673. Cited on page 76.

[87] ZYGMUND, A.; FEFFERMAN, R. *Trigonometric Series*. [S.l.]: Cambridge University Press, 2003. (Cambridge Mathematical Library). ISBN 9780521890533. Cited on page 76.

[88] REN, Z.; XU, C.; WANG, Z. New perspective on complex cluster radioactivity of heavy nuclei. *Physical Review C—Nuclear Physics*, APS, v. 70, n. 3, p. 034304, 2004. Cited on page 79.

[89] GAMOW, G. *The quantum theory of the atomic nucleus*. [S.l.]: US Atomic Energy Commission, Division of Technical Information Extension, 1963. Cited on page 79.

[90] TAYLOR, J. R. *An Introduction to Error Analysis: the study of uncertainties in physical measurements*. 2nd. ed. [S.l.]: University Science Books, 1997. ISBN 0935702423. Cited on page 80.

Appendix A – Volume of a Hypersphere

In this appendix, we present the calculation of the volume of a hypersphere of radius r in an n-dimensional space $\mathbb{R}^n$. The aim is to provide a general formulation that makes it possible to understand how the volume of this geometric region behaves as the number of dimensions increases. This result is relevant in various contexts of theoretical physics and applied mathematics, especially in scenarios involving extra dimensions. We begin by considering the simpler cases of the spheres $S^1(r)$ and $S^2(r)$, defined by

$$S^1(r) = x_1^2 + x_2^2 = r^2 \ , \tag{A.1}$$

and

$$S^2(r) = x_1^2 + x_2^2 + x_3^2 = r^2 \ . \tag{A.2}$$

The volumes of $S^1(r)$ and $S^2(r)$ are given by:

$$\text{vol}(S^1(r)) = 2\pi r \quad \text{and} \quad \text{vol}(S^2(r)) = 4\pi r^2 \ .$$

For simplicity, let us denote the volumes of the unit spheres as $\text{vol}(S^1) = \text{vol}(S^1(r=1))$ and $\text{vol}(S^2) = \text{vol}(S^2(r=1))$. The volume of $S^{n-1}(r)$ can be written as follows:

$$\text{vol}(S^{n-1}(r)) = r^{n-1}\text{vol}(S^{n-1}) \ . \tag{A.3}$$

In the space $\mathbb{R}^n$, we consider the coordinates $x_1, x_2, ..., x_n$ and let r be the radial coordinate. Then,

$$r^2 = x_1^2 + x_2^2 + \cdots + x_n^2 \ . \tag{A.4}$$

Let's divide our analysis into two stages. First, let's look at the following integral:

$$I = \int_{\mathbb{R}^n} e^{-r^2} dx_1 dx_2 \cdots dx_n \ . \tag{A.5}$$

Using Eq.(A.4) in the exponential factor, the integral becomes a product of n Gaussian integrals:

$$I = \prod_{i=1}^{n} \int_{-\infty}^{+\infty} e^{-x_i^2} dx_i = \pi^{n/2} \ . \tag{A.6}$$

In the next step, we will solve the integral by dividing $\mathbb{R}^n$ into shells. Since the space of r is $S^{n-1}(r)$, the volume of each shell lying between r and $r + dr$ is the volume of $S^{n-1}(r)$ times dr.

$$I = \int_0^\infty \text{vol}(S^{n-1}(r)) e^{-r^2} dr = \text{vol}(S^{n-1}) \int_0^\infty r^{n-1} e^{-r^2} dr \ . \tag{A.7}$$

Let's make the following change of variable:

$$r^2 = t \Rightarrow r dr = \frac{1}{2} dt \ . \tag{A.8}$$

Like this,

$$r^{n-1} dr = r^{n-2} r dr = r^{2(n/2-1)} r dr = \frac{1}{2} t^{n/2-1} dt \ . \tag{A.9}$$

Thus, our integral becomes

$$I = \frac{1}{2}\mathrm{vol}(S^{n-1}) \int_0^\infty t^{n/2-1} e^{-t} dt \ . \tag{A.10}$$

The integral of the above equation is known and can be expressed using the gamma function:

$$I = \frac{1}{2}\mathrm{vol}(S^{n-1})\Gamma(n/2) \ . \tag{A.11}$$

Therefore, from Eqs.(A.6) and (A.11), we have that the volume of the $(n-1)$-sphere will be [33, 34, 85]:

$$\mathrm{vol}(S^{n-1}(r)) = \frac{2\pi^{n/2} r^{n-1}}{\Gamma(n/2)} \ . \tag{A.12}$$

Appendix B – Poisson Summation Formula

The Poisson Summation Formula (PSF) for a periodic function f is defined as follows [86, 87]:

$$\sum_{p=-\infty}^{+\infty} f(t+pT) = \sum_{k=-\infty}^{+\infty} g(k/T)\frac{e^{\frac{2\pi ikt}{T}}}{T} \ , \tag{B.1}$$

where T is the period and $g(k/T)$ the Fourier transform of $f(t)$, given by

$$g(k/T) = \int_{-\infty}^{+\infty} e^{-\frac{2\pi ik\tau}{T}} f(\tau)d\tau \ . \tag{B.2}$$

Appendix C – Integral of an Infinitesimal δ-dimensional Volume in Spherical Coordinates

The calculation of a δ-volume in spherical coordinates is analogous to that of a three-dimensional volume. However, it is necessary to pay attention to some details present during its resolution. So, let's begin by recalling what happens to the integral of an infinitesimal volume d^3V when we change the Cartesian coordinates x, y, z to spherical r, θ, ϕ:

$$\begin{aligned}\int_{\mathbb{R}^3} d^3V &= \int_{-\infty}^{+\infty}\int_{-\infty}^{+\infty}\int_{-\infty}^{+\infty} dxdydz \\ &= \int_0^{2\pi}\int_0^{\pi}\int_0^{\infty} |J|\, drd\theta d\phi \\ &= \int_0^{2\pi}\int_0^{\pi}\int_0^{\infty} r^2\sin\theta drd\theta d\phi \\ &= 4\pi\int_0^{\infty} r^2 dr\ .\end{aligned}$$

Rewriting it another way, we have

$$\int_{\mathbb{R}^3} d^3V = \mathrm{vol}(S^2)\int_0^{\infty} r^2 dr\ , \tag{C.1}$$

where $r^2 = x^2 + y^2 + z^2$. In the most general case, in δ dimensions, the integral of an infinitesimal volume $d^\delta V$ would be of the form[1]:

$$\int_{\mathbb{R}^\delta} d^\delta V = \int_0^{2\pi}\int_0^{\pi}\cdots\int_0^{\pi}\int_0^{\infty} |J|\, drd\theta_1\cdots d\theta_{\delta-2}d\theta_{\delta-1}\ . \tag{C.2}$$

To find the Jacobian determinant, J, in δ dimensions, recall that, in 3D, the total infinitesimal displacement in spherical coordinates is given by the vector:

$$d\mathbf{l} = dl_r\hat{\mathbf{r}} + dl_\theta\hat{\theta} + dl_\phi\hat{\phi} = dr\hat{\mathbf{r}} + rd\theta\hat{\theta} + r\sin\theta d\phi\hat{\phi}\ . \tag{C.3}$$

In turn, the infinitesimal volume d^3V in spherical coordinates is given by:

$$d^3V = dl_r dl_\theta dl_\phi = \underbrace{r^2\sin\theta}_{|J|\text{ in 3D}} drd\theta d\phi\ . \tag{C.4}$$

In δD, the total infinitesimal displacement is

$$\begin{aligned}d\mathbf{l} &= dl_r\hat{\mathbf{r}} + dl_{\theta_1}\hat{\theta}_1 + dl_{\theta_2}\hat{\theta}_2 + \cdots + dl_{\theta_{\delta-1}}\hat{\theta}_{\delta-1} \\ &= dr\hat{\mathbf{r}} + rd\theta_1\hat{\theta}_1 + r\sin\theta_1 d\theta_2\hat{\theta}_2 + r\sin\theta_1\sin\theta_2 d\theta_3\hat{\theta}_3 + \cdots \\ &\quad + r\sin\theta_1\sin\theta_2\cdots\sin\theta_{\delta-2}d\theta_{\delta-1}\hat{\theta}_{\delta-1}\ .\end{aligned}$$

Thus, the infinitesimal δ-volume $d^\delta V$ in spherical coordinates will be:

[1] For simplicity, we will use the notation $(\theta_1, \theta_2, \cdots, \theta_{\delta-1})$ to represent the angular variables.

$$d^\delta V = \underbrace{r^{\delta-1}\sin^{\delta-2}\theta_1 \sin^{\delta-3}\theta_2 \cdots \sin\theta_{\delta-2}}_{|J| \text{ in } \delta\text{D}} dr d\theta_1 d\theta_2 \cdots d\theta_{\delta-1} \ . \tag{C.5}$$

Therefore, the general expression for the integral of an infinitesimal δ-volume in spherical coordinates is:

$$\begin{aligned}
\int_{\mathbb{R}^\delta} d^\delta V &= \int_0^{2\pi}\int_0^{\pi}\cdots\int_0^{\pi}\int_0^{\infty} r^{\delta-1}\sin^{\delta-2}\theta_1 \sin^{\delta-3}\theta_2\cdots\sin\theta_{\delta-2} dr d\theta_1\cdots d\theta_{\delta-1} \\
&= \mathrm{vol}(S^{\delta-2})\int_0^{\pi}\int_0^{\infty} r^{\delta-1}\sin^{\delta-2}\theta_1 dr d\theta_1 \\
&= \mathrm{vol}(S^{\delta-1})\int_0^{\infty} r^{\delta-1} dr \ .
\end{aligned} \tag{C.6}$$

Appendix D – The Geiger-Nuttall Law

In nuclear physics, the Geiger–Nuttall Law (GNL) establishes a relationship between the decay constant of a radioactive isotope and the energy of the emitted alpha particles. In general terms, the law indicates that isotopes with shorter half-lives emit alpha particles with higher energies, whereas long-lived isotopes emit less energetic ones.

This relationship also implies that the half-life of an isotope depends exponentially on its decay energy. Consequently, large variations in half-life correspond to relatively small changes in decay energy and, therefore, in the energy of the emitted alpha particles. As a result, despite the wide range of half-lives among alpha-emitting isotopes, spanning many orders of magnitude, their decay energies have relatively close values.

Originally formulated in 1911 by Hans Geiger and John Mitchell Nuttall as a relation between the decay constant and the range of alpha particles in air [55], the modern form of the GNL is expressed as

$$\log_{10} T_{1/2} = \frac{A(Z)}{\sqrt{E}} + B(Z), \tag{D.1}$$

where $T_{1/2}$ is the half-life, E is the total kinetic energy (of both the alpha particle and the daughter nucleus), and A and B are coefficients that depend on the atomic number Z of the isotope [61]. The law shows the strongest agreement for nuclei with even atomic and mass numbers, while the same trend persists, though less distinctly, for nuclei with odd nucleon configurations.

The GNL has also been extended to describe cluster decays [88], processes in which nuclei heavier than helium, such as carbon or silicon, are emitted.

A simple interpretation of this law can be obtained by modeling the alpha particle as being confined within the nucleus, analogous to a particle in a potential well. The particle remains bound due to the strong nuclear interaction and repeatedly reflects within the potential. However, owing to the quantum mechanical phenomenon of tunneling, there exists a finite probability that the particle escapes each time it interacts with the potential barrier.

This quantum mechanical description provides the foundation for deriving the GNL, including the numerical coefficients, through direct calculation, a result first achieved by George Gamow in 1928 [26, 89].

Appendix E – Reduced Chi-Squared

A statistical tool widely employed in the scientific literature to evaluate the consistency of a theoretical model with a given set of observational data is the chi-squared test for a distribution. This test quantifies the degree of agreement between the values predicted by a model and the available experimental data, providing an objective measure of the quality of the fit.

In the present work, to simplify the interpretation of the results, we adopt the Reduced Chi-Squared (RCS) form (also known as the chi-squared per degree of freedom), denoted by $\tilde{\chi}^2$ [90]. Accordingly, for a set of experimental data on the alpha decay of N isotopes, the RCS can be defined as

$$\tilde{\chi}^2 = \frac{1}{d} \sum_{i=1}^{N} \frac{\left(\log_{10} T_{1/2i}^{\mathrm{exp}} - \log_{10} T_{1/2i}^{\mathrm{th}}\right)^2}{\sigma^2}, \tag{E.1}$$

where $T_{1/2i}^{\mathrm{exp}}$ represents the experimental half-life of the i-th isotope, $T_{1/2i}^{\mathrm{th}}$ is the corresponding theoretical prediction, d is the number of degrees of freedom of the fit (typically given by $d = N - n_{\mathrm{p}}$, where n_{p} is the number of free parameters in the model), and σ is the standard deviation associated with the experimental uncertainties.

The expected mean value of $\tilde{\chi}^2$ is equal to 1. Thus, regardless of the number of degrees of freedom, the interpretation criterion is as follows: if the obtained value of $\tilde{\chi}^2$ is of order unity or smaller, the theoretical model can be considered consistent with the observational data within the experimental uncertainties. Conversely, significantly larger values of $\tilde{\chi}^2$ indicate that the discrepancy between theory and experiment is sufficiently large to suggest that the adopted model does not adequately describe the phenomenon under study.

Appendix F – Parameter Fitting Using Approximate Expressions

For this appendix, we present the discussion of the results obtained from the approximate expressions for the Gamow factor, Eq.(3.47), as well as the approximate expressions for its variation in the presence of extra dimensions under the power-law potential, Eq.(4.26), and the Yukawa-type parametrization, Eq.(4.41). These expressions are applied to the theoretical formula for the half-life of radioactive nuclei, Eq.(3.49), through Eq.(4.13).

F.1 Fit for the Power Law

In this analysis, for the short-distance regime, we examine how $\tilde{\chi}^2$ behaves depending on the particular choice used to define the nuclear radius r_1 (see Eqs.(5.1)). The results obtained for each fit are presented[1] in Tables 3, 4 and 5. The corresponding fitting regions for the first four scenarios with extra dimensions are shown in Figs. 15, 16 and 17. Unlike Fig. 13, these plots do not display restricted regions. This difference arises because the approximate expressions in Eqs.(3.47) and (4.26) always yield real values for γ and $\delta\gamma$. In contrast, when evaluating the integral in Eq.(4.3), certain critical parameter combinations may lead to an imaginary result, indicating the absence of tunneling. Consequently, such nonphysical regions appear as restrictions in Fig. 13, but not in the figures based on the approximate formulas.

In Table 3, we observe that the smallest value of $\tilde{\chi}_0^2$ among the scenarios analyzed corresponds to the case $\delta = 1$, for which the best-fit value of the parameter R_1 differs slightly from those obtained in the other scenarios. Furthermore, based on the fitted value of the higher-dimensional Planck length for this case, we see that the result is consistent with the theoretical expectations of the braneworld model: a higher-dimensional Planck length on the order of 4.5×10^{-17} m suggests subnuclear scales for the hidden dimensions, which is significantly larger than the usual Planck-scale estimate proposed by KK theory [5, 7–9]. Similarly, from the results presented in Tables 4 and 5, we can reach analogous conclusions.

Now, examining the behavior of $\tilde{\chi}^2$ for the different extra-dimensional scenarios shown in Figs. 15, 16, and 17, we observe that for the model with only one extra dimension ($\delta = 1$), the region corresponding to the best parameter fit, the darkest area, spans a wider interval of the atomic nucleus radius parameter than in the other cases. Note also that, similar to what was seen in Fig. 13, the leftward-curving boundary at the upper part of the best-fit region becomes increasingly pronounced as the number of extra dimensions grows.

Comparing Figs. 15, 16, and 17, we see that the lower parts of the best-fit regions in Fig. 15 are centered approximately at $R_1 = 1.5$ fm, whereas in Figs. 16 and 17, considering their respective variables R_2 and R_3, this value is closer to 1.2 fm. Furthermore, by

[1] For all extra-dimensional scenarios examined in Table 4, the fit of the free parameter R_α yielded the same common value: $R_\alpha = 1.699$ fm.

Table 3 – Parameter fitting for the power-law case using approximate expressions for the Gamow factor in extra dimensions, where the nuclear radius r_1 is described as in Eq.(5.1a). The values shown for the free parameters R_1 and $l_{\mathrm{P}}^{(4+\delta)}$ are those that minimize the RCS.

δ	$\tilde{\chi}_0^2$	R_1 (fm)	$l_{\mathrm{P}}^{(4+\delta)}$ (m)
1	0.8869	1.24	4.5×10^{-17}
2	0.8932	1.49	2.0×10^{-20}
3	0.8932	1.49	3.1×10^{-19}
4	0.8927	1.48	4.7×10^{-16}
5	0.8922	1.48	7.4×10^{-16}
6	0.8921	1.48	1.0×10^{-15}
7	0.8916	1.48	1.3×10^{-15}

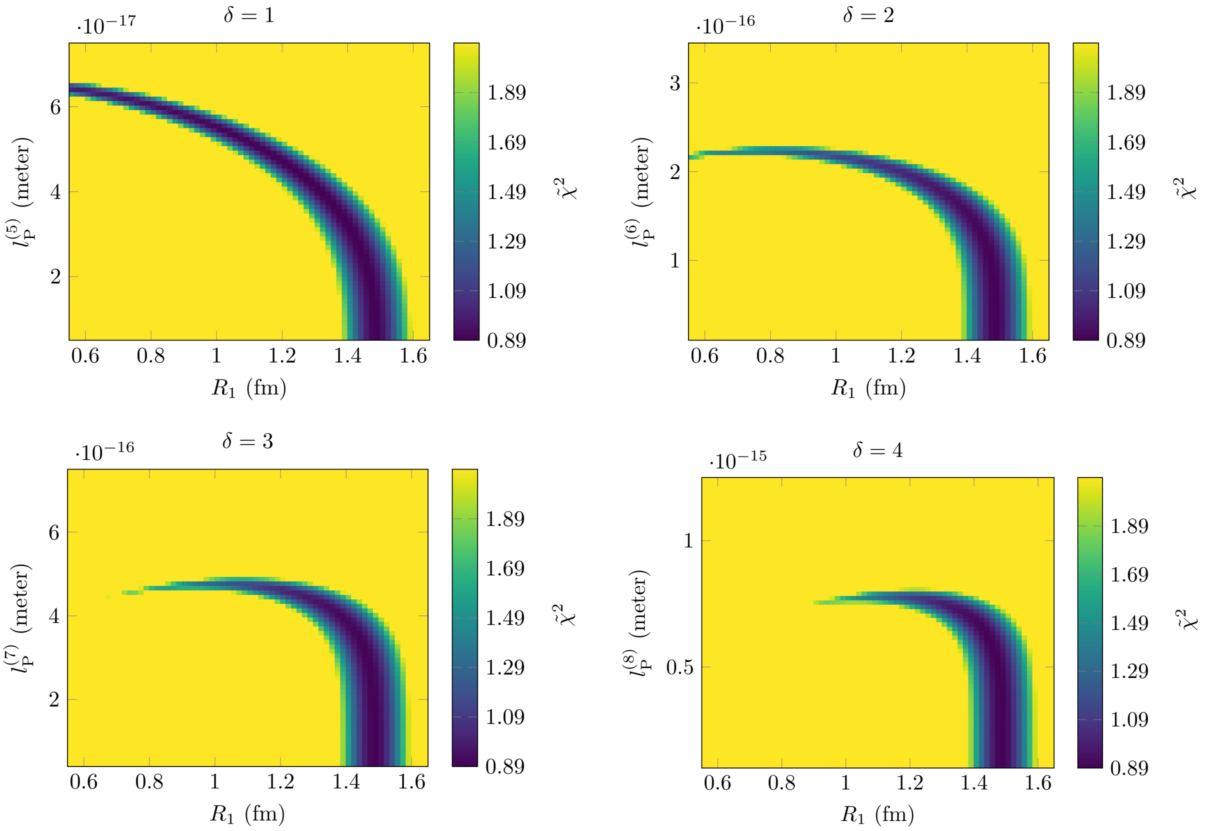

Figure 15 – Color map showing the behavior of $\tilde{\chi}^2$ as a function of the free parameters R_1 and $l_{\mathrm{P}}^{(4+\delta)}$.

analyzing Figs. 15 and 16, it is noticeable that the widths of the lower parts of their best-fit regions are slightly broader than those in Fig. 17. This result suggests that there is less flexibility in the possible values of R_3 compared with the parameters R_1 and R_2 considered in the other cases.

Taken together, these results indicate that the overall quality of the fits obtained using the approximate expressions is stable across the different prescriptions for the nuclear

Table 4 – Parameter fitting for the power-law case using approximate expressions for the Gamow factor in extra dimensions, where the nuclear radius r_1 is described as in Eq.(5.1b). The values shown for the free parameters R_2 and $l_{\mathrm{P}}^{(4+\delta)}$ are those that minimize the RCS.

δ	$\tilde{\chi}_0^2$	R_2 (fm)	$l_{\mathrm{P}}^{(4+\delta)}$ (m)
1	0.9002	1.22	9.6×10^{-18}
2	0.9044	1.21	8.4×10^{-17}
3	0.9043	1.21	2.4×10^{-16}
4	0.9046	1.21	4.7×10^{-16}
5	0.8870	1.27	1.0×10^{-15}
6	0.8914	1.26	1.3×10^{-15}
7	0.8919	1.25	1.6×10^{-15}

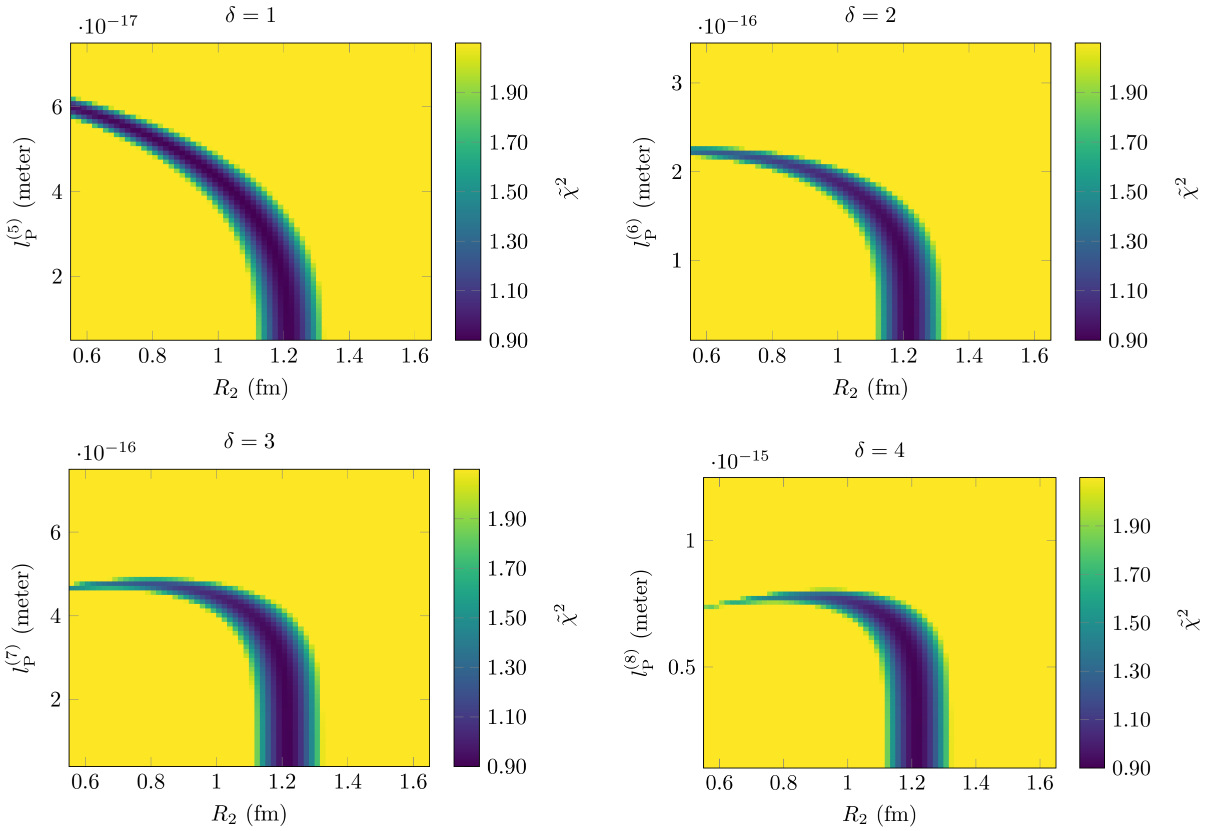

Figure 16 – Color map showing the behavior of $\tilde{\chi}^2$ as a function of the free parameters R_2 and $l_{\mathrm{P}}^{(4+\delta)}$.

radius, but not entirely insensitive to the chosen parametrization. In particular, the slightly narrower best-fit region associated with R_3 suggests that this functional form imposes stronger constraints on the admissible parameter space, reducing the range of R_3 values compatible with the experimental data. Conversely, the broader and more flexible regions obtained for R_1 and R_2 reflect a greater robustness of these parametrizations within the context of the short-distance power-law model. Despite these differences, all three choices yield comparable minimum values of $\tilde{\chi}_0^2$, and all lead to consistent estimates of

Table 5 – Parameter fitting for the power-law case using approximate expressions for the Gamow factor in extra dimensions, where the nuclear radius r_1 is described as in Eq.(5.1c). The values shown for the free parameters R_3 and $l_{\mathrm{P}}^{(4+\delta)}$ are those that minimize the RCS.

δ	$\tilde{\chi}_0^2$	R_3 (fm)	$l_{\mathrm{P}}^{(4+\delta)}$ (m)
1	0.8909	1.01	4.3×10^{-17}
2	0.8980	1.18	5.7×10^{-17}
3	0.8980	1.18	1.8×10^{-16}
4	0.8981	1.18	3.6×10^{-16}
5	0.8982	1.18	5.7×10^{-16}
6	0.8982	1.18	8.0×10^{-16}
7	0.8983	1.18	1.0×10^{-15}

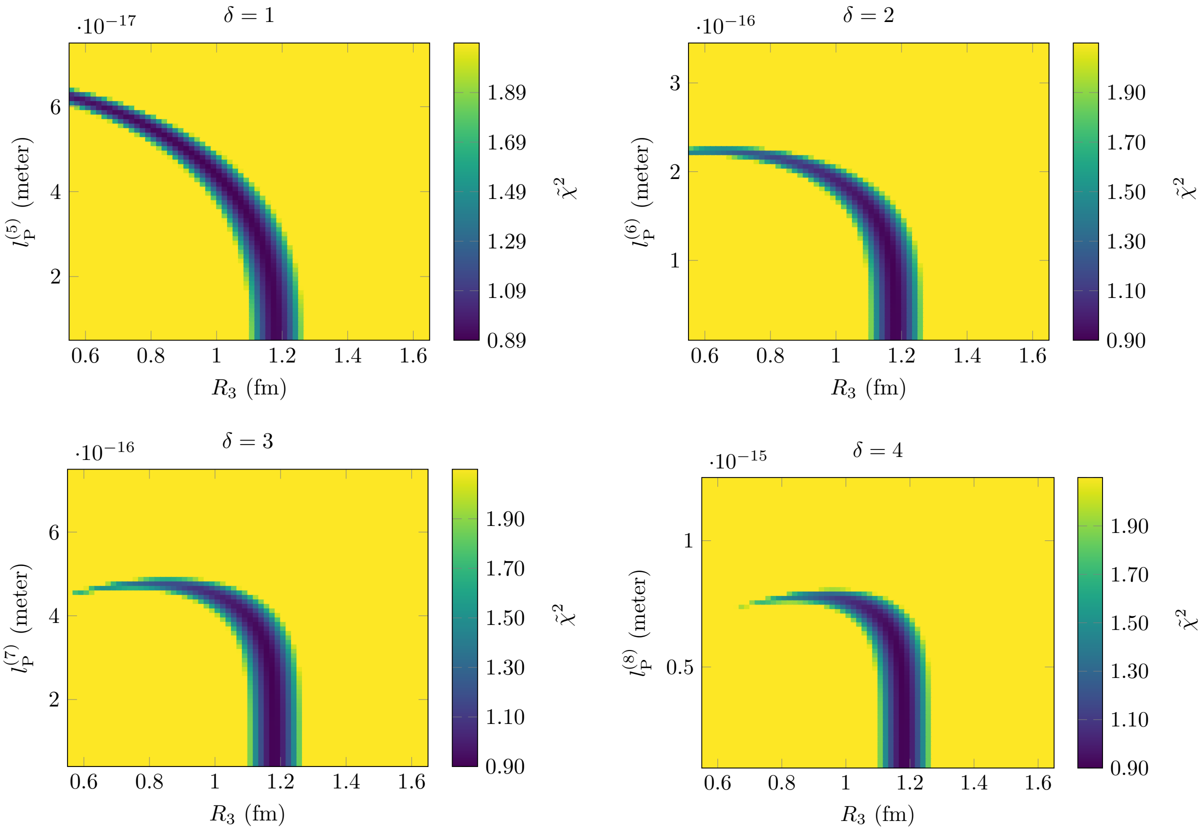

Figure 17 – Color map showing the behavior of $\tilde{\chi}^2$ as a function of the free parameters R_3 and $l_{\mathrm{P}}^{(4+\delta)}$.

the higher-dimensional Planck length in each extra-dimensional scenario. This reinforces the conclusion that the secondary results of this study, namely, the extraction of viable ranges for the nuclear radius and the higher-dimensional Planck scale, are not artifacts of a particular definition of r_1, but remain qualitatively stable under reasonable alternative parametrizations.

F.2 Fit for Yukawa Parameterization

For the analysis performed using the Yukawa parametrization in conjunction with the approximate theoretical expressions from Eqs.(3.47) and (4.41), and applying the fitting procedure through the RCS method, we obtained the results shown in Table 6. A direct comparison between these results and those presented previously in Table 2 reveals that the discrepancies between the two sets of fitted values are remarkably small. This close agreement reinforces the robustness of the fitting strategy and indicates that the approximate expressions capture, to a high degree of accuracy, the same physical trends obtained through the full numerical treatment.

Table 6 – Parameter fitting for the Yukawa parametrization using approximate expressions for the Gamow factor in extra dimensions. The values shown for the free parameters R_1, λ and α are those that minimize the RCS.

$\tilde{\chi}_0^2$	R_1 (fm)	λ (m)	α
0.8669	1.36	7.0×10^{-13}	9.0×10^{33}

However, a more detailed inspection of the upper plot in Fig. 18 shows a qualitative change compared to the corresponding diagram in Fig. 14. This upper panel displays the values that the nuclear parameter R_1 must take for each pair (λ, α) in order for the RCS to achieve its minimum value, and the color gradient forms a well-defined silhouette featuring a sharp "tip". Interestingly, this silhouette mirrors the shape observed in the lower panel of Fig. 18, which depicts the full behavior of $\tilde{\chi}^2$ as a function of λ, α, and R_1, whose values are shown in the upper plot.

A particularly notable feature is the abrupt change in the fitted values of R_1 that occurs along the upper boundary of the top panel. This transition takes place precisely at the midpoint of the plot's width in the λ-direction, aligned with the position of the tip-like structure. The abruptness of this variation strongly suggests that the behavior of R_1 is being driven by the scale associated with the parameter λ. Indeed, the fact that the tip appears exactly at $\lambda = 1.0 \times 10^{-14}$ m in both the upper and lower panels indicates that this length scale acts as a transition point separating two distinct regimes in the (λ, α) parameter space. In other words, near $\lambda = 1.0 \times 10^{-14}$ m, small changes in λ drastically alter the value of R_1 required for optimal fitting, signaling a heightened sensitivity of the model to the Yukawa-range parameter in this region.

Turning to the lower plot in Fig. 18, we observe a pronounced qualitative difference in the behavior of $\tilde{\chi}^2$ relative to the results displayed in Fig. 14. In particular, the RCS now develops a narrow and prominent "spike" centered at $\lambda = 1.0 \times 10^{-14}$ m. This feature reveals that, for this specific value of λ, the interaction-amplitude parameter α is only weakly constrained, producing a ridge-like structure in parameter space. Such a spike corresponds to a region where the model becomes comparatively insensitive to variations in α, which explains why the fitted values of R_1 shift abruptly in the upper plot.

In addition to these distinctive traits, the lower plot of Fig. 18 shows that the best-fit region (the darker blue zone) transitions sharply to higher values of $\tilde{\chi}^2$ as one moves away from the optimal combination of (λ, α). These sudden changes in the RCS, manifesting as steep gradients and abrupt color shifts, indicate a particularly strong boundary separating the region compatible with the observational data from the region that must be excluded. This behavior underscores the high sensitivity of the Yukawa parametrization, within the framework of the approximate expressions, to variations in the free parameters, and it highlights a sharply defined optimal region in the parameter space.

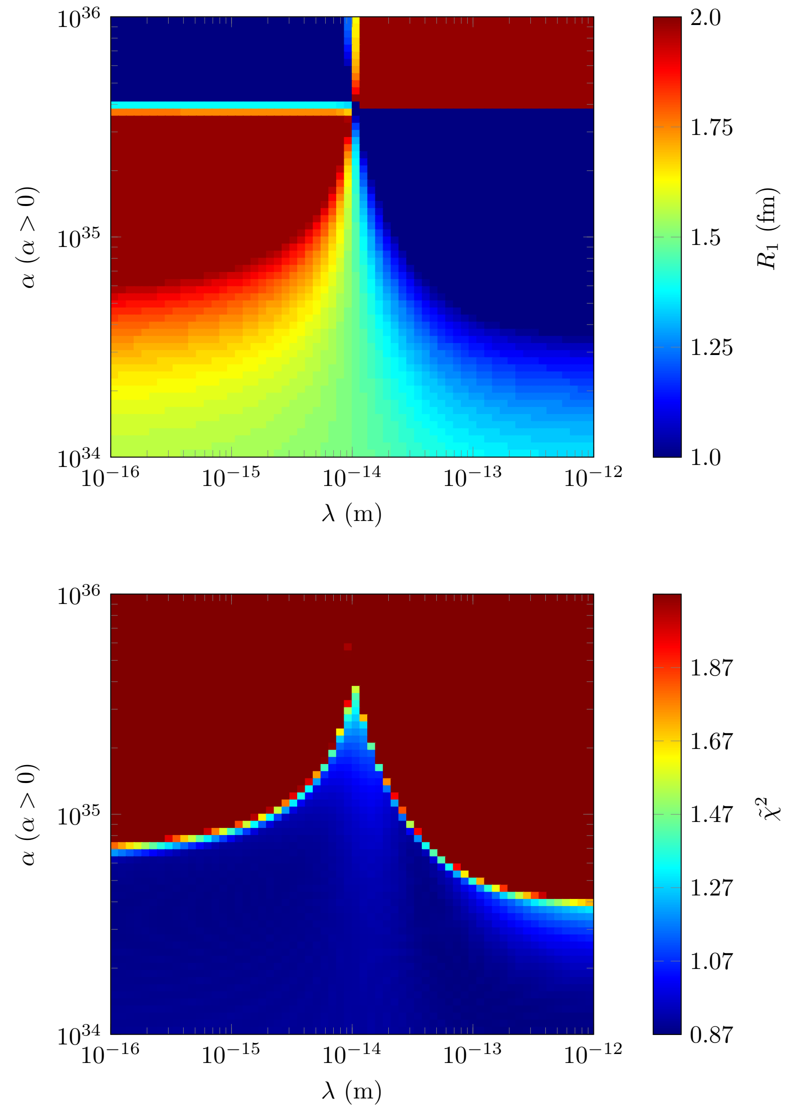

Figure 18 – *Above:* Fit region showing only the free parameters. The color gradient indicates the values of R_1. *Below:* Fit region showing the behavior of $\tilde{\chi}^2$ for the values of α, λ, and R_1.